HYDROGEN PRODUCTION BY *PARAGEOBACILLUS THERMOGLUCOSIDASIUS*

– Genomic insights and process investigation –

Zur Erlangung des akademischen Grades eines

DOKTORS DER NATURWISSENSCHAFTEN (DR. RER. NAT)

von der KIT- Fakultät für Chemieingenieurwesen und Verfahrenstechnik
des Karlsruher Instituts für Technologie (KIT)
genehmigte

DISSERTATION

von

M. Sc. Teresa Mohr

Aus Forst, Baden

Tag der mündlichen Prüfung: 4.12.2019

Erstgutachter: Prof. Dr. rer. nat. Christoph Syldatk

Zweitgutachter: Prof. Dr. Nicolaus Dahmen

Drittgutachterin: Dr. rer. nat. Anke Neumann

Zwischen Wahnsinn und Verstand

ist oft nur eine dünne Wand.

Daniel Düsentrieb

ACKNOWLEDGMENT

My sincere gratitude to Prof. Dr. Christoph Syldatk for the opportunity to work in his group. Thank you for your help and support. I also would like to thank my supervisor Anke Neumann for her consistent support and guidance during my PhD.

I am indebted to all the people whose knowledge and experience have been so valuable to the success of my work. Special thanks to Habibu Aliyu and Pieter de Maayer. Without your guidance I would not be the scientist I am today. Thank you for being my advisor, supporter, mentor and friend!

I would like to thank everyone at TeBi for their friendship, their motivation, help and of course, for the thousand cake days! I am very grateful to all those who supported me in any way at the institute. However, some deserve special mention: Jens (for all the parties and nights we went out), Olga&Aline (being the best colleagues someone can have during a PhD), André (for being my favorite French person), Alba&Michaela (for all your support and help). Becky (for entertaining) and Stefan&Olli&Sarah&Christin&Sascha (for a great time and friendship). Thanks to Pascali (for taking care about lunch), Sandra&Beate&Susanne (for the nice talks). Further, I would also like to thank my wonderful students Raphael, Katrin, Stephanie, Lars, Alex, Roman, Karo, Laura, Eva and Pembe.

I am grateful for the financial support from the Bundesministerium für Bildung und Forschung.

I would like to express my heartfelt gratitude to all my friends. Especially I want to thank Lena, Janina 🏋, David & Benni (131), Ferdi and Vera. Thanks for making bad times good and good times unforgettable ❤

To my beloved grandparents who were often in my thoughts – you are missed. To my family for their encouragement, patience and endless support during my life. Thanks to Mohrenbräu for sponsoring.

PREAMBLE

This thesis is based on peer reviewed research articles. All articles have been drafted during this work and describe the major results of the investigation of hydrogen production by the facultatively anaerobic thermophile *P. thermoglucosidasius*. Chapters based on a publication or are arranged for submission are indicated as such at the beginning of the chapter. The text of those are partly identical to the content of the publication. Citation style, figures and layout have been modified to match the formatting of this dissertation.

Chapter 2 encompasses the original identification of the *Parageobacillus thermoglucosidasius* carbon monoxide dehydrogenase-hydrogenase gene locus responsible for catalyzing the water-gas shift reaction and experimental evidence of hydrogen production via this mechanism. This chapter is largely based on the publication:

"CO-dependent hydrogen production by the facultative anaerobe Parageobacillus thermoglucosidasius."

Microbial Cell Factories, 2018

Chapter 3 describes the results of a screening study of different *P. thermoglucosidasius* strains with distinct hydrogenogenic capacities and their comparative genomic analysis. This chapter is based on the publication:

"Comparative genomic analysis of Parageobacillus thermoglucosidasius strains with distinct hydrogenogenic capacities."

BMC Genomics, 2018

Chapter 4 outlines the versatility of possible application in industrial processes to remove oxygen in syngas. This study was submitted for publication.

Chapter 5 presents the results of parametric optimization for enhanced hydrogen production. This study was submitted for publication.

LIST OF PUBLICATIONS

Peer reviewed original publications

2018

CO-DEPENDENT HYDROGEN PRODUCTION BY THE FACULTATIVE ANAEROBE *PARAGEOBACILLUS THERMOGLUCOSIDASIUS*

Teresa Mohr, Habibu Aliyu, Raphael Küchlin, Shamara Polliak, Michaela Zwick, Anke Neumann, Don Cowan, Pieter de Maayer

Microbial Cell Factories 17:108. DOI: 10.1186/s12934-018-0954-3

COMPARATIVE GENOMIC ANALYSIS OF *PARAGEOBACILLUS THERMOGLUCOSIDASIUS* STRAINS WITH DISTINCT HYDROGENOGENIC CAPACITIES.

Teresa Mohr, Habibu Aliyu, Raphael Küchlin, Michaela Zwick, Anke Neumann, Don Cowan, Pieter de Maayer

BMC Genomics, 19:880. DOI: 10.1186/s12864-018-5302-9

2019

INVESTIGATION OF THE EFFECTS OF DIFFERENT OPERATING PARAMETERS ON HYDROGEN PRODUCTION BY *PARAGEOBACILLUS THERMOGLUCOSIDASIUS* DSM 6285

Teresa Mohr, Habibu Aliyu, Lars Biebinger; Roman Gödert; Alexander Hornberger, Don Cowan, Pieter de Maayer, Anke Neumann

Submitted for publication

ACETOGENIC FERMENTATION FROM OXYGEN CONTAINING WASTE GAS

Teresa Mohr, Alba Infantes, Lars Biebinger; Pieter de Maayer, Anke Neumann

Submitted for publication

Conference poster

FERMENTATION OF OXYGEN CONTAINING SYNGAS

Teresa Mohr, Alba Infantes, Lars Biebinger, Anke Neumann

VAAM Jahrestagung (2018)

ABSTRACT

The overreliance on dwindling fossil fuel reserves and the negative climatic effects of using fuels are driving the development of new clean energy sources. One such alternative source of clean and renewable energy is hydrogen (H_2). Thus, there is an urgent need of developing biological strategies to produce H_2 via biological processes since the existing production strategies are not sustainable and mainly rely on fossil fuels.

This thesis provides the investigation of the microbial hydrogen production by the thermophilic *Parageobacillus thermoglucosidasius*. Comparative genomics performed in this study showed that *P. thermoglucosidasius* encodes two evolutionary distinct H_2-uptake [Ni-Fe]-hydrogenases and one H_2-evolving hydrogenase. In addition, genes encoding an anaerobic CO dehydrogenase (CODH) are co-localized with genes encoding a putative H_2-evolving hydrogenase. The co-localized of CODH and uptake hydrogenase form an enzyme complex that might potentially be involved in catalyzing the water-gas shift (WGS) reaction: $CO + H_2O \rightleftharpoons CO_2 + H_2$ (Chapter 2). To proof the ability to catalyse the WGS reaction, *P. thermoglucosidasius* DSM 2542^T was cultivated with an initial gas atmosphere of 50% CO and 50% air. After the oxygen was exhausted, the H_2 production commenced after a lag phase resulting at an equimolar conversion with a final yield of 1.08 H_2/CO. Hence, *P. thermoglucosidasius* DSM 2542^T is capable of tolerating elevated CO concentration and metabolizing CO at the same time.

In a further step, H_2 production of several *P. thermoglucosidasius* strains were evaluated (Chapter 3). The capacity to produce H_2 of four *P. thermoglucosidasius* was determined by cultivation and gas analysis. Along with DSM 2542^T, two other strains were hydrogenogenic (DSM 2543, DSM 6285), while one strain (DSM 21625) did not produce H_2. As in Chapter 2 shown, *P. thermoglucosidasius* first consumes O_2 and after a lag phase, H_2 production starts. Among the hydrogenogenic strains, the duration of the lag phase varied. The production of H_2 during the cultivation of DSM 6285 was substantially faster than with DSM 2542^T and DSM 2543. In a further step, comparative genomic analysis of the four strains were conducted. The disparities in the hydrogenogenic capacities of the strains might be explained by extensive differences in the protein complement and differences (polymorphisms and deletions) in the CODH-NiFe hydrogenase loci.

Besides a change in the energy sector to ensure a sustainable society, the chemical industry also has to find alternative strategies to processes depending on fossil c-sources. The unique feature of *P. thermoglucosidasius* shown in Chapter 2 and 3 to tolerate high concentrations of CO and metabolizing CO via the WGS reaction to H_2 and CO_2 can find application in industry besides the production of hydrogen as an energy carrier. Recently, anaerobic organism gained great interest in the production of bulk chemicals such as acetate or ethanol by using industrial waste gas (CO, CO_2, H_2). To make waste gas accessible to the strict anaerobes, a cost-prohibitive chemical O_2 removal step is necessary. Here, in Chapter 4, a sequential cultivation was established, where in the first phase the facultative anaerobic *P. thermoglucosidasius* first removes residual O_2 and produce H_2 and CO_2. The latter were subsequently utilized by the acetogen *C. ljungdhalii* in the second phase to produce acetate. In the presented system, *P. thermoglucosidasius* was successfully established as a biological cleaning tool for waste gases and providing building blocks for acetate production via the Wood-Ljungdahl pathway.

However, with a view of up-scaling the process for H_2 production, different process parameters were investigated in bottle experiments (Chapter 5). In total seven operating parameters on H_2 production were tested, including different growth temperatures, pre-culture ages and inoculum sizes, as well as different pHs and concentrations of nickel and iron in the fermentation medium, respectively. Cultivations were conducted with *P. thermoglucosidasius* DSM 6285 due to the shorter lag phase showed in Chapter 3. Optimum cultivation conditions were observed for 55 °C, an initial pH of 7.0, addition of 0.08 mM $FeSO_4.7H_2O$, 75:25 (CO:air ratio), 10% inoculum, 4 h inoculation time of the 2nd pre-culture.

Thus, the potential of *P. thermoglucosidasius* to produce H_2 via the WGS reaction combined with the thermophilic nature of the organism and the capacity to tolerate high concentrations of CO and O_2, may contribute to develop new strategies for biohydrogen production.

ZUSAMMENFASSUNG

Die starke Abhängigkeit von schwindenden fossilen Brennstoffressourcen und die negativen klimatischen Auswirkungen von Brennstoffen treiben die Entwicklung neuer sauberer Energiequellen voran. Eine dieser alternativen Quellen für saubere und erneuerbare Energie ist das Verwenden von Wasserstoff (H_2). Die Entwicklung neuer Strategien zur H_2-Produktion über biologische Prozesse ist daher dringend erforderlich, da die bestehenden Produktionsstrategien nicht nachhaltig sind und überwiegend auf fossilen Brennstoffen basieren.

Diese Arbeit befasst sich mit der Untersuchung der mikrobiellen Wasserstoffproduktion durch den thermophilen Organismus *Parageobacillus thermoglucosidasius*. Vergleichende genomische Analysen zeigten, dass *P. thermoglucosidasius* Gene für zwei evolutionär unterschiedliche H_2-*uptaking* [Ni-Fe]-Hydrogenasen und eine H_2-bildende Hydrogenase besitzt. Zusätzlich wurden Gene, die für eine anaerobe CO-dehydrogenase (CODH) codieren, identifiziert. Die co-lokalisierten Gene der CODH und der H_2-*uptaking* Hydrogenase können einen Enzymkomplex bilden, welcher möglicherweise an der Wassergas-Shift (WGS) Reaktion beteiligt ist: $CO + H_2O \rightleftharpoons CO_2 + H_2$. Um die Fähigkeit der Katalyse der WGS Reaktion zu zeigen, wurde *P. thermoglucosidasius* DSM 2542^T unter einer Anfangsgasatmosphäre von 50% CO und 50% Luft kultiviert. Nachdem O_2 verbraucht war, startete nach einer Lag-Phase die H_2 Produktion, die zu einer äquimolaren Umwandlung von CO zu H_2 mit einer Endausbeute von 1,08 H_2/CO führte.

P. thermoglucosidasius DSM 2542^T ist somit in der Lage, sowohl eine erhöhte CO-Konzentration zu tolerieren als auch gleichzeitig CO zu metabolisieren (Kapitel 2).

In einem weiteren Schritt wurden vier *P. thermoglucosidasius* Stämme auf ihre Kapazität zur Herstellung von H_2 durch Kultivierung und Gasanalyse untersucht (Kapitel 3). Neben DSM 2542^T waren zwei weitere Stämme (DSM 2543, DSM 6285) zur H_2 Bildung fähig, während ein Stamm (DSM 21625) kein H_2 produzierte. Wie in Kapitel 2 dargestellt, verbraucht *P. thermoglucosidasius* zunächst O_2 bis nach einer Lag-Phase die H_2-Produktion beginnt. Diese Lag-Phase variierte zwischen den wasserstofferzeugenden Stämmen in ihrer Dauer. Die Produktion von H_2 während der Kultivierung von DSM 6285 war wesentlich schneller als bei DSM 2542^T und DSM 2543. In einem weiteren Schritt wurde eine vergleichende genomische Analyse der vier Stämme durchgeführt. Die Disparitäten in den wasserstofferzeugenden Stämmen könnten durch große Unterschiede im Protein-Komplement sowie durch Polymorphismen und Deletionen in den CODH-NiFe-Hydrogenase-Loci erklärt werden.

Neben einem Wandel im Energiesektor zur Gewährleistung einer nachhaltig orientierten Gesellschaft muss auch die chemische Industrie alternative Strategien zu den bisherigen Prozessen finden, die überwiegend auf fossilen Brennstoffen basieren. Die in den Kapiteln 2 und 3 dargestellte Eigenschaften von *P. thermoglucosidasius*, hohe CO-Konzentrationen zu tolerieren und CO über die WGS-Reaktion zu H_2 und CO_2 zu metabolisieren, kann neben der Produktion von H_2 als Energieträger auch in der chemischen Industrie Anwendung finden. In den vergangenen Jahren haben anaerobe Organismen großes Interesse im Bereich der Herstellung von Chemikalien wie Acetat oder Ethanol unter Verwendung von Industrieabgasen (CO, CO_2, H_2) erlangt. Um das Abgas für die anaeroben Bakterien verträglich zu machen, ist ein teurer chemischer Schritt zur Entfernung von O_2 erforderlich. In Kapitel 4 wurde eine sequentielle Kultivierung etabliert, bei der in der ersten Phase der fakultative anaerobe *P. thermoglucosidasius* zunächst Restsauerstoff entfernt und anschließend H_2 und CO_2

produziert. Letztere wurden anschließend vom acetogenen *C. ljungdhalii* in der zweiten Phase zur Herstellung von Acetat genutzt. Im dargestellten System konnte *P. thermoglucosidasius* erfolgreich zur Sauerstoffentfernung für Abgase eingesetzt werden und gleichzeitig Bausteine für die Acetatproduktion über den Wood-Ljungdahl-Weg liefern.

Um den Prozess zur H_2-Produktion in einem größeren Maßstab zu etablieren, wurden in Flaschenversuchen verschiedene Prozessparameter untersucht (Kapitel 5). Insgesamt wurden sieben Parameter getestet, darunter verschiedene Wachstumstemperaturen, Vorkulturalter und Inokulumgrößen sowie unterschiedliche pH-Werte und Konzentrationen von Nickel und Eisen im Fermentationsmedium. Die Kultivierung erfolgte mit *P. thermoglucosidasius* DSM 6285 aufgrund der in Kapitel 3 dargestellten kürzeren Lag-Phase. Als optimale Kultivierungsbedingungen zeigten sich: 55 °C, einen Anfangs-pH von 7,0, Zugabe von 0,08 mM $FeSO_4.7H_2O$, einer Gasatmosphäre von 75:25 (CO:Luft Verhältnis), 10% Inokulum und einer 4 h Inkubationszeit der zweiten Vorkultur beobachtet.

Die Fähigkeit von *P. thermoglucosidasius* H_2 über die WGS-Reaktion zu produzieren, in Kombination mit der thermophilen Natur des Organismus und seiner Fähigkeit hohe Konzentrationen von CO und O_2 zu tolerieren, können dazu beitragen, neue Strategien für die Bio-Wasserstoffproduktion zu entwickeln.

TABLE OF CONTENTS

1 Theoretical Background and Research Proposal

1.1 THINK GREEN: RENEWABLE ENERGY

By the year 2040, the global energy demand is set to grow by more than 40%, mainly due to increased and rapid urbanization and industrialization (World Energy Outlook 2018). Most of the World's energy demand today is met with fossil fuels (e.g. petroleum, natural gas and coal) due to their convenient usage and their easy availability. These fossil fuel resources are, however, limited and their use as energy source results in the emission of greenhouse gases, mainly pollutants such as CO_2, CH_4, N_2O and O_3, which have a substantive negative effect on climate change (Jeoung *et al*., 2014). As such, there is an imperative need for a change in the energy sector to remedy the over-burdening of fossil fuels and the negative downstream effects of their implementation. Therefore, there has been an increasing interest in renewable energy sources to sustain economic growth concomitantly with reduced greenhouse effects (Ellabban *et al.*, 2014). Commonly employed renewable energy sources include wind energy, solar energy, geothermal energy and hydropower (Ellabban *et al.*, 2014). Biomass is also seen as a promising renewable resource. Energy from biomass can be gained by e.g. pyrolysis and anaerobic digestion of biomass feedstocks (e.g. from plants, microorganisms or forestry waste) (Srirangan *et al.*, 2012). A promising alternative to the fossil-based energy is the use of H_2 as an energy carrier. In comparison to fossil fuels, H_2 has the highest energy content with 141.9 MJ/kg higher heating value (Nikolaidis & Poullikkas, 2017). Because its combustion does not contribute to the greenhouse effect, with only heat and water produced during this process ($2\ H_2 + O_2 \rightleftharpoons 2\ H_2O$), H_2 can help in addressing increasing pollution issues and global warming to ensure a sustainable modern society. The production of H_2 is thus needed to be explored via biological processes because the existing production strategies are not sustainable.

1.2 HYDROGEN

Hydrogen is the most abundant element on Earth, although it is only present in combination with other elements (e.g. with O_2 in water). It can be generated via any primary energy source like wind, sun or natural gas and serve then as a fuel. H_2 stands out as an energy carrier because it is the only carbon-free fuel and features the highest energy content (141.9 MJ/kg) compared to other fuels (Nikolaidis & Poullikkas, 2017). Furthermore, in contrast to the combustion of fossil fuels, such as coal, oil and natural gas, combustion of H_2 gas does not result in the emission of greenhouse gases, thereby improving air quality (Marbán & Valdés-Solís, 2007). Given its inherent properties, H_2 plays a pivotal role in a wide range of industrial applications. In the chemical industry, H_2 is deployed for the production of ammonia (a major component of fertilizer) via the Haber process (Timm, 1963). It is also used in the production of methanol and refined petroleum (Ramachandran & Menon, 1998). These three products use two-thirds of the annual H_2 output (Ramachandran & Menon, 1998). It is also used as an O_2 scavenger to remove O_2 chemically for preventing corrosion and oxidation and finds application in the field of aeronautics as fuel in rockets (Sharma & Ghoshal, 2014). Furthermore, its easy conversion to electricity in fuel cells make H_2 very attractive as a clean and sustainable energy source (Nikolaidis & Poullikkas, 2017). H_2 is been seen as a suitable energy carrier for domestic consumption using applicable storage technologies such as compressed gas, cryo-compressed H_2 or as liquid H_2 (Preuster *et al.*, 2017). As such H_2 represents an attractive energy carrier and is currently being explored extensively as alternative fuel for cars, public transport vehicles and in the production of electricity (Figure 1) (Marbán & Valdés-Solís, 2007).

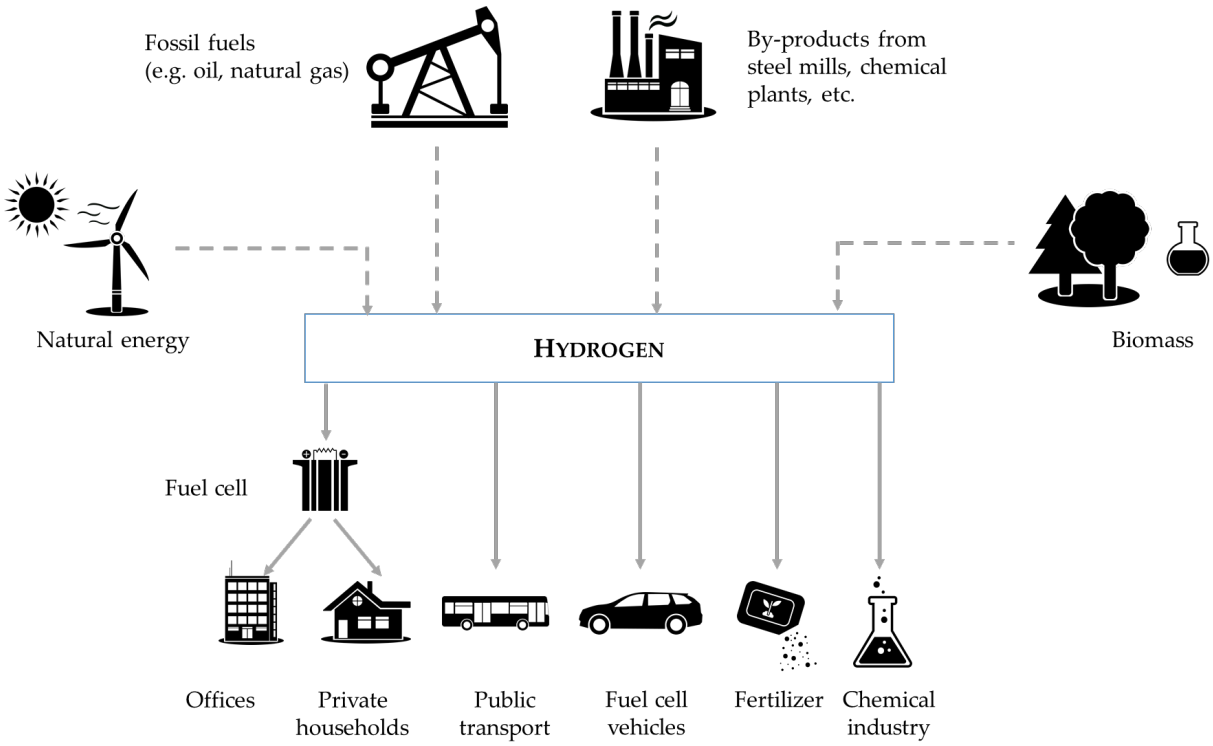

Figure 1: Hydrogen resources and applications.

1.3 INDUSTRIAL HYDROGEN PRODUCTION FROM FOSSIL FUELS

With its broad range of industrial and energy-related applications, several approaches have been developed for the production of H_2 gas. Current industrial H_2 production strategies depend primarily on fossil fuels. This includes steam reforming, partial oxidation or the combination of both. Other processes include the usage of biomass via pyrolysis and gasification. In a third approach, H_2 is produced from water by electrolysis (Nikolaidis & Poullikkas, 2017).

Hydrocarbon reformation strategies

Hydrocarbon reformation involves the conversion of hydrocarbons such as methane or natural gas to H_2 (Reimert *et al.*, 2011). The most commonly employed approach is steam reformation. In this process, the raw material (e.g. natural gas or biogas) is first cleaned. Then it is combined with steam and heat in the reformation reaction, resulting in the production of H_2 and carbon monoxide (CO) (Reimert *et al.*, 2011). In a following

process – after a heat recovery step – the resultant CO is converted via a catalytic water-gas shift (WGS) reaction to H_2 and carbon dioxide (CO_2) (Reimert *et al.*, 2011). If needed, carbon dioxide is removed in a final step by CO_2 capture and storage to increase H_2 yield (Figure 2A).

Another H_2 production approach is the partial oxidation process in which steam, O_2 and hydrocarbon are converted to H_2 and carbon oxides. After the substrate (e.g. methane) is cleaned, an oxidization step is undertaken with syngas (comprised of H_2, CO and some CO_2) as a product (Reimert *et al.*, 2011). The H_2 yield can again be increased by using the catalytic WGS reaction and CO_2 capture as is frequently employed in steam reforming strategies (Figure 2B) (Sørensen & Spazzafumo, 2011).

The combination of steam reforming and partial oxidation is termed the autothermal reformation method (Reimert *et al.*, 2011). In this approach, either steam or O_2 and CO_2 are used in a reaction with methane to produce syngas. Both reactions take place simultaneously (Figure 2C) (Sørensen & Spazzafumo, 2011).

Pyrolysis strategies

In a further approach, H_2 can be gained via pyrolysis. The word pyrolysis has its origin in Greek ("pyro" = fire; "lysis" = separating). It describes the thermal decomposition of organic material at high temperatures in the absence of O_2. Possible feedstocks are natural gas liquids and gases from crude oil (Reimert *et al.*, 2011). The process emits mainly H_2, CO_2, CO and CH_4 (Figure 2D) (Albright *et al.*, 1983).

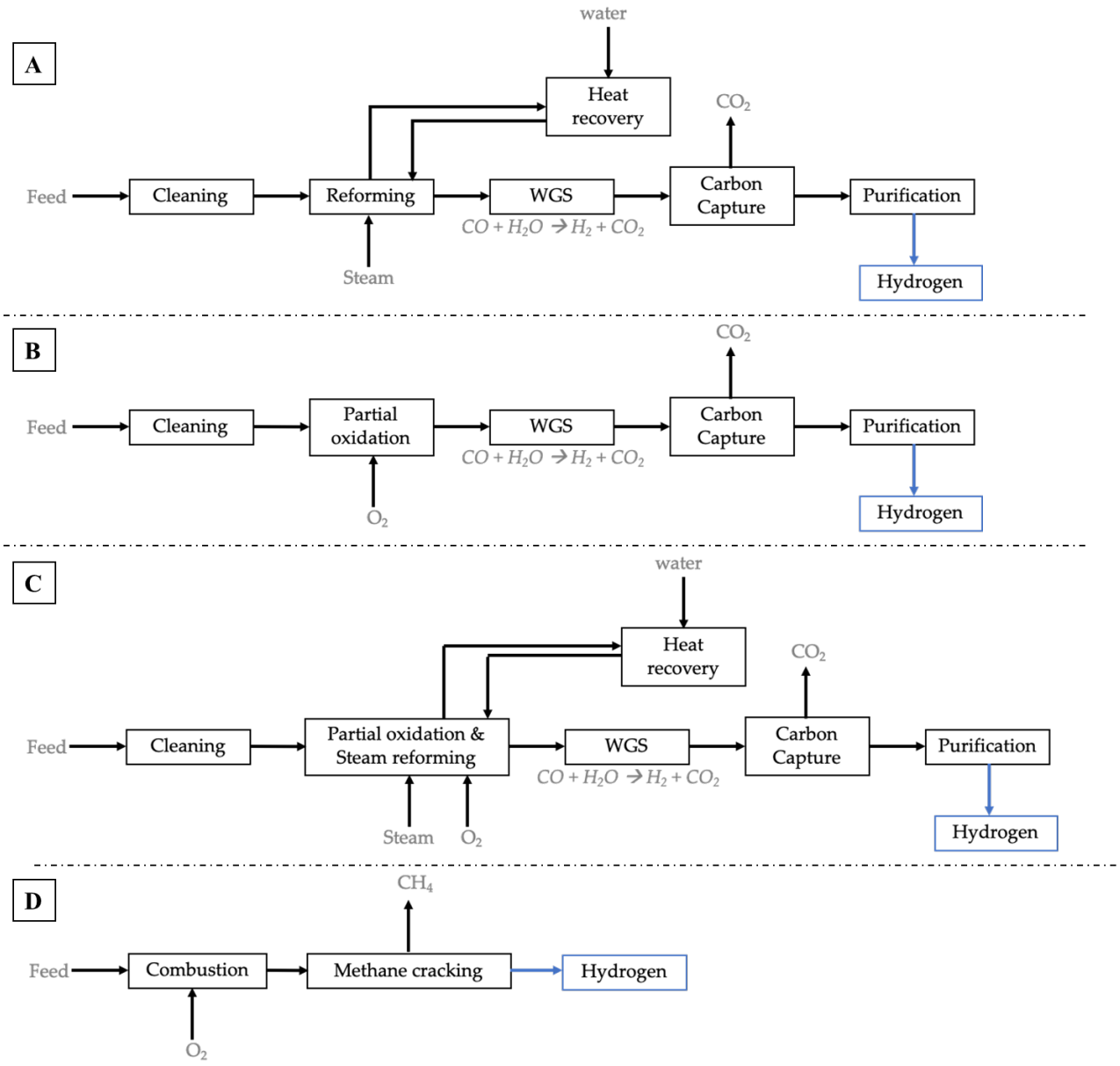

Figure 2: Schematic overview of different strategies for hydrogen production based on fossil fuels. (A) Stream reforming process. (B) Partial oxidation process. (C) Auto thermal reforming process: combination of partial oxidation and steam reforming. (D) hydrocarbon pyrolysis process.

Electrochemical strategies

The decomposition of water into H_2 and O_2 is termed electrolysis (Figure 3). This process is primarily undertaken in alkaline-water or solid-oxide electrolyzer cells. Positive ions (H_3O^+) move to the cathode, the negative hydroxide ions (OH^-) move towards the anode resulting in potential difference (Ebbesen & Mogensen, 2009; Zeng & Zhang, 2010). O_2 is produced at the anode and H_2 at the cathode: $2\ H_2O \rightarrow O_2 + 2\ H_2$.

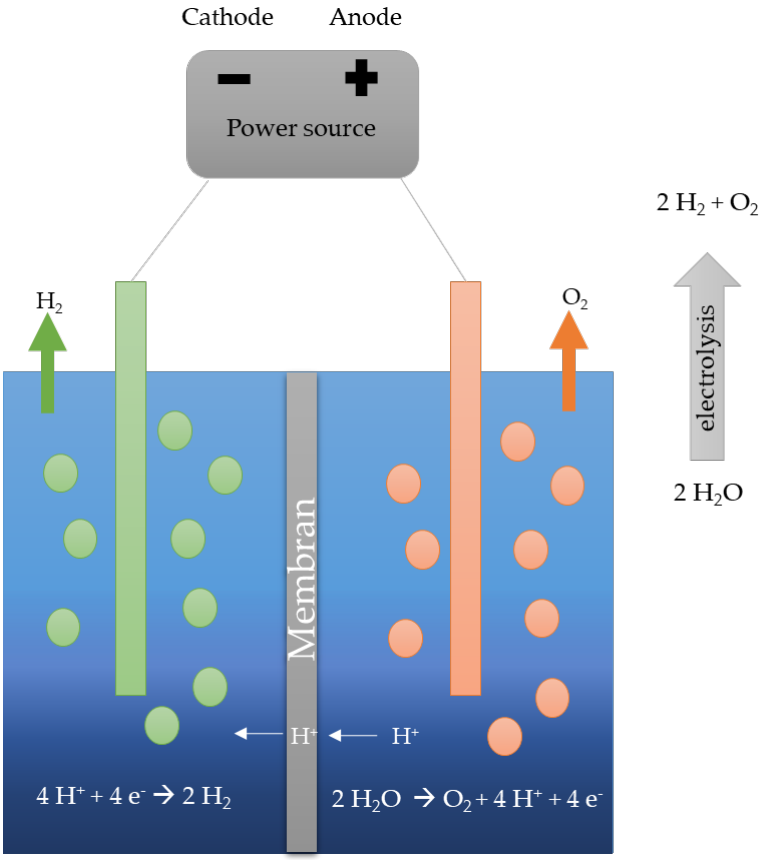

Figure 3: Electrolysis of water.

The hydrocarbon-based H_2 strategies described above represent the primary means by which most H_2 is produced at present. In particular, steam reformation and partial oxidation account for ~95% of all H_2 produced (Ogden, 1999). However, there are several constraints to the viability and sustainability of these H_2 production practices. As these processes involve heating and cooling steps, high pressures and electricity-driven equipment, the high energy and cost investment makes these processes largely

economically unviable (Preuster *et al.*, 2017). For example, H_2 production via electrolysis of methane is substantially more expense than if it were to be used directly in heating (Preuster *et al.*, 2017). Furthermore, these H_2 production strategies are primarily dependent on the availability of fossil fuels. At present, it is estimated that there is only enough natural coal, natural gas and oil to meet our current energy demands for another 114, 52.8 and 50.7 years, respectively (BP, 2016). The combustion of fossil fuels for the production of H_2 also results in the emission of greenhouse gases (H_2O, CO_2, CH_4, N_2O, O_3). Other primary pollutants like CO, SO_2 and volatile organic compounds are also released into the atmosphere during the combustion of fossil fuels (Flachsbart, 1999; Philip *et al.*, 2013). The pollutants are either hazardous in their native forms or in combination with other reagents (which are actually benign). The most concerning pollutant is CO_2, the major compound produced when fossil fuels are burned. As a consequence of the release of greenhouse gases, the average surface and ocean temperature is increasing, with dramatic climatic consequences (Schneider, 1989). There has thus been increased interest in the use of biological strategies.

1.3.1 Biological hydrogen production strategies

A variety of organisms (archaea, anaerobic bacteria, cyanobacteria and lower eukaryotes) are able to produce H_2 via biological mechanisms (Das & Veziroğlu, 2001). The mechanisms of H_2 production can be divided into light independent or light dependent processes. Dark fermentation is a light-independent process that is undertaken by heterotrophic bacteria, whereas biophotolysis and photofermentation are light dependent processes which occur in photoauthotrophic microalgae and cyanobacteria, and photosynthetic bacteria (Figure 4) (Rahman *et al.*, 2016).

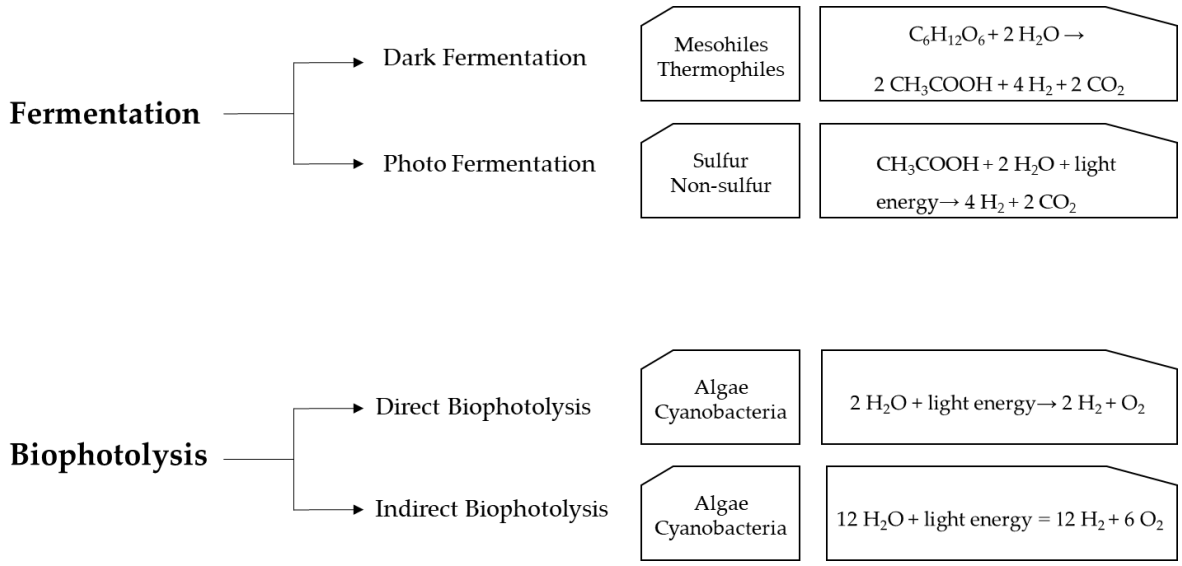

Figure 4: Schematic overview of biological strategies for hydrogen production.

Biophotolysis

Biophotolysis is the light driven decomposition of water into molecular hydrogen and O_2 (Nagarajan *et al.*, 2016). Biophotolysis can be further categorized into direct and indirect biophotolysis. In direct biophotolysis water is being converted into O_2 and H_2 in the presence of light and solar energy by green algae (e.g. *Chlamydomonas reinhadtii*) or cyanobacteria (e.g. *Synechocystis* spp.) (Yu & Takahashi, 2007):

$$2\ H_2O + light\ energy \rightarrow 2\ H_2 + O_2$$

During this reaction, light is absorbed by photosystem I (PSI) and photosystem II (PSII). Electrons from PSI are transferred to ferredoxin (Fd). In PSII, the absorbed light is used for the cleavage of water into electrons, protons (H^+) and O_2. The electrons are then transferred through the electron transport chain to hydrogenase enzymes that catalyze the production of H_2 gas (Hallenbeck & Benemann, 2002).

Indirect photolysis describes a two-step process for H_2 production via the microalgal and cyanobacterial photosynthetic systems. During the first step, water molecules are splitted in the presence of light energy resulting in the formation of protons and O_2. In the second step, CO_2 is fixed when storage carbohydrates are produced. H_2 production follows via a hydrogenase (Nath & Das, 2004). These two steps are strictly separated from each other to ensure that the hydrogenase enzyme is not inhibited by

O_2. In the first step, electrons derived from the carbon source of the intracellular energy reserves in contrast to direct photolysis (derived from water splitting) (Ni *et al.*, 2006):

$$6\ H_2O + 6\ CO_2 + \text{light energy} \rightarrow C_6H_{12}O_6 + 6\ O_2$$

$$C_6H_{12}O_6 + 12\ H_2O + \text{light energy} \rightarrow 12\ H_2 + 6\ CO_2$$

Due to the sensitivity of the hydrogenase enzymes to O_2 the H_2 yield of biophotolysis is typically low (Levin *et al*, 2004; Kapdan & Kargi, 2006). When applying biophotolysis in a bioindustrial process, partial O_2 pressure should be controlled below 0.1%, which is problematic because of the required diluent gas and power input for gas transfer (Hallenbeck & Benemann, 2002).

Photofermentation

Photosynthetic bacteria can also produce H_2 using light energy and reducing organic acids through photofermentation:

$$CH_3COOH + 2\ H_2O + \text{light energy} \rightarrow 4\ H_2 + 2\ CO_2$$

Microorganisms that can catalyze this reaction include purple non-sulfur, purple bacteria or green (gliding and green sulfur) bacteria (Rahman *et al.*, 2016). The organic acids serve as the source of electrons. Organic compounds are oxidized with light energy, and also produce electrons. The electrons are pumped through electron carriers and a proton gradient is built. Due the gained energy, an ATP synthase enzyme can produce adenosine triphosphate (ATP) from adenosine diphosphate (ADP). ATP can then be used to transport the electrons to ferredoxin. In a final step, nitrogenase enzymes catalyze the formation of H_2 by using the electrons derived from ferredoxin (Rahman *et al.*, 2016).

Dark fermentation

Dark fermentation produces H_2 through the catabolism of a wide range of carbon sources (e.g. glucose, sucrose and starch mixtures) and organic acids (e.g. acetate, propionate and butyrate). This process occurs in a wide range of microorganisms, including *Clostridium*, *Enterobacter*, *Thermoanaerobacterium* and *Thermococcus* spp., which carry out several distinct anaerobic fermentative pathways (Fabiano & Perego, 2002; Zhang *et al.*, 2003; Kanai *et al.*, 2005; Chen *et al.*, 2008; Ghimire *et al.*, 2015). For example, during the dark fermentation of glucose, glucose is converted to pyruvate through glycolysis producing ATP from ADP and NAD^+. In a further step, a pyruvate ferredoxin oxidoreductase and hydrogenase oxidize pyruvate to CO_2, acetyl-CoA and H_2. Additionally – depending on the microorganism and the environmental conditions – pyruvate can be also converted to formate. Formate can be further converted to CO_2 and H_2, while acetyl-CoA can be converted to other products such as acetate, butyrate and ethanol (Ni *et al.*, 2006; Li & Fang, 2007a). The biochemical reaction that takes place when glucose serves as substrate is:

$$C_6H_{12}O_6 + 2\ H_2O \rightarrow 2\ CH_3COOH + 4\ H_2 + 2\ CO_2$$

Light-dependent processes and dark fermentation represent the most pertinent biological avenues which are being exploited for bioindustrial H_2 production (Rahman *et al.*, 2016). However, several other biological pathways may also yield H_2 and may serve as the basis for bioindustrial H_2 production. One relatively underexplored pathway involves the production of H_2 via the biological WGS reaction with CO serving as substrate.

1.4 CO- DEPENDENT METABOLISM - MICROORGANISM

Carbon monoxide (CO) is a tasteless and odorless gas. It can be toxic due to its binding to metallocenters in haeme proteins (haemoglobin, myoglobin and cytochrome oxidase) (Blumenthal, 2001). It is a product of either natural processes or partial combustion of carbon-containing fuels in anthropogenic processes (Blumenthal, 2001). Anthropogenic sources include emissions from gasoline- and diesel-powered motors and from industrial processes (e.g. combustion of municipal waste) (Flachsbart, 1999; Philip *et al*., 2013). In biological reactions, CO can also occur as a byproduct. It is formed by anaerobic bacteria in aquatic environments (Schmidt & Conrad, 1993), during the oxidation of methane (Taylor *et al*., 1996), during haeme oxidation (Engel *et al*., 1972) or aromatic amino acid degradation (Hino & Tauchi, 1987). CO furthermore plays a crucial role in tropospheric chemistry, where it removes the hydroxyl radicals (OH^-) from the air. Hydroxyl radicals have a positive effect on air quality in that they decrease greenhouse gases (CH_4, CO_2) levels. Higher concentrations of CO result in a decrease of hydroxyl radicals and consequently an increase in retention of the greenhouse gases in the atmosphere (Lu & Khalil, 1993; Lelieveld *et al*., 2004).

Its toxicity aside, CO represents a potent energy (electron) and carbon source for microorganisms. A wide range or microorganisms is capable of metabolizing CO directly from the atmosphere and from the ocean including both aerobes and anaerobes (King, 1999; Zafiriou *et al*., 2003). Anaerobic organism that are capable of metabolizing CO include acetogenic bacteria and sulfate-reducing bacteria (Conrad & Seiler, 1980; King & Weber, 2007; Techtmann *et al*., 2009).

CO metabolizing bacteria are classified as carboxydotrophs and 'carboxydovores'. Most of the carboxydotrophs are found in high-temperature niches. The ability to convert CO is likely a self-protection strategy to reduce toxic concentrations of CO to produce H_2 and CO_2 which can then be used in energy generation. Carboxydotrophs

contain *a*-, *b*- and *c*-type cytochromes and tolerate high concentrations of CO (up to 90%) (Zavarzin & Nozhevnikova, 1977; Meyer & Schlegel, 1978). In contrast to carboxydotrophs, carboxydovores are unable to use CO as a C-source for growth. Higher CO concentrations inhibit growth of some carboxydovores because of their inability to assimilate CO_2. CO is used rather as a supplementary energy source in the latter microorganisms (King & Weber, 2007).

Both aerobic and anaerobic CO metabolizing organisms contain an enzyme, Carbon monoxide Dehydrogenase (CODH), which is essential for CO metabolism. With this enzyme, microorganisms are able to use CO as an energy source and CO_2 as a carbon source (Mörsdorf *et al.*, 1992). In aerobic bacteria, the CODH contains either iron or molybdenum, while the anaerobic CODH contains nickel in its active site (King & Weber, 2007; Oelgeschläger & Rother, 2008). The CODHs are thus classified on the basis of their metallocentre into Mo- and Ni-containing CODHs. They are further subdivided on the basis of their metabolic roles and catalytic activities, with some CODHs being mono-functional, while others are bifunctional (e.g. CODH/acetyl-coenzyme A (-CoA) synthase) (Ferry 1995; Lindahl 2002; Ragsdale 2004). In aerobic bacteria, CODH-catalyzed CO conversion results in the production of biomass and CO_2 (King & Weber, 2007). By contrast, CO metabolism occurs in anaerobic bacteria via several distinct pathways, yielding distinct products.

As such, anaerobic CO-utilizing microorganisms are further classified on the basis of the product resulting from CO oxidation and include acetogens, sulphate-reducing bacteria and methanogens. Acetogens produce acetate via the reductive acetyl-CoA pathway (Wood-Ljungdhal pathway). Hereby, CO_2 is first reduced to CO by a carbon monoxide dehydrogenase, which is then combined with a methyl group to acetyl-CoA. Acetal-CoA is then further converted to acetate (Diekert, 1990). Acetogenic bacteria have gained biotechnological interest as acetate can serve as a precursor for the production of value-added products (e.g. cellulose acetate and polyvinyl acetate (Köpke *et al.*, 2011). However, many acetogens are also capable of producing other

value-added by-products such as ethanol, butyrate or butanol. For example, *Clostridium carboxidovorans* also produces substantial amounts of ethanol, butyrate and butanol during growth on CO (Liou *et al*., 2005).

Sulfate reducing microorganisms (desulfuricants) are frequently isolated from hot springs, soils, natural gas wells, anaerobic sludge and marine sediments (Sipma *et al*., 2006). They are able to use CO to reduce sulfate. Hereby, CO is converted into CO_2 and the reducing equivalents are used to reduce water to H_2. The latter product is then used for sulfate reduction (Sipma *et al*., 2006). *Desulfomonile tiedjei* or *Desulfotomaculum carboxydivorans* and the archaea *Thermoproteus tenax* are well-known examples of carboxydotrophic sulfate reducers (Fischer *et al*., 1983; DeWeerd *et* al., 1990; Parshina *et al*., 2005). In hydrogenotrophic methanogenesis, CO is first oxidized to CO_2 by the CODH. In a second step, CO_2 is reduced by using H_2 as an electron donor (Daniels *et al*., 1977). This metabolic process occurs in a diverse group of Euryarchaeota (Methanobacteriales, Methanococcales, Methanomicrobiales, Methanipyrales and Mehanosarcinales) which inhabit anoxic environments such as white smoker chimneys (Jones *et al*., 1983; Garcia *et al*., 2000).

In addition to acetogens, sulfate-reducing bacteria and methanogens, some bacterial and archaeal taxa have also evolved to couple CO metabolism to the production of hydrogen gas. Due to their ability to undertake the conversion of CO concomitant with the production of H_2, these organisms are designated as hydrogenogens.

1.4.1 CO-metabolism and the WGS reaction

Hydrogenogenic bacteria are capable of oxidizing CO via a Ni-Fe Carbon Monoxide Dehydrogenase (CODH, EC 1.2.7.4, Oxidoreductases) at a complex metal center containing Ni, Fe and S. This is coupled with the reduction of protons to H_2 by a hydrogenase enzyme in the water-gas shift (WGS) reaction: $CO + H_2O \rightleftharpoons CO_2 + H_2$ (ΔG°= -41.2 kj/mol). The WGS reaction occurs in mesophilic and thermophilic bacterial taxa, while it appears to be more prevalent in the latter. This might be explained by the increased gas diffusion rates at higher temperatures (Diender *et al*., 2015).

However, the WGS reaction is a two-step reaction, catalyzed by two enzymes: Carbon Monoxide Dehydrogenase and hydrogenase.

Structure and function of the [NiFe]- Carbon Monoxide Dehydrogenase (CODH) enzyme

The CODH enzyme catalyzes the reaction $CO + H_2O \rightleftharpoons 2e^- + H_2O + CO_2$ during the first step of the WGS reaction. The CODH involved in the WGS reaction contains nickel and is hence a [NiFe]-CODH. In general, [NiFe]-CODH are found in anaerobic bacteria and archaea and do play a role in different energy-yielding pathways (Lindahl, 2002; Ragsdale, 2004). They all contain iron-sulfur center and nickel as a cofactor to ensure binding and coordinating CO in its active side (Dobbek *et al*., 2001). The function and regulation of the CODH is well studied in two organisms, namely the mesophilic photosynthetic bacterium *Rhodospirillum rubrum* and the thermophilic anaerobe *Carboxydothermus hydrogenoformans* (Svetlichny *et al*., 1991; Kerby *et al*., 1995). The mechanism of CO metabolism is similar in both taxa, but unlike *R. rubrum C. hydrogenoformans* is capable of using CO as the sole C-source for growth (Svetlichny *et al*., 1991). In both bacteria, CO metabolism and hydrogenogenesis involves a set of distinct proteins which are coded on several gene cluster. The transcription of the gene cluster *cooFSCTJ* involved in CO oxidation is coupled to the binding of CO to the heme groups of the protein CooA. The gene cluster encodes for active CODH (*cooS*), nickel inserting complex (*cooCTJ*) and the electron carrier (*cooF*). After CO is oxidized, the resulting electrons are transferred to the CooF protein (iron-sulfur protein), which acts as a shuttle to an energy conserving hydrogenase complex (Kerby *et al*., 1995).

Structure and function of the hydrogenase enzyme

During the second step of the WGS reaction a hydrogenase catalyzes the reaction $2H^+ + 2e^- \rightleftharpoons H_2$. Based on their metal content, hydrogenases can be distinguished into [Fe]-, [FeFe] and [NiFe] hydrogenases (Vignais *et al*., 2001). The latter can be classified further into four groups: membrane-associated H_2 uptake hydrogenase (group 1),

soluble uptake and sensory hydrogenases (group 2), heteromultimeric cytoplastic hydrogenases (group 3) and energy converting hydrogenases (group 4). Group 4 is involved in the WGS reaction (Alfano & Cavazza, 2018). Members of the [NiFe]-Group 4a hydrogenases, also called formate hydrogenlyase complex I (FHL-1), are membrane bound, O_2 sensitive and mostly found among the facultatively fermentative Proteobacteria (in particular enterobacteria) (Greening *et al.*, 2016). All [NiFe]- hydrogenases consist of an αβ heterodimer. The larger subunit (α- subunit) carries the bimetallic active site, while the smaller (β- subunit) carries the Fe-S cluster (Greening *et al.*, 2016; Vignais & Billoud, 2007). In *R. rubrum* and *C. hydrogenoformans* the gene cluster *cooMKLXUH* codes for a hydrogenase complex (Svetlichny *et al.*, 1991; Kerby *et al.*, 1997).

Preliminary comparative genomic analysis in our laboratory, identified a locus coding for a [NiFe]-CODH adjacent to genes coding for a [NiFe]-hydrogenase in the thermophilic bacterium *Parageobacillus thermoglucosidasius*. As this bacterium represents the organism of interest in this study, the following section will discuss key aspects of the biology, genetics and biotechnological potential of this bacterium.

1.5 *PARAGEOBACILLUS THERMOGLUCOSIDASIUS*

In 1983, Suzuki *et al*. described *Bacillus thermoglucosidasius* as a new species of obligately thermophile (growth range: 42 °C – 69 °C) in the family *Bacillaceae* and the phylum Firmicutes, which was isolated from soil in Japan, Kyoto. Subsequent molecular and phylogenetic analysis of *B. thermoglucosidasius* led to its reclassification to the genus *Geobacillus* (Nazina *et al.*, 2001). A phylogenomic study has since led to the splitting of the genus *Geobacillus* into the former genus, as well a novel genus *Parageobacillus*, which cluster distinctly in a genome-wide taxonomy and are furthermore, distinguished by a distinct G+C content range of 42.1-44.4% compared to 48.8-53.1% in the genus *Geobacillus* (Aliyu *et al.*, 2016). As a result, *G. thermoglucosidasius* was re-classified to its current taxonomic status, *Parageobacillus*

thermoglucosidasius (Aliyu *et al.*, 2016). *P. thermoglucosidasius* belongs to the family of *Bacillaceae* and have been isolated from a wide range of environmental sources including flax plants, river sediments and hot springs (Gurujeyalakshmi & Oriel, 1988; Valladares Juárez *et al.*, 2009; Brumm *et al.*, 2015).

1.5.1 Insights in metabolic pathways

P. thermoglucosidasius is classified as a heterotroph, utilizing organic compounds as carbon source. Its metabolism is mainly via aerobic respiration but it is capable of mixed acid fermentation in the absence of O_2 as terminal electron acceptor (Hussein *et al.*, 2015). *P. thermoglucosidasius* shows extensive metabolic versatility in that it is able to utilize a broad range of different carbohydrates including mono- and di-saccharides, starch and xylan (De Maayer *et al.*, 2014; Zeigler, 2014; Daas *et al.*, 2016).

It has been noted that, although the organism is a facultative anaerobe, *P. thermoglucosidasius* requires small amounts of O_2. The supplied amounts of O_2 is not required for the central metabolism, but to ensure that some of the cell processes, that requires O_2, are still active. For example, the production of thiamine (vitamin B1) by *P. thermoglucosidasius* requires O_2 (Hussein *et al.*, 2015).

Central metabolism of carbohydrates involves three pathways, the Embden-Meyerhof-Parnas (EMP) pathway, oxidative pentose phosphate pathway and the tricarboxylic acid (TCA) cycle (Tang *et al.*, 2008; Hussein *et al.*, 2015). Via the EMP pathway, which does not require any O_2, glucose is converted through several series of reactions to two molecules of pyruvate. During this pathway ATP and NADH are produced (1 molecule of glucose result in two molecules of pyruvate, ATP and NADH (Stettner & Segrè, 2013). The pentose phosphate pathway can serve as an alternative glucose pathway with the aim of producing NADPH for reductive biosynthetic reactions such as fatty acid synthesis. The six carbons sugar glucose is converted to the five carbon sugar ribose-5-phosphate, which is essential for pyrimidine and purine nucleotide biosynthesis (Krueger & von Schaewen, 2003). During one turn of the TCA cycle, three NADH, one $FADH_2$ and one ATP (or GTP) are produced and two CO_2

molecules released. In the absence of O_2, *P. thermoglucosidasius* undertakes mixed acid fermentation, hereby producing acetate, formate, lactate, succinate and ethanol (Cripps *et al*., 2009). The production of the latter, particularly from renewable biomass sources such as xylan, has led to increased interest in *P. thermoglucosidasius* for the production of first- and second-generation fuels. Additionally, due to its thermophilic nature and its metabolic versatility, this organism can be useful for a broad range of biotechnological applications (Hussein *et al.*, 2015).

1.5.2 Applications in Biotechnology

The thermophilic nature and metabolic versatility of *P. thermoglucosidasius* make it an ideal candidate for implementation in a broad range of biotechnological applications (Hussein *et al*., 2015). Thermophiles produce thermostable enzymes which have adapted through key changes in amino acids (Reed *et al.*, 2013). These extremozymes are characterized by higher activity and efficiency under high temperatures and extreme pH values compared to their mesophilic counterparts and are thus applicable in high temperature industrial processes. Higher temperature in industrial applications are also less prone to contamination. Furthermore, there has been increased interest in the use of *P. thermoglucosidasius* in different industrial approaches. As this organism is capable of biosorption of heavy metals, it can e.g. desulfurize sulfur-containing compounds in oil (Peng *et al*., 2019). In the textile industry, *P. thermoglucosidasius* can find application to produce finer fibers by reduction of the pectin content of the fibers (Valladares Juárez *et al*., 2009). *P. thermoglucosidasius* has been used to generate large amounts of ethanol, for instance it has been demonstrated that a genetic engineered strain of *P. thermoglucosidasius* (DSM TM242) was able to produce ethanol with 90% of the theoretical yield (Cripps *et al*., 2009). Furthermore, a recombinant *P. thermoglucosidasius* strain successfully produced isobutanol from cellobiose (Lin *et al*. 2014).

1.6 RESEARCH PROPOSAL

At present, the global energy demand is largely met through the use of fossil fuels. As fossil fuel supplies are dwindling and their use has a negative effect on the air quality and climate change, there is an urgent need for the development of environmentally friendly and sustainable energy strategies. H_2, which usage results in zero carbon emission, may serve as an environmentally friendly energy alternative. However, its use is largely hampered by a lack of cost-effective and sustainable production processes, and there is a thus a need for research in the field of biological H_2 production.

The facultatively anaerobic thermophilic bacterium *Parageobacillus thermoglucosidasius* carries the genetic complement coding for enzymes involved in the water-gas shift (WGS) reaction ($CO + H_2O \rightleftharpoons CO_2 + H_2$). This capacity has to date only been described in anaerobic bacteria, and as such, *P. thermoglucosidasius* may serve as an advantageous biological agent for H_2 production

The aim of this thesis was to characterize and optimize the hydrogenogenic potential of *P. thermoglucosidasius*. This was addressed through the following objectives:

- Analysis of the hydrogenogenic capacity of *P. thermoglucosidasius* and evolutionary analysis of this unique feature (Chapter 2).
- Evaluation of distinct *P. thermoglucosidasius* strains for their capacity to produce H_2 via the WGS reaction (Chapter 3).
- Possible application in industry as a biological cleaning tool for waste gas (Chapter 4).
- Process optimization by evaluating the effects of different process parameters on H_2 yield and production rate (Chapter 5).

REFERENCES FOR CHAPTER 1

Aliyu H, Lebre P, Blom J, Cowan D, De Maayer P (2016) Phylogenomic re-assessment of the thermophilic genus *Geobacillus*. *Systematic and Applied Microbiology*. **39(8):**527-533. DOI:10.1016/j.syapm.2016.09.004.

Albright L, Crynes B, Corcoran W, Pyrolysis: Theorie and Industrial Practice (Eds.: Albright L, Crynes B, Corcoran W) Academic Press, New York 1983.

Alfano A, Cavazza C (2018) The biologically mediated water-gas shift reaction: structure, function and biosynthesis of monofunctional [NiFe]- carbon monoxide dehydrogenase. *Sustainable Energy & Fuels*. **2**:1653-1670. DOI:10.1039/C8SE00085A.

Blumenthal I (2001) Carbon monoxide poisoning. *Journal of the Royal Society of Medicine*. **94(6)**:270-272.

BP (2016). Statistical Review of World Energy 2016. 68th edition.

Brumm PJ, Land ML, Mead DA (2015) Complete genome sequence of *Geobacillus thermoglucosidasius* C56-YS93, a novel biomass degrader isolated from obsidian hot spring in Yellowstone National Park. *Standards in Genomic Science*. **10(73)**:73. DOI:10.1186/s40793-015-0031-z.

Chen SD, Lee KS, Lo YC, Chen WM, Wu JF, Lin CY, Chang JS (2008) Batch and continuous bio-hydrogen production from starch hydrolysate by *Clostridium* species. *International Journal of Hydrogen Energy*. **33**:3289-3294. DOI:10.1016/j.ijhydene.2008.01.028.

Conrad R, Seiler W (1980) Role of microorganism in the consumption and production of atmospheric carbon monoxide by soil. *Applied Environmental Microbiology*. **40**:437-445.

Cripps RE, Eley K, Leak DJ, Taylor M, Todd M, Boakes S, Martin S, Atkinson T (2009) Metabolic engineering of *Geobacillus thermoglucosidasius* for high yield ethanol production. *Metabolic Engineering*, **11**: 398-408. DOI:10.1016/j.ymben.2009.08.005.

Daas MJA, van de Weijer AHP, de Vos WM, van der Oost J, van Kranenburg R (2016) Isolation of a genetically accessible thermophilic xylan degrading bacterium from compost. *Biotechnology for Biofuels*. **9**:210. DOI:10.1186/s13068-016-0618-7.

Daniels L, Fuchs G, Thauer RK, Zeikus JG (1977) Carbon monoxide oxidation by methanogenic bacteria. *Journal of Bacteriology*. **132**:118–126.

Das D, Veziroğlu TN (2001) Hydrogen production by biological processes: a survey of literature. *International Journal of Hydrogen Energy*. **26**:13-28. DOI:10.1016/S0360-3199(00)00058-6.

De Maayer P, Brumm PJ, Mead DA, Cowan DA (2014) Comparative analysis of the *Geobacillus* hemicellulose utilization locus reveals a highly variable target for improved hemicellulolysis. *BMC Genomics*. **15**:836. DOI:10.1186/1471-2164-15-836.

DeWeerd KA, Mandelco L, Tanner RS, Woese CR, Suflita JM (1990) *Desulfomonile tiedjei* gen. nov. and sp. nov., a novel anaerobic, dehalogenating, sulfate-reducing bacterium". *Archives of Microbiology*. **154(1)**:22-30. DOI:10.1007/BF00249173.

Diekert G (1990) CO_2 reduction to acetate in anaerobic bacteria. *FEMS Microbiology Review*. **87**:391-396. DOI:10.1016/0378-1097(90)90484-8.

Diender M, Stams AJM, Sousa DZ (2015) Pathways and Bioenergetics of Anaerobic Carbon Monoxide Fermentation. *Frontiers in Microbiology*. **6**:1275. DOI:10.3389/fmicb.2015.01275.

Dobbek H, Svetlitchnyi V Gremer L, Huber R, Meyer O (2001) Crystal structure of a carbon monoxide dehydrogenase reveals a [Ni-4Fe-5S] cluster. *Science*. **293**:1281–1285. DOI:10.1126/science.1061500.

Ebbesen SD, Mogensen M (2009) Electrlysis of carbon dioxid in Solid Oxide Electrolysis cells. *Journal of Power Sources*. **193(1)**:349-358. DOI:10.1016/j.jpowsour.2009.02.093.

Ellabban O, Abu-Rub H, Blaabjerg F (2014) Renewable energy resources: Current status, future prospects and their enabling technology. *Renewable and Sustainable Energy*, **39**:748-764. DOI:10.1016/j.rser.2014.07.113.

Engel RR, Matsen JM, Chapman SS, Schwartz S (1972) Carbon monoxide production from heme compounds by bacteria. *American Society for Microbiology*. **112(3)**: 1310-1315.

Fabiano B, Perego P (2002) Thermodynamic study and optimization of hydrogen production by *Enterobacter aerogenes*. *International Journal of hydrogen Energy*. **27**:149-156. DOI:10.1016/S0360-3199(01)00102-1.

Ferry JG (1995) CO dehydrogenase. *The Annual Review of Microbiology*. **49**:305–333. DOI:10.1146/annurev.mi.49.100195.001513.

Fischer F, Zillig W, Stetter KO, Schreiber G (1983) Chemolithoautotrophic metabolism of anaerobic extremly thermophilic archaebacteria. *Nature*. **301**:511–513. DOI:10.1371/journal.pone.0024222.

Flachsbart PG (1999) Human exposure to carbon monoxide from mobile sources. *Chemosphere – Global Change Science*. **1**: 301-329). DOI:10.1016/S1465-9972(99)00030-6.

Garcia JL, Patel BK, Ollivier B (2000) Taxonomic, phylogenetic, and ecological diversity of methanogenic Archaea. *Anaerobe*. **6**:205–226. DOI:10.1006/anae.2000.0345.

Ghimire A, Frunzo L, Pirozzi F, Trably E, Escudie R, Lens PNL, Esposito G (2015) A review on darf fermentative biohydrogen production from organic biomass: Process parameters and use of by-products. *Applied Energy*. **144**:73-95. DOI:10.1016/j.apenergy.2015.01.045.

Greening C, Biswas A, Carere CR, Jackson CJ, Taylor MC, Stott MB, Cook GM, Morales SE (2016) Genomic and metagenomic surveys of hydrogenase distribution indicate H_2 is a widely utilised energy source for microbial growth and survival. *ISME Journal*. **10(3)**:761-77. DOI:10.1038/ismej.2015.153.

Gurujeyalakshmi G, Oriel P (1988) Isolation of Phenol-Degrading *Bacillus stearothermophilus* and Partial Characterization of the Phenol Hydroxylase. *Applied and Environmental Microbiology*. **55(2)**:500-502.

Hallenbeck PC, Benemann JR (2002) Biological hydrogen production; fundamental and limiting processes. *International Journal of Hydrogen Energy*. **27**:1185-1193. DOI:10.1016/S0360-3199(02)00131-3.

Hino S, Tauchi H (1987) Production of carbon monoxide from aromatic amino acid by *Morganella morganii*. *Archieves of Microbiology*. **148(3)**:167-171. DOI:10.1007/BF00414807.

Hussein AH, Lisowska BK, Leak DJ (2015) The Genus *Geobacillus* and their biotechnological potential. *Advances in Applied Microbiology*. **92**:1-48. DOI:10.1016/bs.aambs.2015.03.001.

Jeoung JH, Fesseler J, Goetzl S, Dobbek H (2014) Carbon Monoxide. Toxic Gas and Fuel for Anaerobes and Aerobes: Carbon Monoxide Dehydrogenase. *Metal ions in life science.* **14**:37-69. DOI:10.1007/978-94-017-9269-1_3.

Jones WJ, Leigh JA, Mayer F, Woese CR, Wolfe RS (1983) *Methanococcus jannaschii* sp. nov., an extremely thermophilic methanogen from a submarine hydrothermal vent. *Archives Microbiology*. **136**:254–261. DOI:10.1007/BF00425213.

Kanai T, Imanaka H, Nakajima A, Uwamori K, Omori Y, Fukui T, Atomi H, Imanaka T (2005) Continuous hydrogen production by the hyperthermophilic archaeon, *Thermococcus kodakaraensis* KOD1. *Journal of Biotechnology*. **116(3)**:271-282. DOI:10.1016/j.jbiotec.2004.11.002.

Kapdan IK, Kargi F (2006) Bio-hydrogen production from waste materials. *Enzyme and Microbial Technology.* **38**:569–82. DOI:10.1016/j.enzmictec.2005.09.015.

Kerby R, Ludden P, Roberts G (1995) Carbon monoxide-dependent growth of *Rhodospirillum rubrum*. *Journal of Bacteriology*. **177**:2241-2244. DOI:10.1128/jb.177.8.2241-2244.1995.

Kerby R, Ludden P, Roberts G (1997) In vivo nickel insertion into the carbon monoxide dehydrogenase of *Rhodospirillum rubrum*: molecular and physiological characterization of cooCTJ. *Journal of Bacteriology*. **179**:2259-2266. DOI:10.1128/jb.179.7.2259-2266.1997.

King GM (1999) Characteristics and significance of atmospheric carbon monoxide consumption by soils. *Chemosphere*. **1**:53–63. DOI:10.1016/S1465-9972(99)00021-5.

King GM, Weber CF (2007) Distribution, diversity and ecology of aerobic CO-oxidizing bacteria. *Nature Reviews Microbiology*. **5**:107–118. DOI:1 0.1038/nrmicro1595.

Köpke M, Mihalcea C, Liew F, Tizard JH, Ali MS, Conolly JJ, Al- Sinawi B, Simpson SD (2011) 2,3-Butanediol production by acetogenic bacteria, an alternative route to chemical synthesis using industrial waste gas. *Applied Environmental Microbiology*. **77**:5467-5475. DOI:10.1128/AEM.00355-11.

Kotay SM, Das D (2008) Biohydrogen as renewable energy resource – Prospects and potentials. *International Journal of Hydrogen Energy*. **33(1)**:258-263. DOI: 10.1016/j.ijhydene.2007.07.031.

Krueger NJ, von Schaewen A (2003) The oxidative pentose phosphate pathway: structure and organization. *Current Opinion in Plant Biology*. **6(3)**:236-246. DOI:10.1016/S1369-5266(03)00039-6.

Lelieveld J, Dentener FJ, Peters W, Krol MC (2004) On the role of hydroxyl radicals in the self-cleansing capacity of the troposphere. *Atmospheric Chemistry and Physics*. **4**:2337-2344. DOI:10.5194/acp-4-2337-2004.

Levin DB, Pitt L, Love M (2004) Biohydrogen production: prospects and limitations to practical application. *International Journal of Hydrogen Energy*, **29**:173–85. DOI:10.1016/S0360-3199(03)00094-6.

Li C, Fang HHP (2007a) Fermentative hydrogen production from wastewater and solid wastes by mixed cultures. *Critical Reviews in Environmental Science and Technology*. **37(1)**:1-39. DOI:10.1080/10643380600729071.

Lin PP, Rabe KS, Takasumi JL, Kadisch M, Arnold FH, Liao JC (2014) Isobutanol production at elevated temperatures in thermophilic *Geobacillus thermoglucosidasius*. *Metabolic Engineering*. **24**:1-8. DOI:10.1016/j.ymben.2014.03.006.

Lindahl PA (2002) The Ni-containing carbon monoxide dehydroge- nase family: light at the end of the tunnel? *Biochemistry*. **41**:2097–2105. DOI:10.1021/bi015932+.

Liou JS, Balkwill DL, Drake GR, Tanner RS (2005) *Clostridium carboxidivorans* sp. nov., a solvent-producing clostridium iso- lated from an agricultural settling lagoon, and reclassification of the acetogen *Clostridium scatologenes* strain SL1 as *Clostridium drakei* sp. nov. *International Journal of Systematic and Evolutionary Microbiology*. 55:2085–2091. DOI:10.1099/ijs.0.63482-0.

Lu Y, Khalil MAK (1993). Methane and carbon monoxide in OH chemistry: the effects of feedbacks and reservoirs generated by the reactive products. *Chemosphere*. **26**:641–655. DOI:10.1016/0045-6535(93)90450-J.

Marbán G, Valdés-Solís T (2007) Towards the hydrogen economy? *Science Direct*. **32**:1625-1637. DOI:10.1016/j.ijhydene.2006.12.017.

Meyer O, Schlegel HG (1978) Reisolation of the carbon monoxide utilizing hydrogen bacterium *Pseudomonas carboxydovorans* (Kistner) comb. nov. *Archieves of Microbiology*. **118**:35–43.

Mörsdorf G, Frunzke K, Gadkari D, Meyer O (1992) Microbial growth on carbon monoxide. *Biodegradation* **3**:61–82.

Nagarajan D, Lee DJ, Kondo A, Chang JS (2016) Recent insights into biohydrogen production by microalgae – From biophotolysis to dark fermentation. *Bioresource Technology*. **227**:373-387. DOI:10.1016/j.biortech.2016.12.104.

Nath K, Das D (2004) Biohydrogen production as a potential energy resource- Present state-of-art. *Journal of Scientific & Industrial Research*. **63**:729-738.

Nazina TN, Tourova TP, Poltaraus AB, Novikova EV, Grigoryan AA, Ivanova AE, Lysenko AM, Petrunyaka VV, Osipov GA, Belyaev SS, Ivanov MV (2001) Taxonomic study of aerobic thermophilic bacilli: descriptions of *Geobacillus subterraneus* gen. nov., sp. nov. and *Geobacillus uzenensis* sp. nov. from petroleum reservoirs and transfer of *Bacillus stearothermophilus, Bacillus thermocatenulatus, Bacillus thermoleovorans, Bacillus kaustophilus, Bacillus thermoglucosidasius* and *Bacillus thermodenitrificans* to *Geobacillus* as the new combinations *G. stearothermophilus, G. thermocatenulatus, G. thermoleovorans, G. kaustophilus, G. thermoglucosidasius* and *G. thermodenitrificans*. *International Journal of Systematic and Evolutionary Microbiology*. **51**:433-446.

Ni M, Leung DYC, Leung MKH, Sumathy K (2006) An overview of hydrogen production from biomass. *Fuel Processing Technology*. **87**:461-472. DOI:10.1016/j.fuproc.2005.11.003.

Nikolaidis P, Poullikkas A (2017) A comparative overview of hydrogen production processes. *Renewable & Sustainable Energy Reviews*. **67**:597–611. DOI:10.1016/j.abb.2004.08.032.

Odgen JM (1999) Prospects for Building A Hydrogen Energy Infrastructure. *Annual Review of Energy and The Environment*. **24**:227-279. DOI:10.1146/annurev.energy.24.1.227.

Oelgeschläger, E, Rother, M (2008) Carbon monoxide-dependent energy metabolism in anaerobic bacteria and archaea. *Archives of Microbiology*. **190**:257–269. DOI:0.1007/s00203-008-0382-6.

Parshina SN, Sipma J, Nakashimada Y, Henstra AM, Smidt H, Lysenko AM, Lens PN, Lettinga G, Stams AJ (2005) *Desulfotomaculum carboxydivorans* sp. nov., a novel sulfate-reducing bacterium capable of growth at 100% CO. *International Journal of Systematic and Evolutionary Microbiology*. **55**:2159-2165. DOI:10.1099/ijs.0.63780-0.

Peng C, Huang D, Shi Y, Zhang B, Sun L, Li M, Deng X, Wang W (2019) Comparative transcriptomic analysis revealed the key pathways responsible for organic sulfur

removal by thermophilic bacterium *Geobacillus thermoglucosidasius* W-2. *Science of the total Environment*. **676**:639-650. DOI:10.1016/j.scitotenv.2019.04.328.

Philip EA, Clark OG, Londry K, Yu Steven, Leonard J (2013) *Compost science & utilization*. **19(3)**:170-177. DOI:10.1080/1065657X.2011.10736996.

Preuster P, Alekseev A, Wasserscheid P (2017) Hydrogen Storage Technologies for Future Energy Systems. *Annual Review of Chemical and Biomolecular Engineering*. **8**:445-471. DOI:10.1146/annurev-chembioeng-060816-101334.

Ragsdale SW (2004) Life with carbon monoxide. *Critical Reviews in Biochemistry and Molecular Biology*. **39**:165–195. DOI:10.1080/10409230490496577.

Rahman SNA, Msdar MS, Rosli MI, Majlan EH, Husaini T, Kamarudin SK, Daud WRW (2016) Overview of biohydrogen technologies and application in fuel cell technology. *Renewable & Sustainable Energy Reviews*. **66**:137-162. DOI:10.1016/j.rser.2016.07.047.

Ramachandran R, Menon RK (1998) An overview of industrial uses of hydrogen. *International Journal of Hydrogen Energy*. **23(7)**:593-598. DOI:10.1016/S0360-3199(97)00112-2.

Reed CJ, Lewis H, Trejo E, Winston V, Evilia C (2013) Protein adaption in archeael extremophiles. *Archaea*. 373275. DOI:10.1155/2013/373275.

Reimert R, Marschner F, Renner HJ, Boll W, Supp E, Brejc M, Liebner W, Schaub G (2011) Gas production, 2. Processes. *Ullmann's Encyclopedia of Industrial Chemistry*, Wiley-VCH, Weinheim. DOI:10.1002/14356007.o12_o01.

Schmidt U, Conrad R, (1993) Hydrogen, carbon monoxide, and methane dynamics in Lake Constance. *Limnology and Oceanography*, **38**:1214–1226. DOI:10.4319/lo.1993.38.6.1214.

Sharma S, Ghoshal SK (2014) Hydrogen the future transportation fuel: From production to applications. *Renewable and Sustainable Energy Review*. **43**:1151-1158. DOI:10.1016/j.rser.2014.11.093.

Schneider SH (1989) The Greenhouse Effect: Science and Policy. *Science*. **243(4892)**:771-781. DOI:10.1126/science.243.4892.771.

Sipma J, Henstra AM, Parshina SM, Lens PN, Lettinga G, Stams AJ (2006) Microbial CO conversions with applications in synthesis gas purification and bio-desulfurization. *Critical Reviews in Biotechnology*. **26**:41–65. DOI:10.1080/07388550500513974.

Sørensen B, Spazzafumo G (2011) Hydrogen and Fuel Cells. *Emerging Technologies and Application*. DOI:10.1016/C2009-0-63881-2.

Srirangan K, Akawi L, Moo-Young M, Chou CP (2012) Towards sustainable production of clean energy carriers from biomass resources. *Applied Energy*, **100**:172-186. DOI:10.1016/j.apenergy.2012.05.012.

Stettner AI, Segrè D (2013) The cost of efficiency in energy metabolism. *PNAS*. **110(24)**:9629-9630. DOI:10.1073/pnas.1307485110.

Svetlichny V, Sokolova T, Gerhardt M, Ringpfeil M, Kostrikina N (1991) *Carboxydothermus hydrogenoformans* gen. nov., sp. nov., a CO-utilizing thermophilic anaerobic bacterium from hydrothermal environments of Kunashir Island. *Systematic and Applied Microbiology*. **14**:254-260. DOI:10.1016/S0723-2020(11)80377-2.

Suzuki Y, Kishigami T, Inoue K, Mizoguchi Y, Eto N, Takagi M, Abe S (1983) *Bacillus thermoglucosidasius* sp. nov., a New Species of Obligately Thermophilic Bacilli. *Systematic and Applied Microbiology*. **4**:487-495. DOI:10.1016/S0723-2020(83)80006-X.

Tang YJ, Sapra R, Joyner D, Hazen TC, Myers S, Reichmuth D, Blanch H, Keasling JD (2008) Analysis of metabolic pathways and fluxes in a newly discovered thermophilic and ethanol-tolerant *Geobacillus* strain. *Biotechnology and Bioengineering*. **102(5)**:1283-1525. DOI:10.1002/bit.22181.

Taylor, JA, Zimmerman, PR, Erickson III, DJ (1996) A 3-D modeling study of the sources and sinks of atmospheric carbon monoxide. *Ecological Modelling*, **88**:53–71. DOI:10.1016/0304-3800(95)00069-0.

Techtmann SM, Colman AS, Robb FT (2009) 'That which does not kill us only makes us stronger': the role of carbon monoxide in thermophilic microbial consortia. *Environmental Microbiology*. **11**:1027–1037. DOI:10.1111/j.1462-2920.2009.01865.

Timm B (1963) 50 Jahre Ammoniak-Synthese. *Chemie Ingenieur Technik*. **35**(12):817-823. DOI:10.1002/cite.330351202.

Valladares Juárez AG, Dreyer J, Göpel PK, Kosche N, Frank D, Märkl H, Müller R (2009) Characterisation of a new hermoalkaliphilic bacterium for the production of high-quality hemp fibres, *Geobacillus thermoglucosidasius* strain PB94A. *Applied Microbiology and Biotechnology.* **83(3)**:521-527.

Vignais PM, Billoud B, Meyer J (2001) Classification and phylogeny of hydrogenases. *FEMS Microbiology Reviews*. **25**:455–501. DOI:10.1111/j.1574-6976.2001.tb00587.x

Vignais PM, Billoud B (2007) Occurrence, classification, and biological function of hydrogenases: an overview. *Chemical Reviews*. **107**:4206–72. DOI:10.1038/ismej.2015.153.

Yu J, Takahashi P (2007) Biophotolysis-based hydrogen production by cyanobacteria and green microalgae. *Communicating Current Research and Educational Topics and Trends in Applied Microbiology*. **1**:79–89.

Zafiriou OC, Andrews SS, Wang W (2003) Concordant estimates of oceanic carbon monoxide source and sink processes in the Pacific yield a balanced global 'blue- water' CO budget. *Global Biogeochemical Cycles*. **17**:1–13. DOI:10.1029/2001GB001638.

Zavarazin GA, Nozhevnikova AN (1977) Aerobic carboxydobacteria. *Microbial Ecology*. **3**:305-326. DOI:10.1007/BF02010738.

Zeigler DR (2014) The Geobacillus paradox: why is a thermophilic bacterial genus so prevalent on a mesophilic planet? *Microbiology*. **160**:1-11. DOI:10.1099/mic.0.071696-0.

Zeng K, Zhang D (2010) Recent progress in alkaline water electrolysis for hydrogen production and application. *Progress in Energy and Combustion Science*. **36**:307-326. DOI:10.1016/j.pecs.2009.11.002.

Zhang T, Liu H, Fang HHP (2003) Biohydrogen production from starch in wastewater under thermophilic conditions. *Journal of Environmental Management*. **69(2)**:149-156. DOI:10.1016/S0301-4797(03)00141-5.

World Energy Outlook 2018 (www.iae.org) accessed on 04/04/2018.

2 CO-DEPENDENT HYDROGEN PRODUCTION BY *PARAGEOBACILLUS THERMOGLUCOSIDASIUS*

This chapter is partially based on the publication

CO-DEPENDENT HYDROGEN PRODUCTION BY THE FACULTATIVE ANAEROBE *PARAGEOBACILLUS THERMOGLUCOSIDASIUS*.

Teresa Mohr, Habibu Aliyu, Raphael Küchlin, Shamara Polliak, Michaela Zwick, Anke Neumann, Don Cowan, Pieter de Maayer

Microbial Cell Factories

Volume 17, Article 108

Published: July 9, 2018

DOI: 10.1186/s12934-018-0954-3

https://microbialcellfactories.biomedcentral.com/articles/10.1186/s12934-018-0954-3

Authors' contribution to this publication

Teresa Mohr designed the experiments together with Pieter de Maayer and Anke Neumann and performed the cultivation with Raphael Küchlin and Michaela Zwick. The genomic analysis was performed together with Habibu Aliyu and Pieter de Maayer. Drafted the manuscript.

Habibu Aliyu performed genomic analysis and drafted the manuscript.

Raphael Küchlin and **Michaela Zwick** assisted during the cultivation experiments.

Shamara Polliack performed parts of the genomic analysis.

Anke Neumann contributed to the conception of the experiments.

Don Cowan contributed to the manuscript concept.

Pieter de Maayer supervised the project, performed genomic analysis and drafted the manuscript.

2.1 INTRODUCTION AND ABSTRACT

The facultatively anaerobic thermophile *Parageobacillus thermoglucosidasius* is frequently isolated from a range of high temperature environments (Zeigler, 2014). Due to its thermophilic nature, this bacterium has been of extensive biotechnological interest for the production of industrially relevant thermostable enzymes (e.g. lipases and proteases), value-added chemicals and as whole cell biocatalyst in a range of bioindustrial processes (Shahinyan *et al*., 2017; Thebti *et al*., 2016).

This chapter describes the analysis of the hydrogenogenic capacity of the facultative anaerobe *P. thermoglucosidasius* DSM 2542^T grown in 250 ml serum bottles with an initial gas atmosphere of CO and air (50:50 ratio). This organism showed the ability to grow at elevated CO concentrations and the capability to produce H_2 at an equimolar conversion (final yield: 1.08 ± 0.07 H_2/CO). Comparative genomics showed that *P. thermoglucosidasius* encodes two evolutionary distinct H_2-uptake [Ni-Fe]-hydrogenases and one H_2-evolving hydrogenase. Additionally, the genes encoding an anaerobic CO dehydrogenase (CODH) are co-localized with genes encoding a putative H_2-evolving hydrogenase. The co-localization of the CODH and the uptake hydrogenase form an enzyme complex that might potentially be involved in catalyzing the water-gas shift reaction in *P. thermoglucosidasius*. Furthermore, evolutionary analysis showed that this combination of hydrogenases is unique to *P. thermoglucosidasius* and suggests that H_2 plays a pivotal in the bioenergetics of this organism. This highlights the potential of the facultative anaerobic *P. thermoglucosidasius* DSM 2542^T for developing new strategies for the biohydrogen production.

2.2 MATERIALS AND METHODS

2.2.1 Microorganisms

The production of H_2 by *P. thermoglucosidasius* when grown in the presence of CO was tested using *P. thermoglucosidasius* DSM 2542^T. Two related strains, *Geobacillus thermodenitrificans* DSM 465^T and *P. toebii* DSM 14590^T, which lack orthologues of the three hydrogenase loci as well as the CODH locus, were included as controls. All strains were obtained from the DSMZ (Deutsche Sammlung von Mikroorganismen und Zellkulturen GmbH, Braunschweig, Germany).

2.2.2 Culture conditions and media

Pre-cultures and cultures were grown aerobically in mLB (modified Luria-Bertani) medium containing tryptone (1% w/v), yeast extract (0.5% w/v), NaCl (0.5% w/v), 1.25 ml/liter NaOH (10% w/v), and 1 ml/liter of each of the filter-sterilized stock solutions: 1.05 M nitrilotriacetic acid, 0.59 M $MgSO_4.7H_2O$, 0.91 M $CaCl_2.2H_2O$ and 0.04 M $FeSO_4.7H_2O$ (Zeigler, 2001). The first pre-culture was inoculated from glycerol stock (20 µl in 20 ml mLB) and cultivated for 24 h at 60 °C and rotation at 120 rpm in an Infors Thermotron (Infors AG, Bottmingen, Switzerland). A second pre-culture was inoculated from the first one to an OD_{600} of 0.1 and incubated as above for 12 h. For the experiments, 250 ml serum bottles were prepared with 49 ml mLB and a gas phase of 50% CO and 50% atmospheric air at 1 bar atmospheric pressure, which were inoculated with 1 ml from the second pre-culture. The experiments were conducted in quadruplicate for a total duration of 84 h.

2.2.3 Analytical methods

Samples were taken at different time points during the experimental procedure. Before and after the sampling the pressure was measured using a manometer (GDH 14 AN, Greisinger electronic, Regenstauf, Germany). To monitor the growth of the cultures, 1 ml of the culture was aspirated through the stopper and

absorbance was measured at OD_{600} using an Ultrospec 1100 pro spectrophotometer (Amersham Biosciences, USA). The determination of the gas compositions at different time points was conducted using a 3000 Micro GC gas analyzer (Inficon, Bad Ragaz, Switzerland) with the columns Molsieve and PLOT Q. A total of 3 ml was sampled from the head space and injected into the GC. A constant temperature of 80 °C was maintained during the total analysis time of 180 s. The gas compositions at the different sampling points were calculated using the following formulas.

For calculation of the gas composition, the ideal gas law was used:

$n = P * V / R * T$

Where n = number of mols of gas; P = pressure of gas (1.013 bar + gas mixture over/under-pressure (p) * 10^5); V = volume of the gas (Start V - number of ml removed prior to each GC measurement); R = universal gas constant (8.314 $J*Kelvin^{-1} * mol^{-1}$ or $kg * m^2sec^{-2}mol^{-1}Kelvin^{-1}$); T = growth temperature of cells (333.15 K (60 °C))

The formula for calculation of the gas amount was thus:

$n_{TOTAL} = (1.013 + p) * 10^2 * V / 2769.8091$

Due to the fact that water could be present in the gas phase at 60 °C, the number of moles of water must be subtracted from the number of moles of the total gas:

$C_{H2O} = 130\ mg * L^{-3}$

$m_{H2O} = C * V$ (in mg)

$n_{H2O} = m / Mr$

$n_{GAS} = n_{TOTAL} - n_{H2O}$

This was used for the final gas concentration formula of:

E.g. for H_2: $n_{H2} = n_{GAS}$ * GC % of H_2 (or mol % of H_2) /100

2.2.4 Comparative genomic analyses

The large hydrogenase subunits were identified from the annotated genome of *P. thermoglucosidasius* DSM 2542^T (CP012712.1) by comparison against the Hydrogenase DataBase (HyDB) (Søndergaard *et al.*, 2016). The full hydrogenase loci were identified by searching the genome up- and downstream of the large subunit gene, extracted and mapped against the genome using the CGView server (Grant *et al.*, 2008). The proteins encoded on the genome were compared by BlastP against the NCBI non-redundant (nr) protein database to identify orthologous loci. Full loci were extracted from the comparator genomes and all loci were structurally annotated using Genemark.hmm prokaryotic v.2 (Besemer *et al.*, 2001). The resultant protein datasets were compared by local BlastP with Bioedit v 7.2.5 (Hall *et al.*, 1999) to identify orthologues, where orthology was assumed for those proteins sharing > 30% amino acid identity over 70% sequence coverage.

A Maximum Likelihood (ML) phylogeny was constructed based on the amino acid sequences of three commonly used housekeeping markers: translation initiation factor IF-2 (InfB), DNA recombination and repair protein RecN RNA polymerase subunit B (RpoB). The proteins were individually aligned using M-Coffee (Wallace *et al.*, 2006), the alignments concatenated and poorly aligned regions were trimmed using Gblocks (Talavera *et al.*, 2007). Finally, the trimmed alignment was used to generate a ML phylogeny using PhyML-SMS, using the optimal amino acid substitution model as predicted by the Smart Model Selection tool (Guindon & Gascuel, 2003; Lefort *et al.*, 2017). Similarly, ML phylogenies were constructed on the basis of the concatenated orthologous proteins encoded on the Pha, Phb, Phc and CODH loci.

2.3 RESULTS

2.3.1 The genome of *P. thermoglucosidasius* encodes three distinct hydrogenases

Analysis of the complete, annotated genome sequence of *P. thermoglucosidasius* DSM 2542^T showed the presence of three putative [Ni-Fe]-hydrogenase loci on the chromosome. Two of these hydrogenases are encoded on the forward strand, while the third is located on the reverse strand (Figure 5). Given the convoluted nomenclature of hydrogenase genes, we have termed these loci as ***P****arageobacillus* **h**ydrogenase **a**, **b** and **c**, in accordance with their chromosomal locations), to distinguish between them.

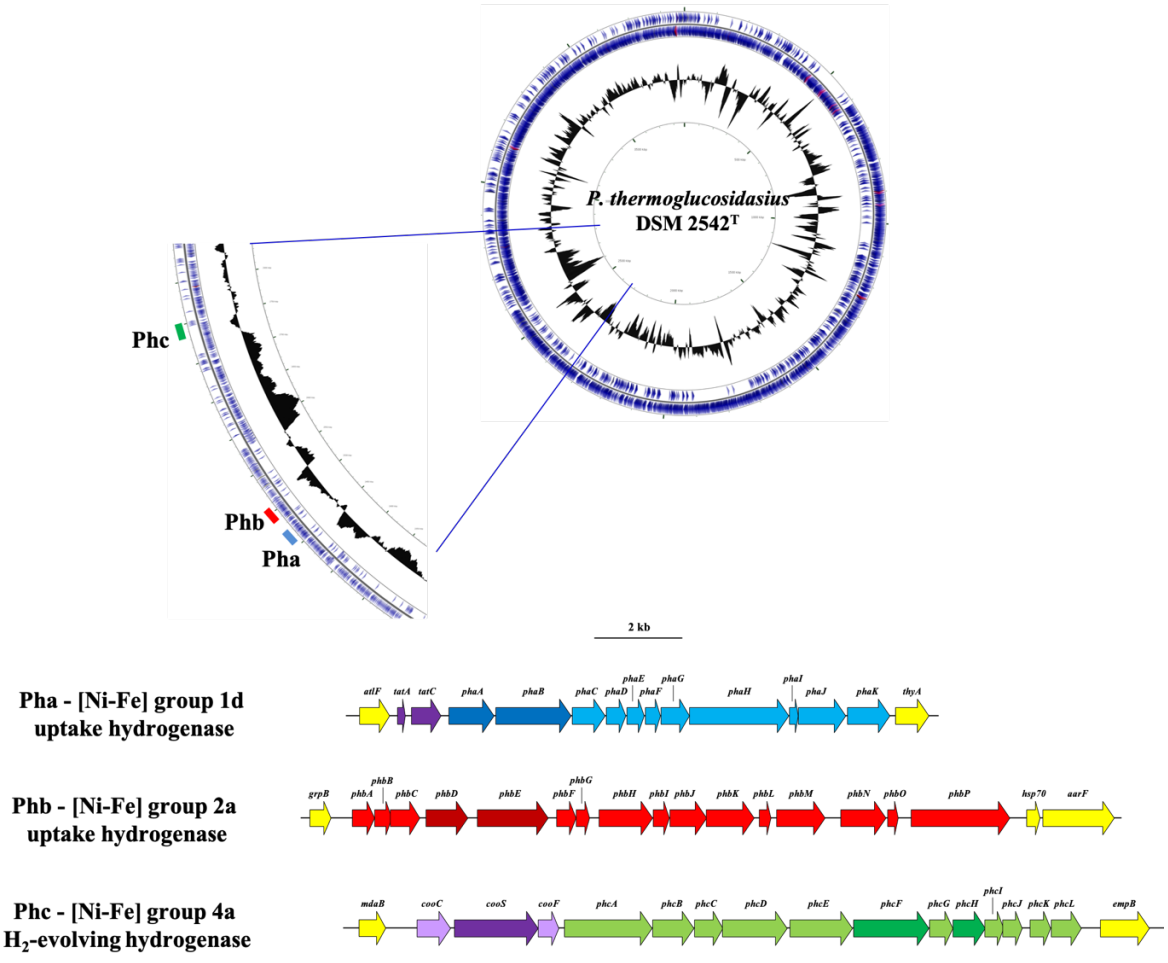

Figure 5: Schematic diagram of the [Ni-Fe] hydrogenase loci and their localization on the chromosome of *P. thermoglucosidasius* DSM 2542^T.

The Pha locus (chromosomal position 2,456,963-2,469,832; 12.9 kb in size) comprises eleven protein coding sequences (NCBI accession ALF10692-10702; PhaA-PhaK) (Figure 5; Appendix 1). Comparison of the amino acid sequence of the predicted catalytic subunit (ALF10727 – PhaB) against HydDB classifies the hydrogenase produced by this locus as a [Ni-Fe] group 1d uptake hydrogenase (E-value = 0.0) (Søndergaard *et al.*, 2016). This unidirectional, membrane-bound, O_2-tolerant hydrogenase is present in a broad range of obligately aerobic and facultatively anaerobic soil-borne, aquatic and host-associated taxa such as *Ralstonia eutropha*, *Escherichia coli* and *Wolinella succinogenes* (Vignais & Billoud, 2007; Greening *et al.*, 2016). The H_2 molecules consumed by group 1d hydrogenases are coupled to aerobic respiration (O_2 as electron acceptor) or to respiratory reduction of various anaerobic electron acceptors including NO^{3-}, SO_4^{2-}, fumarate and CO_2. The *P. thermoglucosidasius* DSM 2542^T hydrogenase locus incorporates genes coding for both small (PhaA; ALF10692; 324 aa) and large (PhaB; ALF10693; 573 aa) catalytic hydrogenase subunits. The strain also encodes seven additional proteins involved in hydrogenase formation, maturation and incorporation of the Ni-Fe metallocenter, including a third hydrogenase subunit (PhaC) which is predicted to serve as cytochrome *b* orthologue and links the hydrogenase to the quinone pools of the respiratory chains (Figure 5; Appendix 1) (Vignais & Billoud, 2007). The *pha* genes are flanked at the 5′ end by two genes coding for orthologues of the Twin-arginine translocation (Tat) pathway proteins TatA and TatC (Figure 5; Appendix 1). These have been shown to form part of the membrane targeting and translocation (Mtt) pathway which targets the fully folded hydrogenase heterodimer to the membrane (Sargent *et al.*, 1998).

The Phb locus (chromosomal position 2,488,614-2,503,714; 15.1 kb in size), located ~ 19 kb downstream of the Pha locus, comprises sixteen protein coding sequences (NCBI accession ALF10723 -738; PhbA-PhbP) (Figure 5.; Appendix 1). The predicted catalytic subunit (ALF10727 – PhbE) compared against HydDB classifies

the product of this locus as a [Ni-Fe] group 2a uptake hydrogenase (E-value = 0.0) (Søndergaard *et al.*, 2016). Members of this group of uptake hydrogenases are widespread among aerobic soil bacteria and Cyanobacteria and play a role in recycling H_2 produced by nitrogenase activity and fermentative pathways (Dutta *et al.*, 2005; Esteves-Ferreira *et al.*, 2017). The recycled H_2 is used in hydrogenotrophic respiration with O_2 serving as terminal electron acceptor, and thus group 2a hydrogenases are often O_2-tolerant (Vignais & Billoud, 2007). This locus encodes both large (PhbE; ALF10727; 544 aa) and small (PhbD; ALF10726; 317) [Ni-Fe] hydrogenase subunits and eight additional proteins with predicted roles in hydrogenase formation, maturation and incorporation of the Ni-Fe metal center in the large subunit (Figure 5; Appendix 1) (Sargent *et al.*, 1998). Furthermore, this locus encodes six proteins whose role in hydrogenase biosynthesis and functioning remains unclear. These include a tetratricopeptide-repeat (PhbH) and NHL repeat (PhbK) containing protein, which also occur in the [Ni-Fe] group 2a hydrogenase loci of *Nostoc punctiforme* ATCC 29133 and *Nostoc* sp. PCC 7120, where they are co-transcribed with the hydrogenase genes and have been suggested to play a role in protein-protein interactions and Fe-S cluster biogenesis (PhbJ) which may mediate electron transport to redox partners in downstream reactions (Holmqvist *et al.*, 2011).

The Phc locus (chromosomal position 2,729,489 – 2,741,372), ~226 kb downstream of the *Phb* locus is 11.9 kb in size and encodes twelve distinct proteins (PhcA-PhcL) (Figure 5; Appendix 1). These include a small (PhcE; ALF10919; 247 aa) and large (PhcG; ALF19021; 574 aa) [Ni-Fe]-hydrogenase catalytic subunit and ten additional proteins involved in hydrogenase formation and maturation (Figure 5; Appendix 1). The HydDB classifies the Phc hydrogenase as a [Ni-Fe] group 4a hydrogenase or formate hydrogenlyase complex I (FHL-1) (Søndergaard *et al.*, 2016). Members of this group are oxygen-sensitive, membrane-bound and are largely restricted to the facultatively fermentative Proteobacteria, particularly

enterobacteria associated with animal intestinal tracts *succinogenes* (Vignais & Billoud, 2007; Greening *et al.*, 2016). FHL-1 couples the reduction of protons from water to the anaerobic oxidation of formate to form CO_2 and H_2 (Andrews *et al.*, 1997; Vignais & Billoud, 2007). BlastP and tBlastN analyses of the protein sequences encoded in the *P. thermoglucosidasius* DSM 2542^T hydrogenase loci showed that the Pha, Phb and Phc loci are universally present in eight other *P. thermoglucosidasius* strains for which genomes are available. These loci are highly syntenous and the encoded proteins share average amino acid identities of 99.73% ([Ni-Fe]-group 1d hydrogenase Pha - 13 proteins), 99.61% ([Ni-Fe]-group 2a hydrogenase Phb -16 proteins) and 99.22% ([Ni-Fe]-group 4a hydrogenase Phc - 12 proteins) with those of DSM 2542^T, respectively. Pairwise BlastP analyses showed limited orthology between the two uptake hydrogenase loci, with 36.29% average amino acid identity in nine proteins encoded on the two loci. The group 1d (Pha) and group 2a (Phb) uptake hydrogenase loci share 33.40% and 62.32% average amino acid identity for three proteins with the H_2 evolving hydrogenase (Phc) locus. The higher level of orthology for Phb and Phc loci proteins can be correlated with the HypA-like (PhbB and PhcK) and the HypB-like (PhbC and PhcL) proteins, which share 75.22 and 86.08% amino acid identity, respectively, and are predicted to play a role in the incorporation of nickel into the hydrogenase enzyme (Chan *et al.*, 2012). Limited orthology is observed between the hydrogenase catalytic subunits or other hydrogenase formation and maturation proteins, suggesting distinct evolutionary histories for the two uptake and one H_2-evolving hydrogenases in *P. thermoglucosidasius*.

2.3.2 *P. thermoglucosidasius* contains a unique profile of hydrogenases with distinct evolutionary histories

The proteins encoded by the Pha, Phb and Phc loci were used in BlastP comparisons against the NCBI non-redundant (nr) protein database and HydDB (catalytic subunits) to identify orthologous loci in other bacterial taxa. This

revealed that, aside from the α-proteobacteria *Azospirillum halopraeferens* DSM 3675^T and *Rhodopseudomonas palustris* BAL398, the combination of [Ni-Fe] group 1- 2- 4 hydrogenases appears to be unique to *P. thermoglucosidasius* (Figure 6). In these two proteobacterial taxa the group 2a uptake hydrogenase is, however, replaced by a group 2b uptake hydrogenase. Group 2b uptake hydrogenases do not have a direct role in energy transduction but are flanked by a PAS domain protein which accepts the hydrogenase-liberated electrons, modulating the activity of a two-component regulator that upregulates the expression of other uptake hydrogenases, thereby serving as H_2-sensing system (Lenz & Friedrich, 1998; Vignais *et al.*, 2005). The Pha uptake hydrogenase locus is relatively well conserved among members of the Firmicutes, including a number of taxa belonging to the Classes Bacilli, Clostridia and Negativicutes, as well as the phyla Proteobacteria and Bacteroidetes (Figure 6; Appendix 2). However, the more distantly related taxa retain little synteny with the Pha locus in *P. thermoglucosidasius* (Figure 7A). Orthologues of the Pha are present in one other *Parageobacillus* spp., namely genomosp. NUB3621, with an average amino acid identity of 92.37% (13 proteins) with the DSM 2542^T Pha proteins. A phylogeny on the basis of nine conserved Pha proteins (PhaABCDGHIJK) showed a similar branching pattern (Figure 7A) as observed for the phylogeny housekeeping protein (InfB-RecN-RpoB) phylogeny, suggesting that this is an ancestral locus that has been vertically maintained. This is supported by the low level of discrepancy in G+C content for the *P. thermoglucosidasius* strains, which are on average 0.87% above the genomic G+C content. Larger discrepancies are, however, evident among the Bacteroidetes, where G+C contents for the locus are on average 4.43% above that of the genome, and the absence of Pha loci in other *Parageobacillus* spp. including *P. toebii* (5 genomes available) and *P. caldoxylosilyticus* (4 genomes available) and *Geobacillus* spp. suggest a more complex evolutionary history for the group 1d hydrogenase.

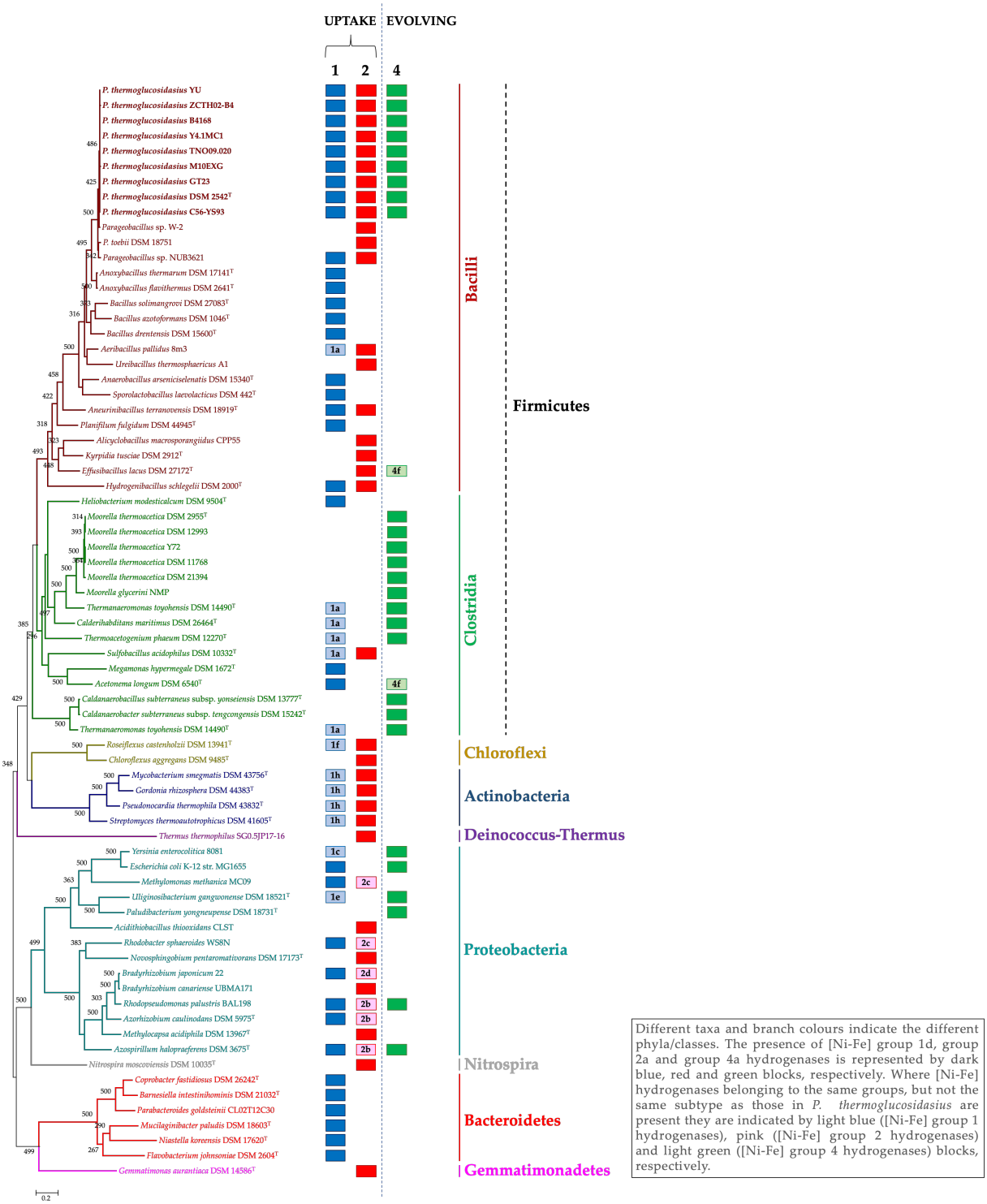

Different taxa and branch colours indicate the different phyla/classes. The presence of [Ni-Fe] group 1d, group 2a and group 4a hydrogenases is represented by dark blue, red and green blocks, respectively. Where [Ni-Fe] hydrogenases belonging to the same groups, but not the same subtype as those in *P. thermoglucosidasius* are present they are indicated by light blue ([Ni-Fe] group 1 hydrogenases), pink ([Ni-Fe] group 2 hydrogenases) and light green ([Ni-Fe] group 4 hydrogenases) blocks, respectively.

Figure 6: Prevalence of [Ni-Fe] hydrogenases orthologous to those in *P. thermoglucosidasius* among other bacterial taxa.

A [Ni-Fe] group 1d hydrogenase - Pha

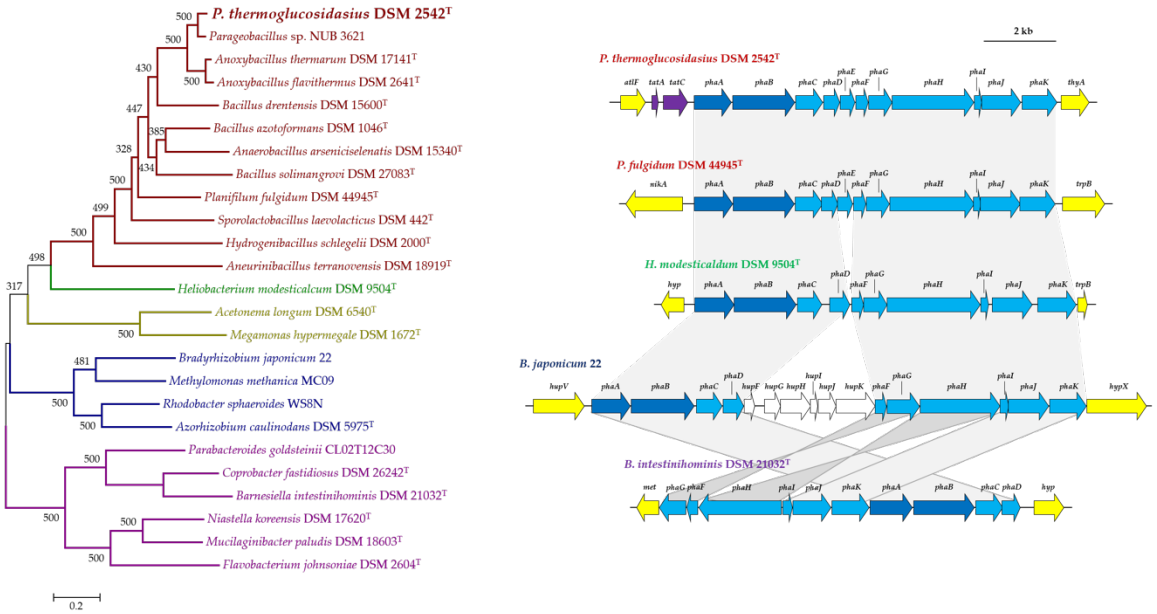

B [Ni-Fe] group 2a hydrogenase - Phb

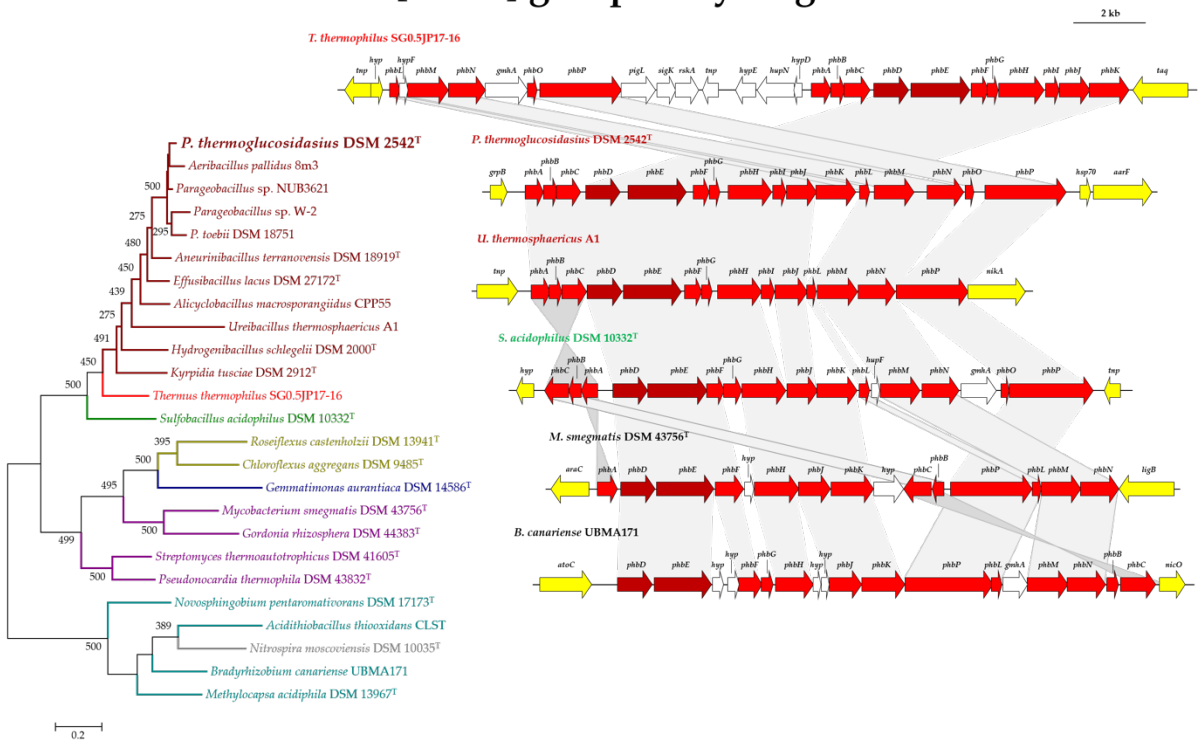

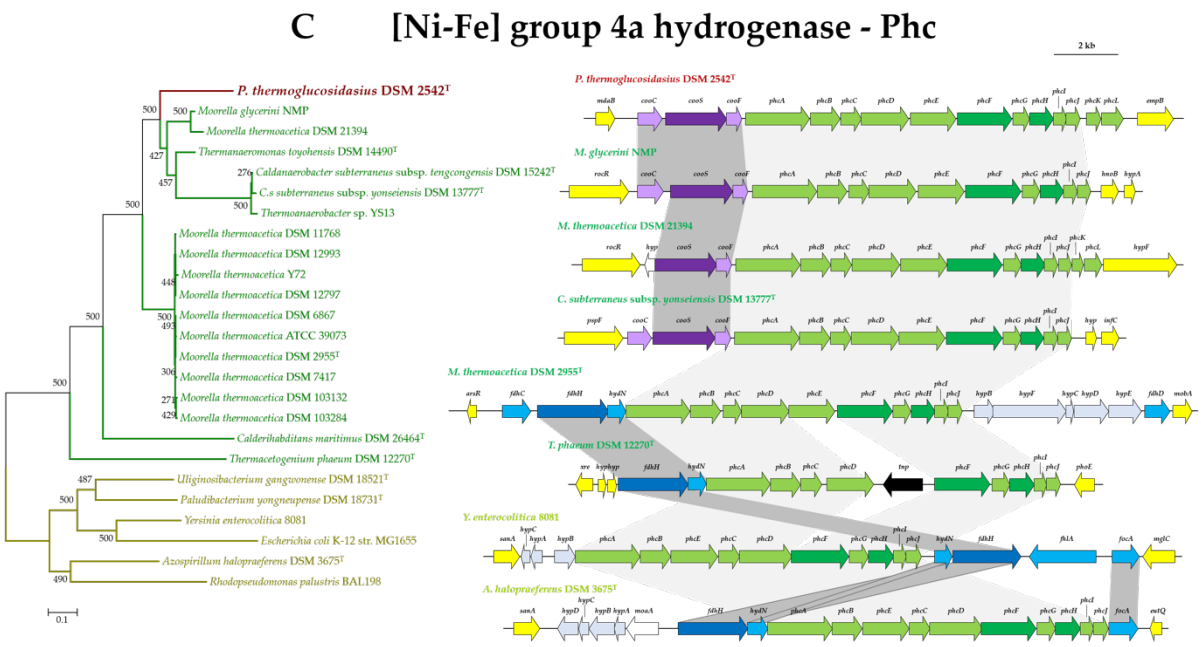

Figure 7: Prevalence and synteny of the *P. thermoglucosidasius*-like [Ni-Fe] hydrogenases. (A) [Ni-Fe] group 1d orthologues. (B) [Ni-Fe] group 2a orthologues. (C) [Ni-Fe] group 4a orthologues. (7A) [Ni-Fe] group 1d orthologues. The ML phylogeny was determined on the basis of the trimmed alignment of nine Pha locus proteins (PhaABCDGHIJK – 2,206 amino acids in length). Hydrogenase genes are coloured in light blue (dark blue for large and small catalytic subunits), tatAE genes in purple and flanking genes in yellow in the synteny diagrams. (7B) [Ni-Fe] group 2a orthologues. The ML phylogeny was determined on the basis of the trimmed alignment of ten Phb locus proteins (PhbBCDEFHJLMN – 2,348 amino acids in length). Hydrogenase genes are coloured in red (dark red for large and small catalytic subunits), genes of no known function in biosynthesis and functioning of the hydrogenase in white and flanking genes in yellow in the synteny diagrams. (7C) [Ni-Fe] group 4a orthologues. The ML phylogeny was determined on the basis of the trimmed alignment of nine Phc locus proteins (PhcABCDFGHIJ – 2,744 amino acids in length). Hydrogenase genes are coloured in light green (dark green for large and small catalytic subunits), anaerobic CODH genes in purple, formate dehydrogenase-related genes in blue and flanking genes in yellow in the synteny diagrams. Values on all trees reflect bootstrap analyses (n= 500 replicates) and all trees were rooted on the midpoint.

Orthologous [Ni-Fe] group 2a uptake hydrogenase (Phb) loci are also common among the Firmicutes, but show a more restricted distribution within the family *Bacillaceae*, with only *Aeribacillus pallidus* 8m3 and *Hydrogenibacillus schlegelii* DSM 2000^T containing orthologues outside the genus *Parageobacillus*. Highly conserved and syntenous loci are, however, present in three non-*thermoglucosidasius* strains: *Parageobacillus* sp. NUB3621, *Parageobacillus* sp. W-2 and *P. toebii* DSM 18751 (Figure 7B; Appendix 2). Orthologous loci are present across a

much wider range of phyla than the Pha locus, including members of the Chloroflexi, Gemmatimonadetes, Actinobacteria, Proteobacteria, Nitrospirae and Deinococcus-Thermus (Figure 6). The latter is of interest as *Thermus thermophilus* SG0.5JP17-16 clusters with the Firmicutes in a phylogeny of ten conserved proteins (PhbBCDEFHJLMN – 72.76% average amino acid identity with *P. thermoglucosidasius* DSM 2542^T) (Figure 7B), but is phylogenetically disparate from the Firmicutes. The *T. thermophilus* locus is present on the plasmid pTHTHE1601 (NC_017273) suggesting that this locus forms part of the mobilome. Furthermore, the G+C content of the Phb locus differs by an average of 4.55% from the average genomic G+C among the eight compared *P. thermoglucosidasius* strains, suggesting recent horizontal acquisition of this locus. The [Ni-Fe] group 4a H_2-evolving hydrogenase (Phc) locus shows the most restricted distribution of the three loci among the Firmicutes, with orthologous loci only present in the eight compared *P. thermoglucosidasius* strains and members of the clostridial family *Thermoanaerobacteraceae* (Figure 6). Further, Phc-like loci appear to be restricted to members of the Proteobacteria. High levels of synteny and sequence conservation can be observed among the Phc loci in both phyla, with the exception of the PhcK and PhcL proteins, which are only present in the *P. thermoglucosidasius* and *Moorella thermoacetica* DSM 21394 Phc loci (Figure 7C). BlastP analyses indicate that PhcK and PhcL show highest orthology with PhbB and PhbC in the Phb locus and may have been derived through gene duplication events.

It is notable that the *P. thermoglucosidasius* Phc locus clusters with a subset of the *Thermoanaerobacteraceae* in the concatenated Phc protein phylogeny, including *Moorella glycerini* NMP, *M. thermoacetica* DSM 21394, *Thermoanaeromonas toyohensis* DSM 14490^T, *Caldanaerobacter subterraneus* subsp. *tencogensis* DSM 15242^T and subsp. *yonseiensis* DSM 13777^T and *Thermoanaerobacter* sp. YS13 (Figure 7C). These differ from the remaining *Thermoanaerobacteraceae* taxa and the proteobacterial orthologous loci in that they are flanked by three genes, *cooCSF*, coding for an

anaerobic carbon monoxide (CO) dehydrogenase, rather than genes coding for a formate dehydrogenase (FdhH) as is typical for the [Ni-Fe] group 4a hydrogenases (Greening *et al.*, 2016). These are generally accompanied by flanking genes coding for the formate dehydrogenase accessory sulfurtransferase protein FdhD, electron transporter HydN, transcriptional activator FhlA and formate transporters FdhC and FocA, which together with FdhH drive the anaerobic oxidation of formate (Figure 7C) (Vignais & Billoud, 2007; Maier *et al.*, 1996; Mukherjee *et al.*, 2017; Thomé *et al.*, 2012). BlastP analysis with the FdhH protein of *M. thermoacetica* DSM 2955^T (AKX95035) shows that an orthologue is present in *P. thermoglucosidasius* DSM 2542^T (ALF09582). The latter protein, however, shares limited orthology (39% amino acid identity; Bitscore: 497; E-value: 6e-614) with its *M. thermoacetica* counterpart and is furthermore localised ~1.5 Mb upstream of the Phc locus, suggesting the *P. thermoglucosidasius* FdhH protein does not function together with the [Ni-Fe] group 4a hydrogenase. Instead, the *P. thermoglucosidasius* Phc hydrogenase may form a novel complex with the adjacent anaerobic CODH locus.

2.3.3 The *P. thermoglucosidasius* [Ni-Fe] group 4a hydrogenase forms a novel complex with the anaerobic (Coo) CO dehydrogenase, with a distinct evolutionary history

The three genes located just upstream of the Phc hydrogenase locus, *cooC*, *cooS* and *cooF* code for a CO dehydrogenase maturation factor (Figure 7C, Figure 8), a CO dehydrogenase catalytic subunit and CO dehydrogenase Fe-S protein, respectively. Together these proteins catalyse the oxidation of CO to generate CO_2 ($CO + H_2O \rightarrow CO_2 + 2\ H^+ + 2\bar{e}$). The electrons are then used in reduction reactions, including sulphate reduction, heavy metal reduction, acetogenesis, methanogenesis and hydrogenogenesis (Ragsdale, 2004; Techtmann *et al.*, 2012).

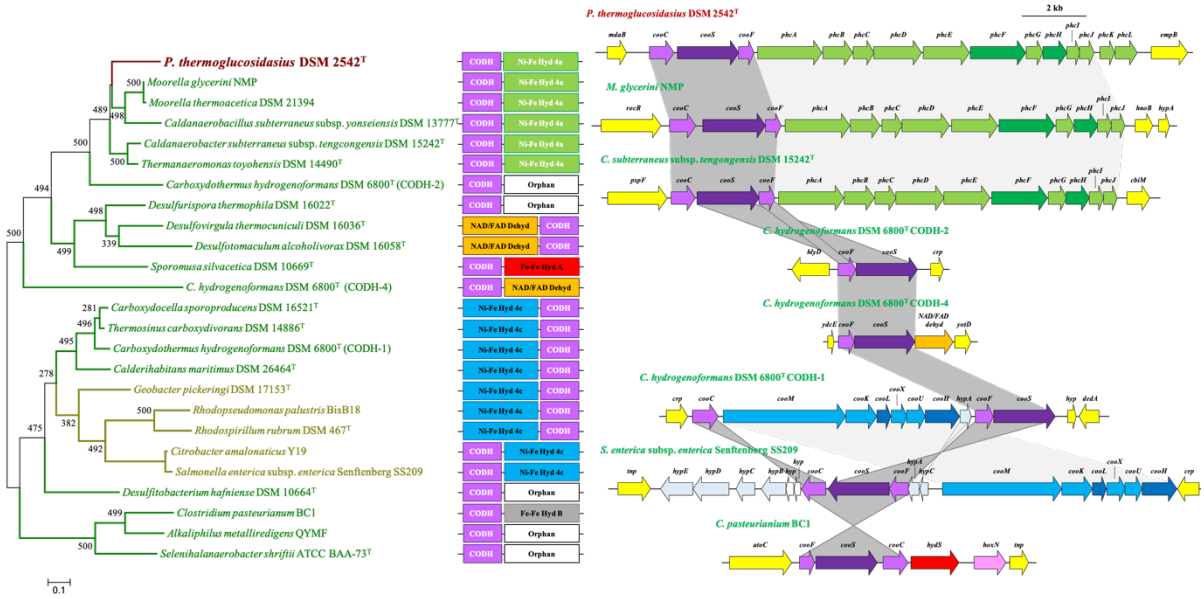

Figure 8: Prevalence and synteny of the *P. thermoglucosidasius*-like CODH loci. A phylogeny was constructed on the basis of the concatenated alignments of two proteins (CooFS – 692 amino acids in length). Boostrap analysis (n = 500 replicates) was performed and the tree was rooted on the mid-point. In the synteny diagrams the CODH genes are coloured in purple (dark purple for the catalytic subunit gene *cooS*), the [Ni-Fe] group 4c hydrogenase genes in blue (dark blue for catalytic subunits), the [Ni-Fe] group 4a hydrogenase genes in green (dark green for catalytic subunits), NAD/FAD oxidoreductase gene in orange, [Fe-Fe] hydrogenase group A genes in red, [Fe-Fe] hydrogenase group B genes in purple and flanking genes in yellow.

The CODH locus is also co-localised with the Phc hydrogenase locus and highly conserved among the eight other *P. thermoglucosidasius* genomes (99.36% average amino acid identity with CooCSF in *P. thermoglucosidasius* DSM 2542^T), while no CODH orthologues are encoded on the genomes of any other *Parageobacillus* or *Geobacillus* spp. A phylogeny on the basis of the conserved CooS and CooF proteins (Figure 8) showed that, as with the Phc locus phylogeny (Figure 7C), those taxa where *cooCFS* flanks the Phc hydrogenase locus cluster together and show extensive synteny in both the *coo* and *phc* gene clusters. This would suggest the co-evolution of the anaerobic CODH and Phc [Ni-Fe] group 4a hydrogenase loci. However, differences in the G+C contents could be observed among the *P. thermoglucosidasius coo* (average G+C content 46.97%) and *phc* (average G+C content 49.02%) loci. This is even more pronounced among the *Thermoanaerobacteraceae* with this CODH-Phc arrangement, where the G+C

contents of the two loci differs by an average of 6.62% and is particularly evident in *C. subterraneus* subsp. *tencongensis* where the G+C contents of the *coo* and *phc* loci differ by 11.77%, suggesting independent evolution of these two loci. This is further support by the phylogeny (Figure 8), where the CODH-Phc loci cluster with CODHs which appear on their own and those flanked by an NAD/FAD oxidoreductase are thought to play a role in oxidative stress response (Wu *et al.*, 2005). The Energy Conserving Hydrogenase (ECH – [Ni-Fe] group 4c hydrogenase)-CODH complex, which has been shown to couple CO oxidation to proton reduction to H_2 in *C. hydrogenoformans* and *Rhodospirillum rubrum*, clusters more distantly from the CODH-[Ni-Fe] group 4a complex (Fox *et al.*, 1996; Soboh *et al.*, 2002). Overall, the results suggest that the CODH and [Ni-Fe] group 4a hydrogenase have evolved independently, but may form a complex linking CO oxidation to reduction of protons to produce CO_2 and H_2.

2.3.4 The CODH-[Ni-Fe] group 4a hydrogenase complex effectively couples CO oxidation to hydrogenogenesis

The predicted function of the co-localized genes encoding the anaerobic CODH and H_2-evolving hydrogenase (Figure 7C) was tested using *P. thermoglucosidasius* DSM 2542^T. Two related strains, *Geobacillus thermodenitrificans* DSM 465^T and *P. toebii* DSM 14590^T, which lack both orthologues of the three hydrogenases and the anaerobic CODH, were included as controls. The cultivation of *P. thermoglucosidasius* DSM 2542^T in serum bottles with a gas atmosphere consisting of 50% CO and 50% air showed that this strain was able to effectively grow in the presence of 50% CO, reaching a maximum absorbance of 0.82 ± 0.02 after 6 hours of cultivation (Figure 9).

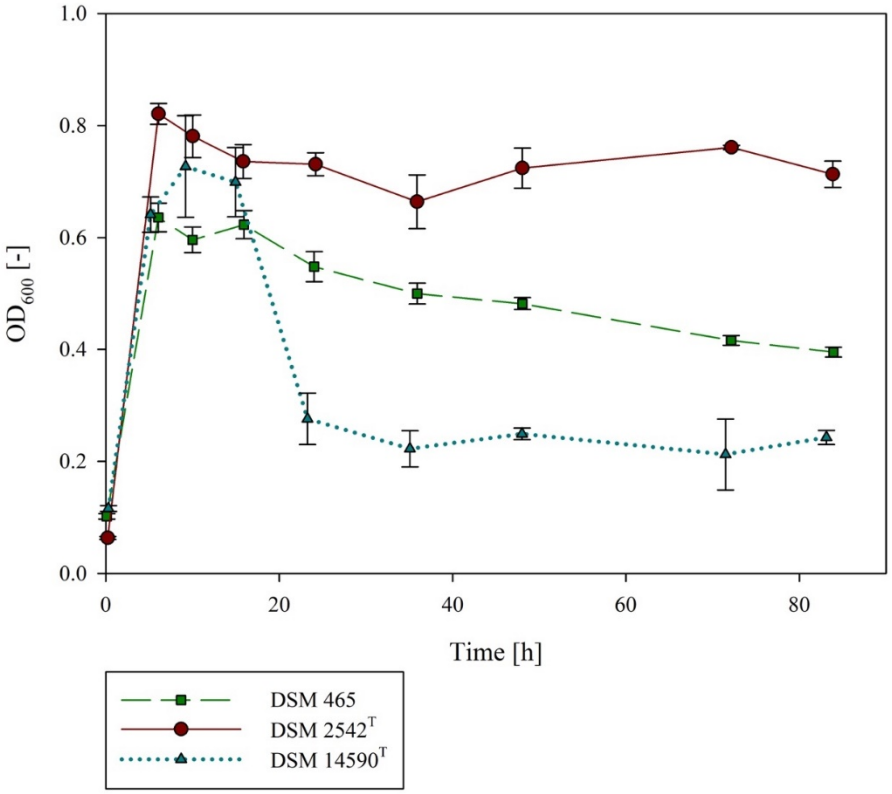

Figure 9: Growth of DSM 465, DSM 2542^T and DSM 14590^T. All strains were grown in quadruplicate in stoppered serum bottles with an initial gas atmosphere composition of 50% CO and 50% air. *P. thermoglucosidasius* DSM 2542^T reached a maximum absorbance (OD_{600}=0.82 ± 0.02) after 6 hours. A maximum absorbance for *P. toebii* DSM 14590^T was reached after 9 hours (OD_{600}=0.73 ± 0.09). For *G. thermodenitrificans* DSM 465 the highest OD_{600}=0.64 ± 0.03 was observed after 6 hours.

A fractional amount of CO was consumed at the beginning of the experiment, when O_2 was still available, by *P. toebii* DSM 14590^T (0.37 ± 0.04 mmol) and *G. thermodenitrificans* DSM 465^T (0.216 ± 0.061 mmol), respectively. This suggests that these strains may possess an alternative mechanism, such as an aerobic CO dehydrogenase, where CO oxidation is coupled to an electron transport chain which finally reduces O_2 (Ragsdale, 2004). For instance, a predicted aerobic CODH is present (CoxMSL – OXB91742-744) in *P. toebii* DSM 14590^T but is absent from *G. thermodenitrificans* DSM 465^T. While the two control strains tolerated the presence of CO, no H_2 production was observed for either strain (Figure 10). By contrast GC analyses revealed the production of H_2 by *P. thermoglucosidasius*

DSM 2542^T after ~36 h (Figure 11). This corresponds with O_2 reaching a plateau value of ~0.03 mmol. After 84 h 2.28 ± 0.11 mmol CO was consumed and 2.47 ± 0.15 mmol H_2 produced. *P. thermoglucosidasius* DSM 2542^T is thus capable of producing H_2 at a near equimolar conversion to CO consumption once most residual O_2 has been exhausted with a final yield of 1.08 ± 0.07 H_2/CO.

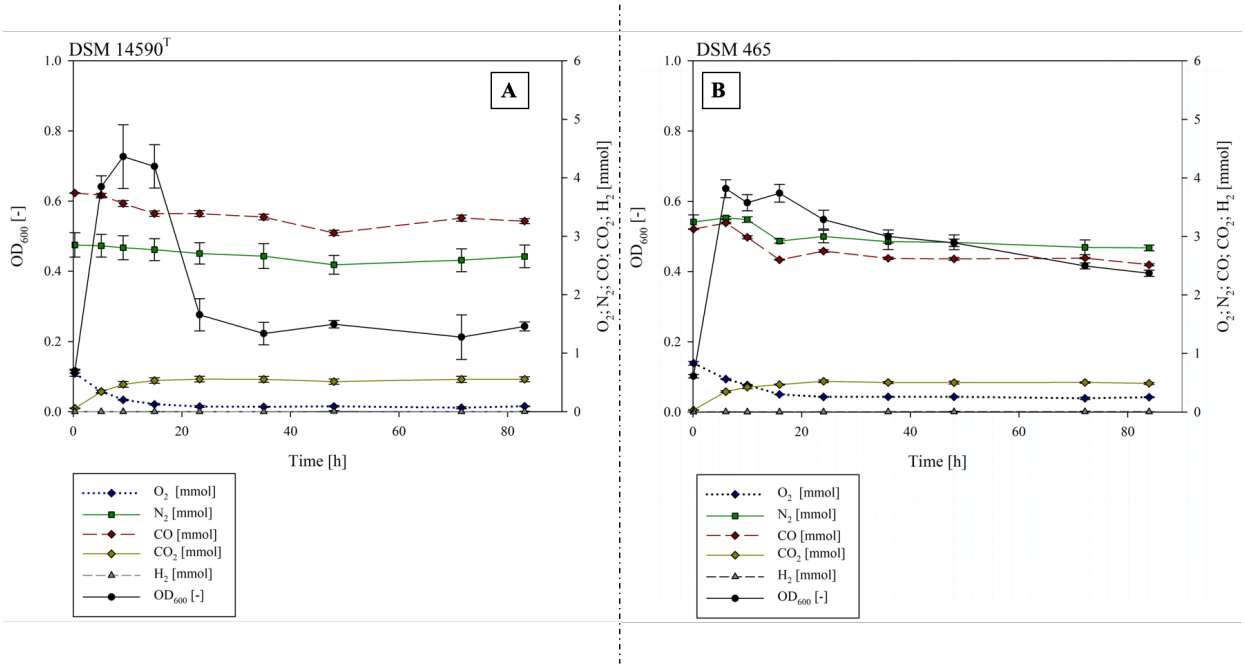

Figure 10: Gas phase composition during the cultivation of (A) *P. toebii* DSM 14590^T and (B) *G. thermodenitrificans* DSM 465 with an initial gas composition of 50% CO and 50% air. (A) O_2 decreased from 0.66 ± 0.05 mmol to ~0.01 mmol after ~23 hours. CO decreased fractionally about 0.37 ± 0.04 mmol. No hydrogen was detected. After 9 hours a maximum absorbance (OD_{600}) with a value of 0.73 ± 0.09 was reached. (B) O_2 decreased from 0.83 ± 0.03 mmol to ~0.03 mmol after 24 hours. CO decreased fractionally about 0.22 mmol. No hydrogen was detected. After 6 hours a maximum absorbance (OD_{600}) with a value of 0.64 ± 0.03 could be detected. O_2 is highlighted in blue, CO in red, hydrogen in grey, CO in yellow and OD_{600} in black.

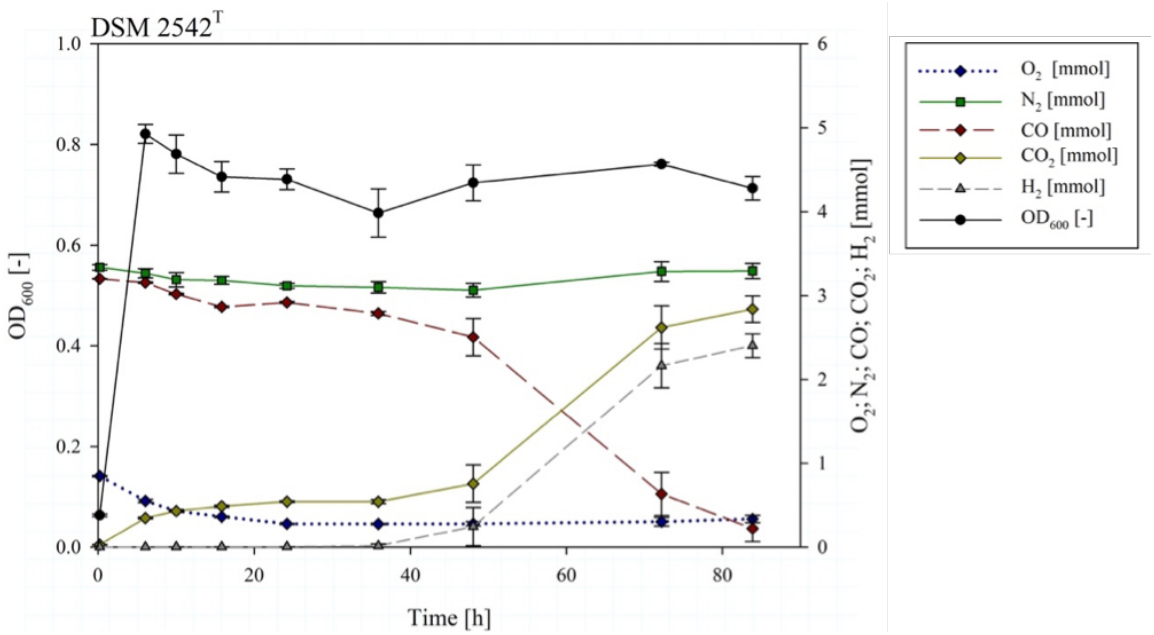

Figure 11: Gas phase composition during the cultivation of *P. thermoglucosidasius* DSM 2542T. O_2 decreased from 0.85 ± 0.01 mmol to ~0.03 mmol after 22 hours. CO decreased until the start of hydrogen production from 3.20± 0.02 mmol to 2.79 ± 0.02 mmol (~36 hours). After 84 hours the CO was consumed completely and 2.47 ± 0.15 mmol hydrogen was produced. After 6 hours a maximum absorbance (OD_{600}) with a value of 0.82 ± 0.02 was reached. O_2 is highlighted in blue, CO in red, hydrogen in grey, CO in dark yellow and OD_{600} in black.

2.4 DISCUSSION

The redox potential and diffusion coefficient of molecular H_2 make it a key component of metabolism and a potent energy source for many microbial taxa (Greening *et al.*, 2016). The ability to utilize this energy source relies on the production of various hydrogenase enzymes, which power both the consumption and production of H_2 and inextricably couple H_2 to energy-yielding pathways such as acetogenesis, methanogenesis and respiration (Vignais & Billoud, 2007; Schwartz *et al.*, 2013). Our comparative genomic analysis revealed that *P. thermoglucosidasius* contains a unique hydrogenase compliment comprised of two uptake hydrogenases (group 1d and 2a) and one H_2-evolving hydrogenase (group 4a). Evolutionary analyses showed that these hydrogenases are derived through three independent evolutionary events. This indicates that H_2 is likely to play a pivotal role in *P. thermoglucosidasius* metabolism and bioenergetics in the ecological niches it occupies. By contrast, members of the sister genus *Geobacillus* lack orthologous hydrogenase loci and, aside from *P. thermoglucosidasius*, only the group 1d and 2a uptake hydrogenases share orthology in one and three *Parageobacillus* spp., respectively, even though they are frequently isolated from the same environments.

The group 4a H_2-evolving hydrogenase of *P. thermoglucosidasius* is not found in any other members of the class Bacilli and is most closely related to those found in members belonging to the class Clostridia, particularly the family *Thermoanaerobacteraceae*. Furthermore, it forms an association with a CODH, which is found in common with a more restricted subclade of strict anaerobes within the family *Thermoanaerobacteraceae*.

2.5 CONCLUSIONS

Our fermentation studies with *P. thermoglucosidasius* in the presence of CO showed that *P. thermoglucosidasius* grows efficiently when exposed to high concentrations of CO and that the CODH-group 4a hydrogenase complex can effectively couple CO oxidation to H_2 evolution. *P. thermoglucosidasius* can do so at a near-equimolar conversion. Furthermore, unlike other CO oxidizing hydrogenogenic bacteria, which are strict anaerobes, *P. thermoglucosidasius* is a facultative anaerobe capable of first removing residual O_2 from CO gas sources prior to producing H_2 via the water-gas shift reaction. The combination of these features makes *P. thermoglucosidasius* an attractive target for potential incorporation in industrial-scale production strategies of biohydrogen.

REFERENCES FOR CHAPTER 2

Andrews SC, Berks BC, McClay J, Ambler A, Quail MA, Golby P, Guest JR (1997) A 12-cistron *Escherichia coli* operon (*hyf*) Encoding a putative proton-translocating formate hydrogenlyase system. *Microbiology*. **143**:3633–47. DOI:10.1099/00221287-143-11-3633.

Besemer J, Lomsadze A, Borodovsky M (2001) GeneMarkS: a self-training method for prediction of gene starts in microbial genomes. Implications for finding sequence motifs in regulatory regions. *Nucleic Acids Research*. **29**:2607–18. DOI:10.1093/nar/29.12.2607.

Chan KH, Lee KM, Wong KB (2012) Interaction between hydrogenase maturation factors HypA and HypB is required for [NiFe]-hydrogenase maturation. PLoS One. 7:e.32592. DOI:10.1371/journal.pone.0032592.

Dutta D, De D, Chaudhuri S, Bhattacharya SK (2005) Hydrogen production by Cyanobacteria. *Microbial Cell Factories*. **4**:36–46. DOI:10.1186/1475-2859-4-36.

Esteves-Ferreira AA, Cavalcanti JHF, Vaz MGMV, Alvarenga LV, Nunes-Nesi A, Araújo WL (2017) Cyanobacterial nitrogenases: Phylogenetic diversity, regulation and functional predictions. *Genetics and Molecular Biology*. **40**:261–75. DOI:10.1590/1678-4685-GMB-2016-0050.

Fox JD, Kerby RL, Roberts GP, Ludden PW (1996) Characterization of the CO-induced, CO-tolerant hydrogenase from *Rhodospirillum rubrum* and the gene encoding the large subunit of the enzyme. *Journal of Bacteriology*. **178**:1515–1524. DOI:10.1128/jb.178.6.1515-1524.

Grant JR, Stothard P (2008) The CGView Server: a comparative genomics tool for circular genomes. *Nucleic Acids Research*. **36**:181–4. DOI:10.1093/nar/gkn179.

Greening C, Biswas A, Carere CR, Jackson CJ, Taylor MC, Stott MB, Cook GM, Morales SE (2016) Genomic and metagenomic surveys of hydrogenase distribution

indicate H_2 is a widely utilised energy source for microbial growth and survival. *ISME Journal*. **10**:761–77. DOI:10.1038/ismej.2015.153.

Guindon S, Gascuel O (2003) A simple, fast, and accurate algorithm to estimate large phylogenies by maximum likelihood. *Systematic Biology*. **52**:696–704. DOI:10.1080/10635150390235520.

Hall TA (1999) Bioedit: a user-friendly biological sequence alignment editor and analysis program for Windows 95/98/NT. *Nucleic Acids Symposiums Series*. **41**:95–8.

Holmqvist M, Lindberg P, Agervald Å, Stensjö K, Lindblad P (2011) Transcript analysis of the extended *hyp*-operon in the cyanobacteria *Nostoc* sp. strain PCC 7120 and *Nostoc punctiforme* ATCC 29133. *BMC Research Notes*. **4**:186. DOI:10.1186/1756-0500-4-186.

Lefort V, Longueville J, Gascuel O (2017) SMS: Smart Model Selection in PhyML. *Molecular Biology and Evolution*. **34**:2422–4. DOI:10.1093/molbev/msx149.

Lenz O, Friedrich B (1998) A novel multicomponent regulatory system mediates H_2 sensing in *Alcaligenes eutrophus*. *Proceedings of the National Academy of Sciences of the United States of America*. **95**:12474–9. DOI:10.1073/pnas.95.21.12474.

Maier T, Binder U, Böck A (1996) Analysis of the hydA locus of *Escherichia coli*: two genes (hydN and hypF) involved in formate and hydrogen metabolism. *Archives of Microbiology*. **165**:333–41. DOI:10.1007/s002030050335.

Mukherjee M, Vajpai M, Sankararamakrishnan R (2017) Anion-selective Formate/ nitrite transporters: taxonomic distribution, phylogenetic analysis and subfamily-specific conservation pattern in prokaryotes. *BMC Genomics*. **18**:1–19. DOI:10.1186/s12864-017-3947-4.

Ragsdale SW (2004) Life with Carbon Monoxide. *Critical Reviews in Biochemistry and Molecular Biology*. **39**:165–95. DOI:10.1080/10409230490496577.

Shahinyan G, Margaryan A, Panosyan H, Trchounian A (2017) Identification and sequence analyses of novel lipase encoding novel thermophillic bacilli isolated from Armenian geothermal springs. *BMC Microbiology*. **17**:1-11. DOI:10.1186/s12866-017-1016-4.

Sargent F, Bogsch EG, Stanley NR, Wexler M, Robinson C, Berks BC, Palmer T (1998) Overlapping functions of components of a bacterial Sec-independent protein export pathway. *EMBO Journal*. **17**:3640–50. DOI:10.1093/emboj/17.13.3640.

Schwartz E, Fritsch J, Friedrich B (2013) H_2-Metabolizing Prokaryotes. In: The Prokaryotes: Prokaryotic Physiology and Biochemistry, Rosenberg E, DeLong EF, Lory S, Stackebrandt E, Thomson F, editors. Berlin: Springer. Berlin. pp 119–199.

Soboh B, Linder D, Hedderich R (2002) Purification and catalytic properties of a CO-oxidizing: H_2-evolving enzyme complex from *Carboxydothermus hydrogenoformans*. *European Journal of Biochemisty*. **269**:5712–21. DOI:10.1046/j.1432-1033.2002.03282.x.

Søndergaard D, Pedersen CNS, Greening C (2016) HydDB: A web tool for hydrogenase classification and analysis. *Scientific Report*. **6**:1–8. DOI:10.1038/srep34212.

Talavera G, Castresana J (2007) Improvement of phylogenies after removing divergent and ambiguously aligned blocks from protein sequence alignments. *Systematic Biology*. **56**:564–77. DOI:10.1080/10635150701472164.

Techtmann SM, Lebedinski AV, Colman AS, Sokolova TG, Woyke T, Goodwin L, Robb FT (2012) Evidence for horizontal gene transfer of anaerobic carbon monoxide dehydrogenases. *Frontiers in Microbiology*. **3**:1–16. DOI:10.3389/fmicb.2012.00132.

Thebti W, Riahi Y, Belhadj O (2016) Purification and Characterization of a New Thermostable, Haloalkaline, Solvent Stable, and Detergent Compatible Serine

Protease from *Geobacillus toebii* Strain LBT 77. *BioMed Research International.* DOI:10.1155/2016/9178962.

Thomé R, Gust A, Toci R, Mendel R, Bittner F, Magalon A, Walburger A (2012) A sulfurtransferase is essential for activity of formate dehydrogenases in *Escherichia coli. Journal of Biological Chemistry*. **287**:4671–8. DOI:10.1074/jbc.M111.327122.

Vignais PM, Elsen S, Colbeau A (2005) Transcriptional regulation of the uptake [NiFe] hydrogenase genes in *Rhodobacter capsulatus*. *Biochemical Society Transactions*. **33**:28–32. DOI:10.1042/BST0330028.

Vignais PM, Billoud B (2007) Occurrence, classification, and biological function of hydrogenases: an overview. *Chemical Reviews*. **107**:4206–72. DOI:10.1038/ismej.2015.153.

Wallace IM, Sullivan OO, Higgins DG, Notredame C (2006) M-Coffee: combining multiple sequence alignment methods with T-Coffee. *Nucleic Acids Research*. **34**:1692–9. DOI:10.1093/nar/gkl091.

Wu M, Ren Q, Durkin AS, Daugherty SC, Brinkac LM, Dodson RJ, Madupu R, Sullivan SA, Kolonay JF, Haft DH, Nelson WC, Tallon LJ, Jones KM, Ulrich LE, Gonzales JM, Zhulin IB, Robb FT, Eisen JA (2005) Life in hot carbon monoxide: the complete genome sequence of *Carboxydothermus hydrogenoformans* Z-2901. *PloS Genetics*. e60.

Zeigler DR (2001) The Genus *Geobacillus*.Introduction and Strain Catalog. *Bacillus Genetic Stock Center. Catalog of Strains*. **7(3)**.

Zeigler DR (2014) The Geobacillus paradox: why is a thermophilic bacterial genus so prevalent on a mesophilic planet? *Microbiology*. **160**:1–11. DOI:10.1099/mic.0.071696-0.

3 EVALUATION OF HYDROGENOGENIC CAPACITIES OF DIFFERENT *P. THERMOGLUCOSIDASIUS* STRAINS

This chapter is partially based on the publication

COMPARATIVE GENOMIC ANALYSIS OF *PARAGEOBACILLUS THERMOGLUCOSIDASIUS* STRAINS WITH DISTINCT HYDROGENOGENIC CAPACITIES.

Teresa Mohr, Habibu Aliyu, Raphael Küchlin, Michaela Zwick, Anke Neumann, Don Cowan, Pieter de Maayer

BMC Genomics

Volume 19, Article 880

Published: December 6, 2018

DOI: 10.1186/s12864-018-5302-9

https://bmcgenomics.biomedcentral.com/articles/10.1186/s12864-018-5302-9

Authors' contribution to this publication

Teresa Mohr designed all experiments, performed the cultivation with Raphael Küchlin and Michaela Zwick, performed together with Habibu Aliyu and Pieter de Maayer the comparative analysis and drafted the manuscript.

Habibu Aliyu performed genomic analysis and drafted the manuscript.

Raphael Küchlin and **Michaela Zwick** performed the experiments with Teresa Mohr.

Anke Neumann contributed to the experimental design.

Don Cowan edited the manuscript.

Pieter de Maayer supervised the project, performed genomic analysis and drafted the manuscript.

3.1 INTRODUCTION AND ABSTRACT

In Chapter 2 we showed that *P. thermoglucosidasius* DSM 2542^T is capable of producing H_2 via the water-gas shift (WGS) reaction, which can be linked to a carbon monoxide dehydrogenase-hydrogenase (CODH) enzyme complex encoded on its genome. The genetic complement for these enzymes furthermore represents a universal molecular feature among those *P. thermoglucosidasius* strains for which genome sequences are available. While the molecular determinants for hydrogenogenesis may be present in all *P. thermoglucosidasius* strains, this does not signify that they all produce H_2 equally efficiently. Identifying a particular *P. thermoglucosidasius* strain(s) with superior hydrogenogenic capacities is a key step in the further development and enhancement of this process on a larger scale.

In this chapter, four *P. thermoglucosidasius* strains (DSM 2542^T, DSM 2543, DSM 6285 and DSM 21625) were evaluated for their capacity to produce H_2 via the WGS reaction. Cultivations in 250 ml serum bottles with an initial gas atmosphere of air and CO (50:50 ratio) were undertaken. In addition, the genomes of all four strains were sequenced and comparative genomic analysis was performed.

Disparities in the hydrogenogenic capacities of the different *P. thermoglucosidasius* strains were identified. While three strains (DSM 2542^T, DSM 2543 and DSM 6285) produced H_2 under the tested conditions, the fourth strain (DSM 21625) did not. Furthermore, in one strain (DSM 6285) H_2 production commenced earlier in the cultivation than the other hydrogenogenic strains. Comparative genomic analysis of the four strains identified extensive differences in the protein complement encoded on the genomes, some of which are postulated to contribute to the different hydrogenogenic capacities of the strains. Furthermore, polymorphisms and deletions in the CODH-NiFe hydrogenase loci may contribute towards this variable phenotype.

3.2 MATERIALS AND METHODS

3.2.1 Bacterial strains and culturing conditions

To verify the production of H_2 of different *P. thermoglucosidasius* strains, four strains *P. thermoglucosidasius* DSM 2542^T, *P. thermoglucosidasius* DSM 2543, *P. thermoglucosidasius* DSM 6285 and *P. thermoglucosidasius* DSM 21625 were grown in presence of CO. All strains were obtained from the DSMZ (Deutsche Sammlung von Mikroorganismen und Zellkulturen GmbH, Braunschweig, Germany).

Pre-cultures and experimental cultures were grown in mLB medium (modified Luria-Bertani): tryptone (1% w/v), yeast extract (0.5% w/v), NaCl (0.5% w/v), 1.25 ml/L NaOH (10% w/v). And 1 ml/L of each of the filter-sterilized stock solutions: 1.05 M nitrilotriacetic acid, 0.59 M $MgSO_4.7H_2O$, 0.91 M $CaCl_2.2H_2O$ and 0.04 M $FeSO_4.7H_2O$ (Zeigler, 2001). A first set of pre-cultures was grown aerobically at 60 °C and 120 rpm (24 h). A second pre-culture was inoculated to an OD_{600}= 0.1 from pre-culture 1 and incubated aerobically for 12 h. The cultivations were conducted in serum bottles (250 ml) with 50 ml medium and an initial gas atmosphere consisting of 50% CO and 50% air at 1 bar atmospheric pressure. The bottles were inoculated with 1 ml of the second pre-culture. All cultivations were undertaken at 60 °C and 120 rpm in an Infors Thermotron (Infors AG, Bottmingen, Switzerland) The experiments ran for 84 h and were performed as quadruplicates in stoppered bottles.

3.2.2 Analytical methods

The gas compositions and culture growth were monitored at nine different time points during the experimental cultivation. For monitoring the growth, 1 ml of the culture was measured at OD_{600} using an Ultrospec 1100 pro spectrophotometer (Amersham Biosciences, USA). The gas composition was monitored at each time point using a 300 Micro GC gas analyzer (Inficon, Bad Ragaz, Switzerland) with

the columns Molsieve and PLOT Q. Before and after taking the liquid and gas samples the pressure in the serum bottles was measured using a manometer (GDH 14 AN, Greisinger electronic, Regenstauf, Germany). Gas analysis and calculation of the gas composition were performed as previously described (Chapter 2.2.3).

3.2.3 Genome sequencing, assembly and annotation

P. thermoglucosidasius DSM 2543, DSM 6285 and DSM 21625 were grown aerobically in mLB medium (60 °C; 120 rpm) to mid-log phase. Total DNA was extracted using Quick-DNA™ Fungal/Bacterial Miniprep Kit (Zymo Research, Irvine, CA, USA). The genome of *P. thermoglucosidasius* DSM 2542^T was sequenced previously (NCBI Acc. #: CP012712.1). Genome sequencing of the other three strains was conducted using the Illumina Hiseq platform at GATC Biotech (Konstanz, Germany). A total of 9,152,896 (1.38 Gb: ~ 353x coverage), 9,467,702 (1.43 Gb: ~362x coverage) and 9,684,759 (1.46 Gb: ~ 369x coverage) paired reads were generated for *P. thermoglucosidasius* DSM 2543, DSM 6285 and DSM 21625, respectively. *De novo* genome assembly was undertaken using SPAdes genome assembler v3.11.1 and the resulting contigs were further assembled (scaffolded) with the aid of Medusa v1.6 and CSAR using all available complete genome sequences of *P. thermoglucosidasius* as reference (Bankevich *et al.*, 2012; Bosi *et al.*, 2015; Chen *et al.*, 2017). The plasmids of *P. thermoglucosidasius* DSM 2542^T were missing from the available complete genome sequence but were obtained from a second available draft genome of this strain (NCBI Acc. #LAKX01000000).

The high-quality draft genome sequences of all four strains were structurally and functionally annotated using the Rapid Annotation RAST using Subsystems Technology (RAST v. 2.0) server (Overbeek *et al.*, 2014). Putative integrated bacteriophages were identified using the Phast server (Zhou *et al.*, 2011). The genomic relatedness of the four strains was determined using the Genome-to-Genome Distance calculator (GGDC 2.0) and OrthoANI 0.93 (Tirado-Acevedeo *et al.*, 2010; Meier-Kolthoff *et al.*, 2013).

3.2.4 Comparative genomic analyses

The protein datasets predicted by RAST for all four strains were compared using Orthofinder 1.1.4 (Emms & Kelly, 2015) with default parameters. This allowed for the identification of protein families (orthologous proteins) found in all four strains (core), shared by two or three strains or unique to individual comparator strains (accessory). Both the core and accessory protein family datasets were functionally annotated by comparison against the EggNOG database (v. 4.5.1) using eggnog-mapper and the NCBI Conserved Domain Database using Batch CD-search (Huerta-Cepas *et al.*, 2016; Marchler-Bauer & Bryant, 2004).

To identify variation in the CODH-NiFe group 4a hydrogenase loci of the four compared strains, these regions were extracted from the genome sequences and compared using Mauve v2.3.1 (Darling *et al.*, 2010). SNPs in the genes in this locus were identified by pair-wise alignment of each gene using ClustalW in Bioedit v. 7.2.6 (Thompson *et al.*, 1994; Hall, 1999). The operon structures of the CODH-NiFe group 4a hydrogenase loci were determined *in silico* using FgenesB (Solovyev *et al.*, 2011). Further, transcription factor binding sites (TFBSs) were identified using the TFSITESCAN tool (http://www.ifti.org/Tfsitescan).

3.3 RESULTS

3.3.1 *P. thermoglucosidasius* strains vary in their ability to produce hydrogen

Four *P. thermoglucosidasius* strains, DSM 2542^T, DSM 2543, DSM 6285 and DSM 21625, were cultivated (in quadruplicate) for a total duration of 84 hours in stoppered 250 ml flasks containing 50 ml of modified Luria Bertani (mLB) medium and an initial gas atmosphere of 50% CO and 50% air. The volume percentage of gases, CO, CO_2, O_2 and H_2, were routinely monitored using Gas Chromatography (GC) analysis. All four strains were able to grow in the presence of CO, but reached a maximum absorbance at different time points in the cultivation (Figure 12; Figure 13). Two strains, DSM 2542^T (OD_{600}=0.821 ± 0.019) and DSM 2543 (OD_{600}=0.625 ± 0.023), reached maximum absorbance after ~6 hours, while DSM 21625 reached a maximum absorbance (OD_{600}=0.645 ± 0.032) ~10 hours after inoculation. By contrast *P. thermoglucosidasius* DSM 6285 reached a maximum absorbance only after ~36 hours (OD_{600}=0.537 ± 0.026). In all four strains, O_2 was consumed ~24 hours post inoculation, plateauing at a final value of 0.278 ± 0.007 mmol (Figure 13).

While three strains reached their maximum absorbance while O_2 was still present, the slower growing *P. thermoglucosidasius* DSM 6285 reached its maximum absorbance nearly twelve hours after O_2 was depleted (Figure 12C). This suggests that this strain possesses the metabolic capacity to support fully anaerobic growth. For two of the faster-growing strains, DSM 2542^T and DSM 2543, a gradual recovery in absorbance was observed following the decline after maximal growth. By contrast, for the fourth strain (*P. thermoglucosidasius* DSM 21625) the absorbance continued to decline following O_2 consumption (Figure 12D).

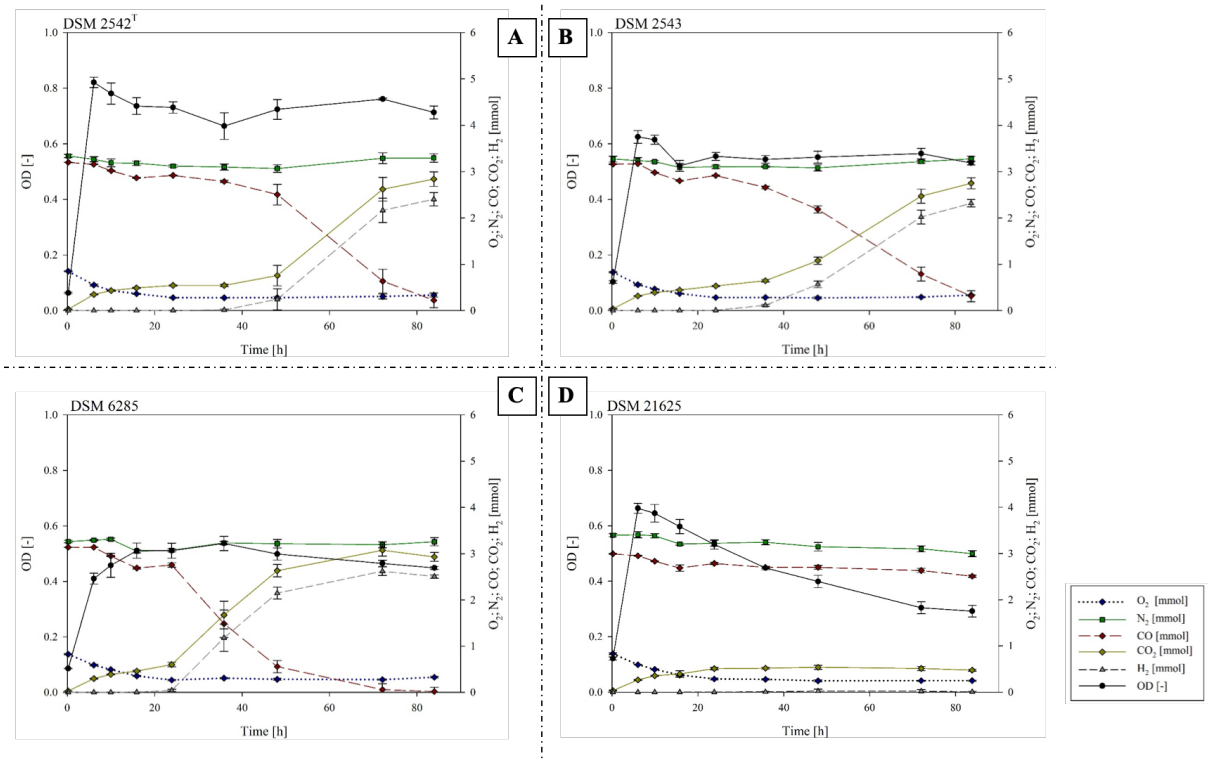

Figure 12: Growth curve and gas composition during the cultivation of (A) *P. thermoglucosidasius* DSM 2542T, (B) DSM 2543, (C) DSM 6285 and (D) DSM 21625.

Analysis of the gas compositions during the cultivation revealed key differences between the four strains. For three of the strains, DSM 2542T, DSM 2543 and DSM 6285, H_2 was produced with the concomitant consumption of CO after O_2 reached its minimal plateau level (Figure 12, Figure 13). By contrast, while a nominal decrease in the amount of CO (0.302 ± 0.373 mmol) could be observed, no H_2 was produced by *P. thermoglucosidasius* DSM 21625 throughout the cultivation (Figure 12D). In the three hydrogenogenic strains, the commencement of H_2 production coincided with a slight increase in absorbance observed in the growth curve (Figure 12). This suggests that the WGS reaction plays a role in the continued growth of these strains under anaerobic conditions. This is supported by the continued decline in absorbance observed for DSM 21625, which was unable to produce H_2 when exposed to CO.

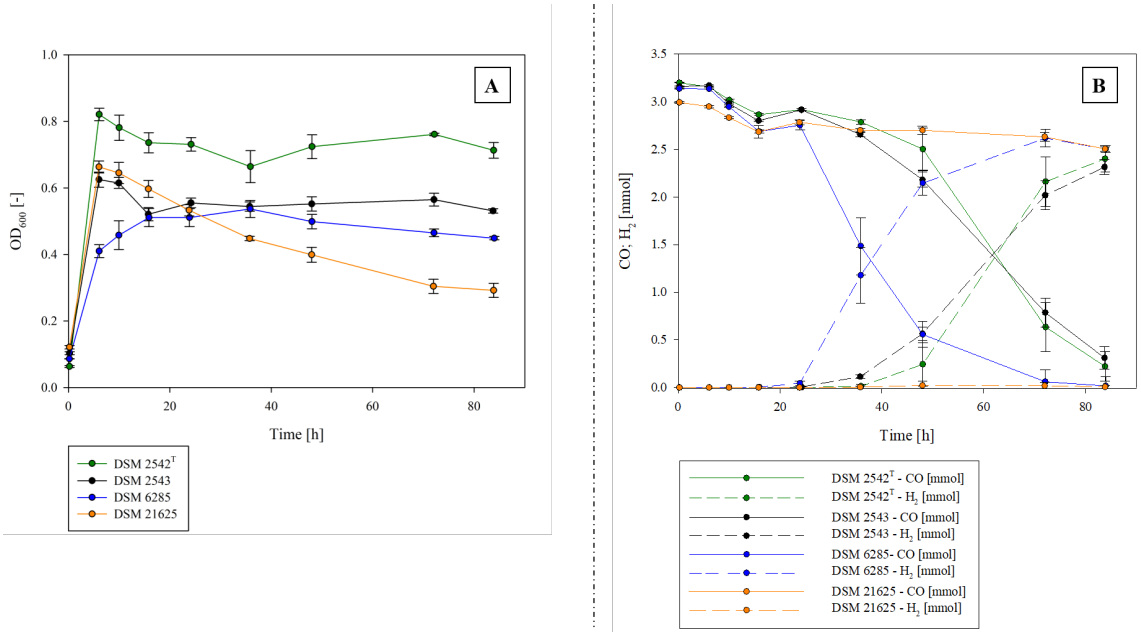

Figure 13: (A) Shows the growth curves of four *P. thermoglucosidasius strains* and (B) shows CO consumption and H_2 production of the strains during the cultivation with an initial gas atmosphere of 50% CO and 50% air.

Only minor differences were observed in terms of the H_2 produced and CO consumed after 84 hours, for DSM 2542^T (H_2 produced: 2.470 ± 0.149 mmol; CO consumed: 2.280 ± 0.11 mmol), DSM 2543 (H_2 produced: 2.389 ± 0 083 mmol; CO consumed: 2.512 ± 0.106) and DSM 6285 (H_2 produced: 2.637 ± 0.058 mmol; CO consumed: 2.552 ± 0.058 mmol), with an average yield of 1.02 H_2/CO (Figure 13B). There was, however, an observable difference in the time taken by the hydrogenogenic strains to start utilizing CO and produce H_2. Whereas DSM 2542^T and DSM 2543 initiated H_2 production after ~36 hours, H_2 production by DSM 6285 commenced ~16 h after inoculation (i.e., the lag phase between growth phase and H_2 production was substantially shorter for *P. thermoglucosidasius* DSM 6285). In order to further characterize the different hydrogenogenic capacities of the *P. thermoglucosidasius* strains, and the faster onset of H_2 production by *P. thermoglucosidasius* DSM 6285 compared to the other two hydrogenogenic strains, the genomes of the four strains were sequenced and compared using *in silico* methodologies.

3.3.2 Comparative genomics reveals substantial genome diversification among the compared *P. thermoglucosidasius* strains

The genomes of *P. thermoglucosidasius* DSM 2543, DSM 6285 and DSM 21625 were assembled to high quality draft status of between five and twenty-two contigs. The complete genome sequence of *P. thermoglucosidasius* DSM 2542^T is comprised of four replicons. The genomes of the four strains range in size between 3.96 and 4.01 Mb with an average G+C content of 43.76% (Figure 14).

Strain	Isolation source	NCBI Acc. #	Genome size (Mb)	# Contigs	G+C %	# predicted plasmids	# CDS	# integrated phages (intact/incomplete)	Total size of phage elements (kb)
DSM 2542^T	Soil, Japan	CP012712.1	3.99	4	43.83	2	4361	0/1	18. 1
DSM 2543	Soil, Japan	PRJNA482718	3.96	5	43.80	2	4329	0/2	25.0
DSM 6285	River sediment, USA	PRJNA482719	3.97	9	43.58	1	4330	01/06	75.2
DSM 21625	Flax plants, Germany	PRJNA482720	4.01	23	43.83	2	4433	02/07	191.2

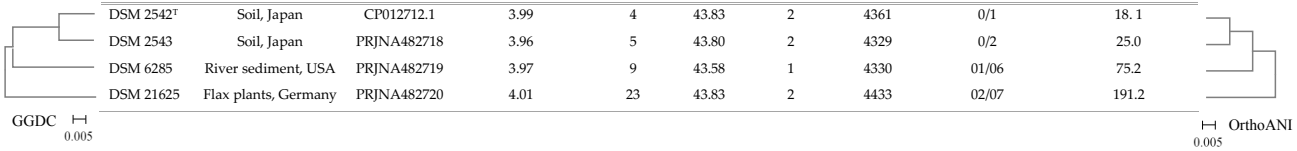

Figure 14: Genome properties of the compared *P. thermoglucosidasius* strains.

DSM 6285 harbours one plasmid while the other three strains have two plasmids. Between 4,329 (DSM 2543) and 4,433 (DSM 21625) proteins are encoded on the genomes. The genomic relatedness of the four strains was determined by calculating the digital DNA-DNA hybridization (GGDC) and OrthoANI values for each paired combination of strains (Meier-Kolthoff *et al.*, 2013; Lee *et al.*, 2016). This showed that *P. thermoglucosidasius* DSM 2542^T and DSM 2543, isolated from the same environmental source, were most closely related. while DSM 21625 was the most distinct strain on the basis of these two genomic values (Figure 14) (Suzuki *et al.*, 1983). However, both GGDC (>70%) and ANI (>95%) values exceed those distinguishing distinct species, confirming that all four strains belonged to the species *P. thermoglucosidasius* (Table 1).

Table 1: Genomic relatedness among the four compared *P. thermoglucosidasius* strains.

	DSM 2542^T	DSM 2543	DSM 6285	DSM 21625	
DSM 2542^T	---	99.99%	99.24%	99.2%	OrthoANI
DSM 2543	97.3%	---	99.27%	99.18%	
DSM 6285	93.5%	93.6%	---	99.14%	
DSM 21625	93.1%	93.1%	92.8%	---	

GGDC

The proteins encoded on the genomes of the four *P. thermoglucosidasius* strains were compared pair-wise using Orthofinder (Emms & Kelly, 2015). This analysis showed that the total protein content of the genomes comprised 5,039 distinct protein families (Figure 15). Of these 3,509 (69.63%) constituted the core protein families shared among all four strains. This core protein family dataset contributes between 83.03 (DSM 21625) and 85.17% (DSM 6285) of the total protein families present on each genome. When considering the unique protein families for each of the strains, the two most closely related strains, *P. thermoglucosidasius* DSM 2542^T and DSM 2543, contained the smallest fraction of strain-unique proteins (<0.65% of total protein families) (Figure 15). *P. thermoglucosidasius* DSM 2542^T and DSM 2543 did, however, have a large shared fraction (317 protein families) which was not found in the other two strains. Larger strain-unique protein fractions were observed for DSM 6285 (7.72%) and DSM 21625 (9.06%) (Figure 15). These differences can be largely attributed to the integration of several prophages within the genomes of these two strains, with phage elements contributing ~1.89 and 4.77% of the total genomic DNA of *P. thermoglucosidasius* DSM 6285 and DSM 21625, respectively.

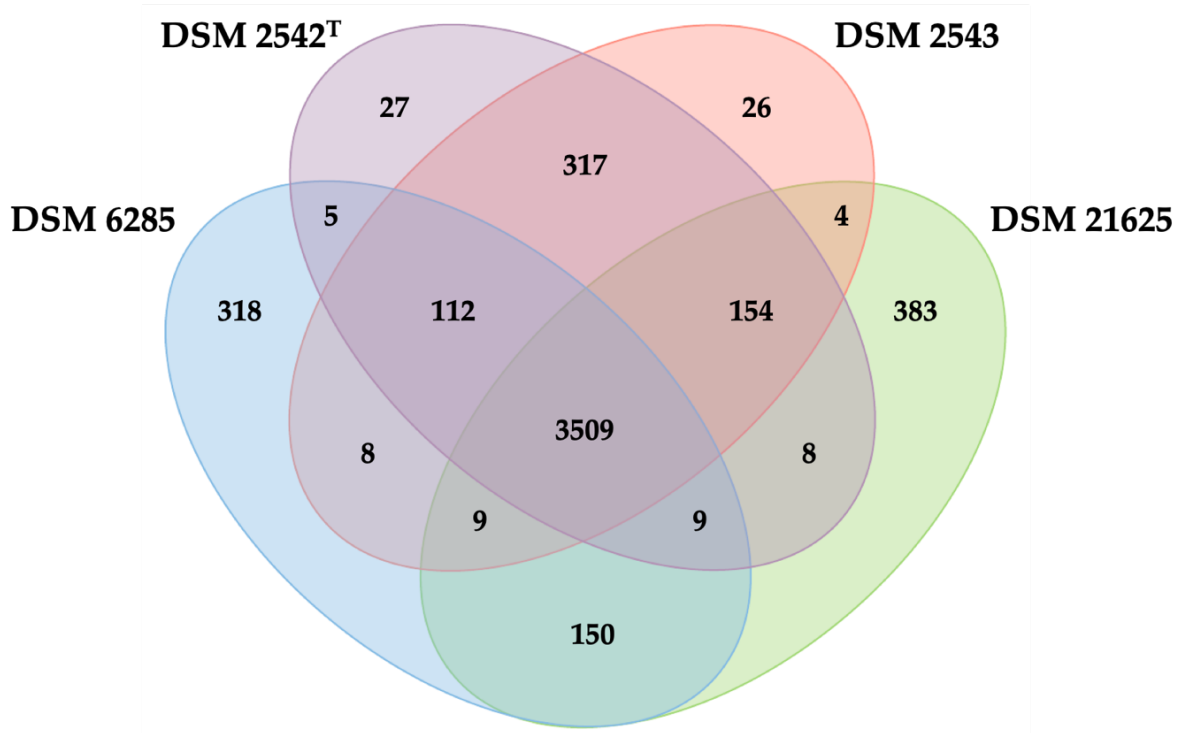

Figure 15: Venn diagram of protein families shared among or unique to the four compared *P. thermoglucosidasius* strains.

3.3.3 Differences in the proteome may contribute to the variable H_2 production capacities of the *P. thermoglucosidasius* strains

The core and accessory protein datasets of the four *P. thermoglucosidasius* strains were compared to assess whether the distinctive H_2 production capacities might be correlated to differences in their protein complement. A total of 383 protein families are unique to the non-hydrogenogenic strain (DSM 21625), while 112 protein families are restricted to the hydrogenogenic strains (DSM 2542^T, DSM 2543 and DSM 6285) (Figure 15; Appendix 3). Functional annotation and classification according to Conserved Orthologous Groups (COGs) (Emms & Kelly, 2015) showed that in both cases the datasets are largely comprised of proteins belonging to the COG functional category S (function unknown), with 73.63% (282 proteins) and 76.79% (86 proteins) of the proteins in the non-hydrogenic and hydrogenic dataset, respectively, belonging to this category (Appendix 3). Most of the remaining proteins unique to the non-hydrogenogenic *P. thermoglucosidasius* DSM 21625 are involved in carbohydrate transport and

metabolism (G – 9.14%), DNA replication, recombination and repair (L – 5.22%) and transcription (K – 3.39%) (Appendix 3). The majority of proteins in COG category G are encoded by the hemicellulose utilization system (HUS) locus, which has previously been identified as a highly variable locus among members of the genera *Geobacillus* and *Parageobacillus*, encoding a broad range of enzymes and metabolic pathways for the degradation of distinct hemicellulose polymers (De Maayer *et al.*, 2014). Proteins linked to the COG category L include phage primases, endonucleases and terminases, a product of the large number of unique phage elements in this strain. Proteins that form part of an L-arabinose transporter (AraFGH) were unique to the hydrogenogenic strains, located within the HUS locus as well as a branched amino acid transporter (LivFGMHJ) (De Maayer *et al.*, 2014).

The shorter H_2 production lag phase for *P. thermoglucosidasius* DSM 6285 suggests that this strain reaches the metabolic state suitable for the WGS reaction sooner than the other hydrogenogenic strains. Analysis of the unique protein family complement of this strain indicated that the majority of the 468 proteins not shared with DSM 2542^T and DSM 2543 belong to the COG category S (function unknown – 76.50%). Considering the proteins in other COG categories, only 24 proteins are involved in metabolic functions, including carbohydrate (G; 5 proteins), amino acid (E; 8 proteins) and inorganic ion transport and metabolism (P; 7 proteins), secondary metabolite biosynthesis, transport and catabolism (Q; 2 proteins) and energy production and conversion (C; 3 proteins) (Appendix 3). Among these metabolic proteins, four are involved in the synthesis of an inorganic ion ABC transporter (NCBI Acc. # DV713_01765-01780). The presence of conserved domains in DV713_01765 (CD08492: PBP2_NikA_DppA_OppA_like_15; E-value: 0e+00), DV713_01770 (TIGR02789: NikB; E-value: 4.52e-77), DV713_01775 (TIGR02790: NikC; E-value: 2.38e-67) and DV713_01780 (TIGR02770: NikD; E-value: 2.93e-79) suggest that this may represent a nickel transport system (Eitinger & Mandrand-

Berthelot, 2000). Nickel is pivotal for the functioning of both anaerobic CODH and Ni-Fe hydrogenases, forming part of the metallocenter of both these enzymes (Eittinger & Mandrand-Berthelot, 2000). Also unique to this strain are three proteins involved in the biogenesis of cytochrome *caa3* oxidase. Cytochrome caa_3 oxidase is the major oxidase involved in the last stages of the respiratory electron transport chain in *B. subtilis* grown under aerobic conditions, transferring electrons from the cytochrome *c* in the respiratory chain to the terminal electron acceptor O_2 (Bengtsson *et al*., 1999; Andrews *et al*., 2005). Deletion of the structural genes for cytochrome *caa3* oxidase in *B. subtilis* showed that this enzyme is not essential for growth (van der Oost *et al.*, 1991). The unique presence of orthologues of three proteins which are central to cytochrome *c* oxidase biosynthesis in *P. thermoglucosidasius* DSM 6285 may imply that this strain could more efficiently oxidise cytochrome *c* and reduce O_2 to H_2O, thereby reaching the critical oxygenic limits for functioning of the anaerobic CODH-hydrogenase enzymes faster than the other strains. However, comparison of the O_2-consumption rates of the hydrogenogenic strains did not show any substantial difference in terms of time taken until O_2 reached its minimum. Differences at the gene level, particularly in the CODH-NiFe hydrogenase loci, may also contribute to the disparity in the hydrogenogenic capacities of the *P. thermoglucosidasius* strains.

3.3.4 Variation in the CODH-hydrogenase locus of hydrogenogenic and non-hydrogenogenic *P. thermoglucosidasius* strains

In order to further distinguish genomic differences underlying the divergent hydrogenogenic capacities of the four *P. thermoglucosidasius* strains, the CODH-NiFe group 4a hydrogenase loci responsible for CO-oxidation dependent hydrogenogenesis (Mohr *et al.*, 2018a) were analysed at both the gene and protein level. In all four strains, the locus encodes three proteins (CooCSF) for the assembly of the CODH enzyme, and twelve proteins (PhcABCDEFGHIJKL) which comprise the NiFe group 4a hydrogenase (Figure 16). *In silico* analysis of the operon structure of this locus using FgenesB (Solovyev *et al.*, 2011) showed that the genes form part of three distinct operons, *cooCSF*, *phcABCDEFGHIJ* and *phcKL*, in all four strains (Figure 16).

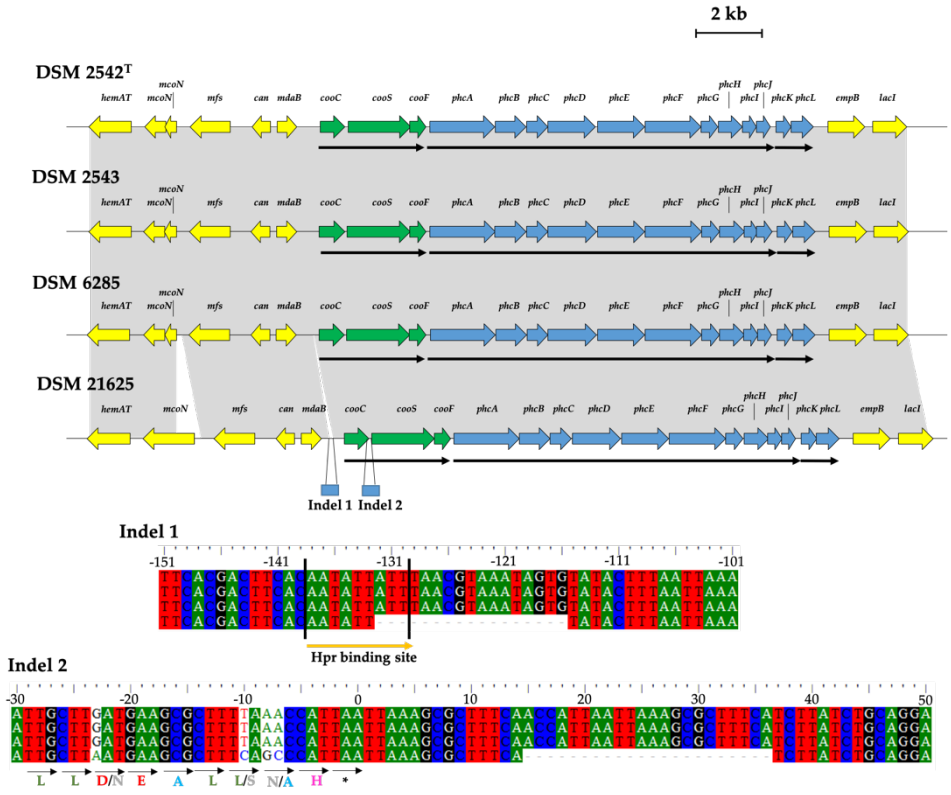

Figure 16: Schematic diagram of the CODH-NiFe group 4a hydrogenase locus of the compared *P. thermoglucosidasius* strains.

To determine whether mutations within the CODH-NiFe hydrogenase genes might be responsible for the difference observed in hydrogenic capacities of the four *P. thermoglucosidasius* strains, the nucleotide sequences for each of the genes in the CODH-NiFe hydrogenase loci of the four strains were aligned and compared. In total, 72 Single Nucleotide Polymorphisms (SNPs) were identified across the fifteen genes, with an average of 4.8 SNPs per gene. SNPs were interspersed across the genes rather than clustered together (Appendix 4). More SNPs was observed in the *cooC* (10 SNPs) and *cooS* (11 SNPs) genes, coding for the CODH maturation factor and CODH catalytic subunit, respectively, as well as *phcA* (8 SNPs), *phcB* (13 SNPs) and *phcF* (9 SNPs), which encode the NiFe group 4a hydrogenase component B, membrane subunit and large subunit, respectively. When comparing the different strains, 45 SNPs (62.5% of the total SNPs) were restricted to the non-hydrogenogenic *P. thermoglucosidasius* DSM 21625, with most of these occurring in the *cooC* (10 SNPs), *cooS* (9 SNPs) and *phcF* (8 SNPs) genes, respectively (Appendix 4). A further 14 SNPs were found in the genes of both DSM 21625 and DSM 6285, while 14 SNPs are only found in the hydrogenogenic *P. thermoglucosidasius* DSM 6285. When the proteins encoded by each of the genes were compared, it was observed that the SNPs resulted in only 29 non-synonymous mutations at the amino acid level (Appendix 4), the majority of which occurred in the proteins of DSM 21625 (19 – 65.72% of the total non-synonymous mutations), with most occurring in CooC (6 mutations) and PhcF (4 mutations). Six distinct non-synonymous mutations were also observed in DSM 6285, which initiates H_2 production more rapidly than the other two hydrogenogenic strains.

Average amino acid identity values were calculated for the CODH-NiFe hydrogenase protein datasets. The three hydrogenogenic strains share an average amino acid identity of 99.87% across the fifteen proteins. The proteins of the non-hydrogenogenic *P. thermoglucosidasius* DSM 21625 shared 99.50% average amino acid identity with those of the hydrogenogenic strains, indicating that this strain

was the most divergent. The highest divergence was observed for CooC, where the DSM 21625 protein shared 97.64% average amino acid identity with the orthologous protein in the other three strains, across 254 amino acids.

Alignment of the entire locus using Mauve v2.3.1 (Darling *et* al., 2010) revealed the presence of two deletions associated with the intergenic regions of the CODH-hydrogenase locus of DSM 21625, which are not observed in the loci of the three hydrogenogenic strains (Figure 16). A twentytwo nucleotide deletion occurs in the intergenic region between *cooC* and *cooS*, fourteen nucleotides downstream of the stop codon of *cooC*. The second deletion of seventeen nucleotides occurred 115 nucleotides upstream of the start codon of *cooC* (and thus upstream of the CODH-NiFe hydrogenase locus). Putative transcription factor binding sites (TFBSs) were identified in a 500 base pair window upstream of the *cooC* start codon using the TFSITESCAN tool (Tfsitescan: http://www.ifti.org/Tfsitescan). One predicted TFBS shared homology with the binding site for the *B. subtilis* transition state regulator Hpr (Ianoka *et al.*, 2009; Kallio *et al.*, 1991; Kodgire & Pao, 2009). Alignment of the flanking regions of the *P. thermoglucosidasius* CODH-NiFe hydrogenase loci showed this transcription factor binds between 139 and 129 bp upstream of *cooC* and the last three nucleotides of this TFBS forms part of the seventeen nucleotide deletion in *P. thermoglucosidasius* DSM 21625 (Figure 16). The deletion within the Hpr binding site might thus explain the lack of H_2 production in this strain. However, further laboratory analysis is required to identify the regulon for the CODH-NiFe hydrogenase locus to confirm this hypothesis.

3.4 DISCUSSION

The ability of four different *P. thermoglucosidasius* strains to produce H_2 via the WGS reaction was evaluated. Our analysis revealed extensive differences in the hydrogenogenic capacities of the strains. In particular, *P. thermoglucosidasius* DSM 21625 was unable to produce H_2 even though a CODH-NiFe hydrogenase locus was shown to be present on the genome. This suggests that the ability to produce H_2 via the WGS reaction is not a universal trait among *P. thermoglucosidasius* strains. We identified one strain, *P. thermoglucosidasius* DSM 6285, with 'superior' hydrogenogenic capacity, with the initiation of H_2 production after a shorter lag phase than for the other hydrogenogenic strains.

Comparative genomic analyses revealed a number of key differences at the molecular level that may underlie the distinct hydrogenogenic capacities observed for the different *P. thermoglucosidasius* strains. These include an extensive protein set which was unique to the hydrogenogenic strains, and differences in the protein complement of DSM 6285 and the other hydrogenogenic strains. The lack of clear phenotypic differences that can be linked to the variation at the protein level suggests that there may be other factors underlying the differences observed in H_2 production times for DSM 6285, DSM 2542^T and DSM 2543. For example, it is possible that some of the proteins assigned to COG category S (unknown function) play a role in these variable phenotypes. Similarly, proteins of unknown function among the protein families unique to the non-hydrogenogenic *P. thermoglucosidasius* DSM 21625 and unique to the hydrogenogenic strains DSM 2542^T, DSM 2543 and DSM 6285 may also have an effect on the ability of the different strains to produce hydrogen.

Furthermore, SNPs in the CODH-NiFe hydrogenase loci, and the associated amino acid mutations and deletions in and adjacent to this locus, may also be responsible for the difference in hydrogenogenic phenotype. In particular, a deletion was

observed in the binding site for the transition state regulator Hpr upstream of the CODH-NiFe hydrogenase locus on the non-hydrogenogenic strain *P. thermoglucosidasius* DSM 21625. In *B. subtilis*, Hpr has been shown to play a role in the up- and down-regulation of a range of genes involved in post-exponential phase processes such as motility, extracellular enzymes synthesis, antibiotic production and sporulation (Inaoka *et al.*, 2009; Kallio *et al.*, 1991; Kodgire & Pao, 2009). As the consumption of CO and production of H_2 by the three H_2-producing *P. thermoglucosidasius* strains occurs in the post-exponential phase, a role for an Hpr-like regulator in the control of this capacity is plausible.

It cannot be excluded that factors other than observable genetic differences may underlie these distinct phenotypes. For example, the shorter lag phase between aerobic growth and the WGS-driven H_2 production may be due to differences in the O_2 sensitivity of the CODH-hydrogenase complex of the hydrogenogenic strains. Proteomic, gene expression and biochemical analyses could shed further light on the phenotypic differences observed in this study.

3.5 CONCLUSIONS

P. thermoglucosidasius strains differ in their capacity to produce H_2 via the CODH-NiFe hydrogenase-catalyzed WGS reaction. This may be correlated to extensive differences we observed in terms of the proteins encoded on the genomes of the strains, as well as to SNPs in the CODH-NiFe hydrogenase loci. Further gene expression, proteomic and physiological characterization will be undertaken to elucidate the factors underlying the distinct hydrogenogenic phenotypes. This data will be crucial in the selection of *P. thermoglucosidasius* strains and the optimization of fermentation conditions for incorporation in bio industrial H_2 production strategies.

REFERENCES FOR CHAPTER 3

Andrews S, Mattatall NR, Arnold D, Hill BC (2005) Expression, purification, and characterization of the Cu_A–cytochrome c domain from subunit II of the *Bacillus subtilis* cytochrome caa_3 complex in *Escherichia coli*. *Protein Expression and Purification*. **2**:227-235. DOI:10.1016/j.pep.2004.11.009.

Bankevich A, Nurk S, Antipov D, Gurevich AA, Dvorkin M, Kulikov AS, Lesin VM, Nikolenko SI, Pham S, Prjibelski AD, Pyshkin AV, Sirotkin AV, Vyahhi N, Tesler G, Alekseyev MA, Pevzner PA (2012) SPAdes: a new genome assembly algorithm and its applications to single-cell sequencing. *Journal of Computational Biology*. **5**: 455-477. DOI:10.1089/cmb.2012.0021.

Bengtsson J, Tjalsma H, Rivolta C, Hederstedt L (1999) Subunit II of *Bacillus subtilis* cytochrome *c* oxidase is a lipoprotein. *Journal of Bacteriology*. **181**: 685-688.

Bosi E, Donati B, Galardini M, Brunetti S, Sagot MF, Lió P, Crescenzi P, Fani R, Fondi M (2015) MeDuSa: a multi-draft based scaffolder. *Bioinformatics*. **31**: 2443–2451. DOI:10.1093/bioinformatics/btv171.

Chen K, Lio C, Huang S, Shen H, Shieh Y, Chiu H, Lu C (2017): CSAR: a contig scaffolding tool using algebraic rearrangements. *Bioinformatics*. **34**: 109-111. DOI:10.1093/bioinformatics/btx543.

Darling AE, Mau B., Perna, NT. (2010) progressiveMauve: multiple genome alignment with gene gain, loss and rearrangement. *PLoS One 5*. e11147. DOI:10.1371/journal.pone.0011147.

De Maayer P, Brumm PJ, Mead DA, Cowan DA (2014) Comparative analysis of the *Geobacillus* hemicellulose utilization locus reveals a highly variable target for improved hemicellulolysis. *BMC Genomics*. **15**: 836. DOI:10.1186/1471-2164-15-836.

Eitinger T, Mandrand-Berthelot MA (2000) Nickel transport systems in microorganisms. *Archives of Microbiology*. **173**: 1-9.

Emms DM, Kelly S (2015) OrthoFinder: solving fundamental biases in whole genome comparisons dramatically improves orthogroup inference accuracy. *Genome Biology*. **16**:157. DOI:10.1186/s13059-015-0721-2.

Hall TA (1999) Bioedit: a user-friendly biological sequence alignment editor and analysis program for Windows 95/98/NT. *Nucleic Acids Symposiums Series*. **41**:95–8.

Huerta-Cepas J, Szklarczyk D, Forslund K, Cook H, Heller D, Walter MC, Rattei T, Mende DR, Sunagawa S, Kuhn M, Jensen LJ, von Mering C, Bork P (2016) eggNOG 4.5: a hierarchical orthology framework with improved functional annotations for eukaryotic, prokaryotic and viral sequences. *Nucleic Acids Research*. **44 D1**: D286-D293. DOI:0.1093/nar/gkv1248.

Inaoka T, Wang G, Ochi K (2009) ScoC regulates bacilysin production at the transcription level in *Bacillus subtilis*. *Journal of Bacteriology*. **191**: 7367-7371. DOI:10.1128/JB.01081-09.

Kallio PT, Fagelson JE, Hoch JA, Strauch MA (1991) The transition state regulator Hpr of *Bacillus subtilis* is a DNA-binding protein. *Journal of Biological Chemistry*. **266**: 13411-13417.

Kodgire P, Rao KK (2009) *hag* expression in *Bacillus subtilis* is both negatively and positively regulated by ScoC. *Microbiology*. **155**: 142-149. DOI:10.1099/mic.0.021899-0.

Lee I, Ouk Kim Y, Park SC, Chun J (2016) OrthoANI: An improved algorithm and software for calculating average nucleotide identity. *International Journal of Systematic and Evolutionary Microbiology*. **66**: 1100-1103. DOI:10.1099/ijsem.0.000760.

Marchler-Bauer A, Bryant SH (2004) CD-Search: protein domain annotations on the fly. *Nucleic Acids Research*. **32**(W): 327-331. DOI:10.1093/nar/gkh454.

Meier-Kolthoff JP., Auch AF, Klenk HP, Göker M. (2013) Genome sequence-based species delimitation with confidence intervals and improved distance functions. *BMC Bioinformatics*. **14:** 1–14. DOI:10.1186/1471-2105-14-60.

Mohr T, Aliyu H, Küchlin R, Polliack S, Zwick M, Neumann A, Cowan D, de Maayer P (2018a) CO-dependent hydrogen production by the facultative anaerobe *Parageobacillus thermoglucosidasius*. *Microbial Cell Factories*. **17**:108. DOI:10.1186/s12934-018-0954-3.

Overbeek R, Olson R, Pusch GD, Olsen GJ, Davis JJ, Disz T. Edwards RA, Gerdes S, Parrello B, Shukla M, Vonsetin V, Wattam AR, Xia F, Stevens R (2014) The SEED and the Rapid Annotation of microbial genomes using Subsystems Technology (RAST). *Nucleic Acids Research*. **42**(Database issue): D206-214. DOI:10.1093/nar/gkt1226.

Solovyev V, Salamov A (2011) Automatic annotation of microbial genomes and metagenomic sequences. In: Metagenomics and its applications in agriculture, biomedicine and environmental studies. *Ed. Robert W, Nova Science Publishers*. New York, USA p. 61-78.

Suzuki Y, Kishigami T, Inoue K, Mizoguchi Y, Eto N, Takagi M, Abe S (1983) *Bacillus thermoglucosidasius* sp. Nov. a new species of obligately thermophilic bacilli. I*nternational Journal of Systematic and Evolutionary Microbiology*. **4**: 487-495

Thompson JD, Higgins DG, Gibson TJ (1994) Clustal W: improving the sensitivity of progressive multiple sequence alignment through sequence weighting, position-specific gap penalties and weight matrix choice. *Nucleic Acids Research*. **22**: 4673-4680.

Tirado-Acevedo O, Chinn MS, Grunden AM (2010) Production of biofuels from synthesis gas using microbial catalysts. *Advances in Applied Microbiology*. **70**:57–92.

Tfsitescan: http://www.ifti.org/Tfsitescan. Accessed 20 April 2018.

van der Oost J, von Wachenfeldt C, Hederstedt L, Saraste M (1991) *Bacillus subtilis* cytochrome oxidase mutants: biochemical analysis and genetic evidence for two aa_3-type oxidases. *Molecular Microbiology*. **5**: 2063-2072.

Zeigler DR (2001) The Genus *Geobacillus*. Introduction and Strain Catalog. *Bacillus Genetic Stock Center. Catalog of Strains*. **7(3)**.

Zhou Y, Liang Y, Lynch KH, Dennis JJ, Wishart DS (2011) PHAST: a fast phage search tool. *Nucleic Acids Research* **39**(Web Server issue):W347-52. DOI:10.1093/nar/gkr485.

4 ACETATE PRODUCTION FROM OXYGEN CONTAINING WASTE GAS

This chapter is partially based on the submitted manuscript

ACETOGENIC FERMENTATION FROM OXYGEN CONTAINING WASTE GAS.

Teresa Mohr*, Alba Infantes*, Lars Biebinger, Pieter de Maayer, Anke Neumann

*co-first author

The findings of this chapter are submitted for publication.

Authors' contribution to this publication

Teresa Mohr designed the experiments together with **Alba Infantes**, conducted experiments, analysed the data and drafted the manuscript.

Alba Infantes performed experiments and edited the manuscript.

Lars Biebinger performed the experiments with Teresa Mohr and Alba Infantes.

Pieter de Maayer contributed to scientific discussion and drafted the manuscript.

Anke Neumann supervised the project and reviewed the manuscript.

4.1 INTRODUCTION AND ABSTRACT

Recently, there has been increased interest in the production of value-added chemicals such as acetate and 2,3-butanediol via environmentally friendly strategies. At present, the production of most of these value-added chemicals is still largely reliant on the use of fossil fuels as substrate (Hatti-Kaul *et al.*, 2007; Zhang *et al.*, ,2017). One potential alternative involves the use of synthesis gas (syngas) which consists primarily of hydrogen (H_2), carbon dioxide (CO_2) and carbon monoxide (CO) (Teixeira *et al.*, 2018). Acetogens can use waste gas substrates (CO, CO_2, H_2) to produce chemicals such as acetate or ethanol, but as the feed gas often contains O_2, which inhibits acetogen growth and product formation, a cost-prohibitive chemical O_2 removal step is necessary.

In this chapter a two-stage microbial system to facilitate acetate production using O_2-containing waste gas was developed. In the first phase the facultatively anaerobic carboxydotrophic thermophile *Parageobacillus thermoglucosidasius* was used to consume residual O_2 and produce H_2 and CO_2 via the WGS reaction. These products were subsequently used by *Clostridium ljungdahlii* for the synthesis of acetate via the W-L pathway.

4.2 MATERIALS AND METHODS

4.2.1 Microorganisms and media

P. thermoglucosidasius DSM 6285 and *Clostridium ljungdahlii* DSM 13528^T were obtained from the Deutsche Sammlung von Mikroorganismen und Zellkulturen (DSMZ, Braunschweig, Germany).

P. thermoglucosidasius DSM 6285 was cultivated in mLB (modified Luria-Bertani) medium: tryptone (10 g/L), yeast extract (5 g/L), NaCl (10 g/L), 1.25 ml/L NaOH (10% w/v), and 1 ml/L of each of the filter-sterilized stock solutions 1.05 M nitrilotriacetic acid, 0.59 M $MgSO_4.7H_2O$, 0.91 M $CaCl_2.2H_2O$ and 0.04 M $FeSO_4.7H_2O$ (Zeigler, 2001). A first (20 ml) pre-culture was grown for 24 h and a second (20 ml) pre-culture was inoculated to an absorbance (OD_{600}) of 0.1 from the first pre-culture and incubated for 4 h. Both pre-cultures were grown aerobically at 60 °C and 120 rpm (Infors Thermotron, Infors AG, Bottmingen, Switzerland) in 20 ml mLB.

Clostridium ljungdahlii DSM 13528^T was pre-cultured in modified GA-based medium (Groher and Weuster-Botz, 2016) containing 20 g/L 2-(N- morpholino) ethansulfonic acid (MES), 1 g/L NH_4Cl, 0.3 g/L KCl, 0.23 g/L KH_2PO_4, 0.5 g/L $MgSO_4.7H_2O$, 2.25 g/L NaCl, 2 g/L yeast extract, 0.15 g/L $CaCl_2.2H_2O$ and 0.001 g/L resazurin (Groher and Weuster-Botz, 2016). The pH of the medium was adjusted to 6.0 with KOH, and distributed in bottles, which were anaerobized using a gas mixture containing 20 vol- % carbon dioxide in nitrogen (Air Liquide, France). After autoclaving, 1 g/L of Cysteine $HCl.H_2O$, 10 g/L of fructose, 1 ml/L of trace element solution (4 g/L $FeSO_4.7H_2O$, 3 mg/L $Na_2SeO_3.5H_2O$, 4 mg/L $Na_2WO_4.2H_2O$, 3 g/L $FeCl_2.4H_2O$, 140 mg/L $ZnCl_2$, 200 mg/L $MnCl_2.4H_2O$, 12 mg/L H_3BO_3, 380 mg/L $CoCl_2.6H_2O$, 4 mg/L $CuCl_2.2H_2O$, 48 mg/L $NiCl_2.6H_2O$, 72 mg/L $Na_2MoO_4.2H_2O$) and 10 ml/L of vitamin solution (4 mg/L biotin, 4 mg/L folic acid, 20 mg/L pyridoxine, 10 mg/L Thiamine-$HCl.2H_2O$, 10 mg/L riboflavin, 10 mg/L

nicotinic acid, 10 mg/L calcium pantothenate, 0.2 mg/L cobalamin, 10 mg/L 4-aminobenzoic acid and 10 mg/L liponic acid) were added.

For pre-cultivation of *C. ljungdahlii* a glycerol stock (1 ml) was transferred anaerobically to a serum bottle containing 50 ml GA medium and incubated for 48 h. A total of 5 ml of the latter culture was transferred anaerobically to 50 ml of fresh GA medium and cultivated at 37 °C and 120 rpm. The latter step was repeated to generate the inoculum for the sequential culture.

4.2.2 Experimental set up

Stoppered flasks (250 ml) containing 50 ml of modified Luria Bertani (mLB) medium and with an initial gas atmosphere of CO and air (50:50 ratio) were inoculated with 1 ml of second pre-culture of *P. thermoglucosidasius* and cultivated for 70 h at 60 °C and 120 rpm. Subsequently (t=70 h), 5 ml of *C. ljungdahlii* pre-culture was added to the *P. thermoglucosidasius* culture. Incubation of the *P. thermoglucosidasius*/*C. ljungdahlii* cultures was performed at 37 °C and 120 rpm. The experiments were performed in quadruplicate for a duration of 240 h (Figure 17)

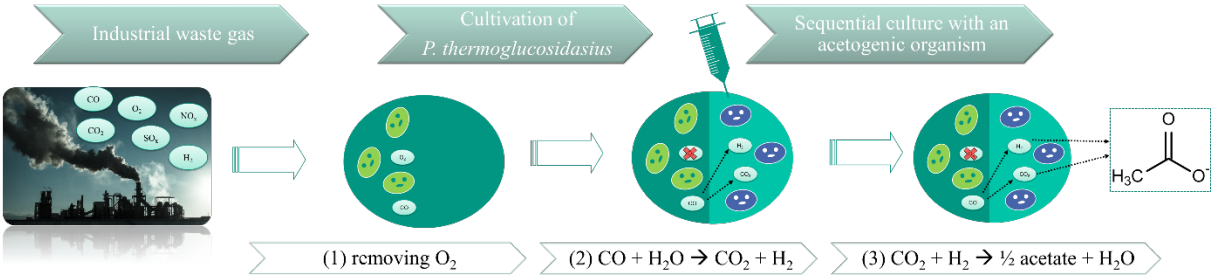

Figure 17: Schematically pathway of the combined WGS reaction and Wood-Ljungdahl pathway.

4.2.3 Analytical methods

Growth was routinely monitored by taking 1 ml culture samples and performing absorbance (OD_{600}) measurements using an Ultrospec 1100 pro spectrophotometer (Amersham Biosciences, USA). Acetate concentrations were similarly monitored using the Roche Yellow line enzymatic assay (Hoffmann- La Roche, Switzerland). The gas composition in the bottles was measured at each sample time using a 300 Micro GC gas analyzer (Inficon, Bad Ragaz, Switzerland). Pressure was measured before and after sample taking using a manometer (GDH 14 AN, Greisinger electronic, Regenstauf, Germany). Gas composition was calculated using the ideal gas law as previously described (Mohr *et al.*, 2018a).

4.3 RESULTS

4.3.1 Pre-culturing with *P. thermoglucosidasius* supports the anaerobic growth of *C. ljungdahlii*

In the first phase of the sequential fermentation *P. thermoglucosidasius* was grown in 50 ml modified Luria Bertani (mLB) medium with an initial gas atmosphere of CO and air (50:50) (Figure 18). After 70 h, when all O_2 was consumed, the culture reached an absorbance (OD_{600}) of 0.732 ± 0.027 and pH of 6.21 ± 0.04 (Figure 18). Previously we have observed that when the O_2 is consumed, the growth of *P. thermoglucosidasius* also plateaus (Mohr *et al.*, 2018a; Mohr *et al.*, 2018b). To ensure that the increase of OD_{600} and acetate during the second phase is not due to *P. thermoglucosidasius* on its own, a control experiment without the addition of *C. ljungdahlii* was conducted (Figure 19). When *C. ljungdahlii* was added to the *P. thermoglucosidasius* culture 70 h after the first phase, the *P. thermoglucosidasius*/*C. ljungdahlii* sequential culture reached a maximum absorbance of 1.316 ± 0.157 approximately 23 h after the latter culture was added (Figure 18). This indicates that the strict anaerobe *C. ljungdahlii* is able to grow in the medium after *P. thermoglucosidasius* exhausts the O_2 from the gas atmosphere. The medium pH dropped drastically once *C. ljungdahlii* was added, from a pH of 6.20 ± 0.04 pre-addition to a pH of 5.61 ± 0.05 post-addition of the latter strain (Figure 18). However, the pH continued to decline throughout the experiment, which can be correlated to active metabolism and acetate production by *C. ljungdahlii*.

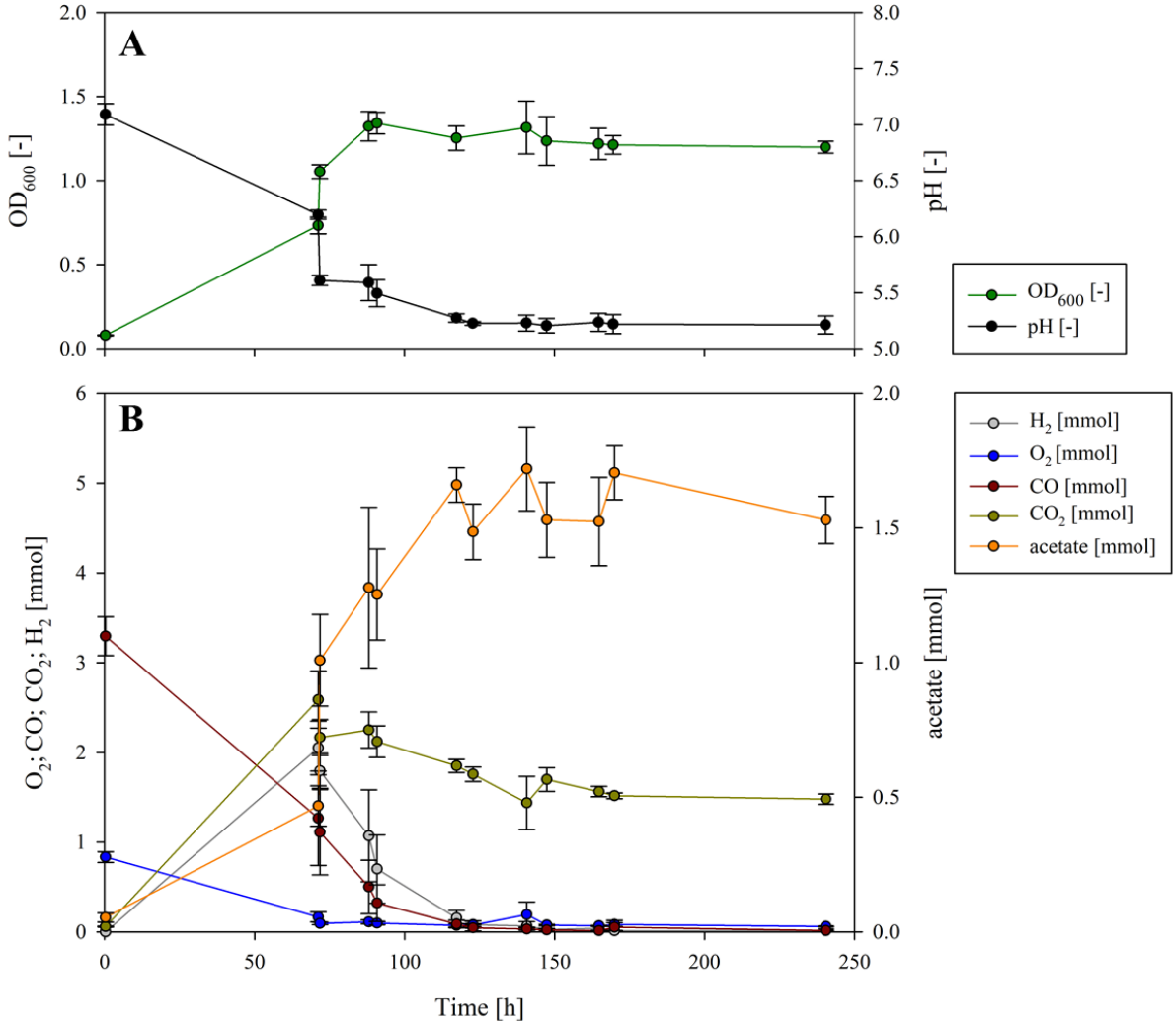

Figure 18: Growth and pH (A) and gas composition and acetate production (B) of the sequential cultivation of *P. thermoglucosidasius* and *C. ljungdahlii*. The dotted line presents the inoculation of *C. ljungdahlii* (A) The measured OD_{600} (dark green) increased after 70 h, and at the same time the pH (black) decreased due to the inoculation with *C. ljungdahlii*. Growth continued until 93 h (23 h after inoculation with the second organism), and then it plateaued. As a result of the metabolic activity, the culture broth was acidified to a pH of 5.2. (B) O_2 (blue) had already been consumed before the second phase, but some CO (dark red) was still left. After inoculation with *C. ljungdahlii*, CO_2 (olive) and H_2 did not accumulate any further, since they were used as building blocks by *C. ljungdahlii* to produce acetate (orange).

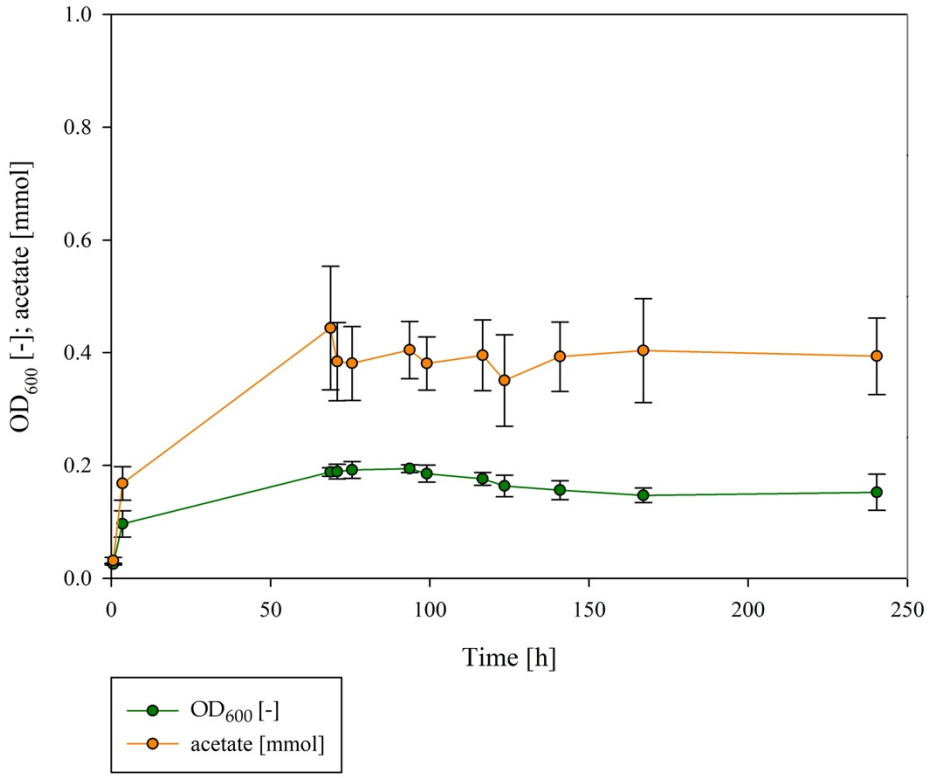

Figure 19: Growth curve and acetate production during the cultivation of *P. thermoglucosidasius* DSM 6285.

4.3.2 Sequential cultivation with *P. thermoglucosidasius* and *C. ljungdahlii* facilitates acetate production

In the post-aerobic phase *P. thermoglucosidasius* consumed 2.050 ± 0.117 mmol of CO, while 2.055 ± 0.023 and 2.646 ± 0.147 mmol of H_2 and CO_2 were produced via the WGS, respectively. Subsequently, both H_2 and CO decreased rapidly, being exhausted ~ 83 h after *C. ljungdahlii* was added. Similarly, CO_2 concentrations decreased, although 1.479 ± 0.058 mmol CO_2 were left at the end of the cultivation (after 240 h), due to the fact that 2 moles of H_2 are needed per mol of CO_2 as per the stoichiometry of the W-L pathway: $2\ CO_2 + 4\ H_2 \rightarrow CH_3COOH + 2\ H_2O$ (Ragsdale, 2008) (Figure 18).

The decrease in concentrations of these three gases correlated with an increase in acetate concentration. Some acetate (0.47 ± 0.07 mmol) was already observed during the first phase. This may be linked to mixed acid fermentation by *P. thermoglucosidasius* after O_2 is consumed (Hussein *et al.*, 2015). However, when

P. thermoglucosidasius was cultivated on its own, no further increase in acetate concentration was observed (Figure 19). The addition of *C. ljungdahlii* resulted in a further spike in acetate concentration (1.01 ± 0.17 mmol – an increase of 0.54 ± 0.22 mmol). This is associated with acetate production by *C. ljungdahlii* in the pre-culture in GA medium containing fructose as carbon source (Tirado-Acevedo *et al*., 2011). However, this spike was unavoidable in the current experimental set-up as the strict anaerobic nature of *C. ljungdahlii* precludes that addition of a washing step of the pre-culture inoculum. However, acetate concentration increased concomitantly with H_2, CO and CO_2 consumption during the second phase, reaching a final concentration of 1.53 ± 0.09 mmol of acetate after *C. ljungdahlii* was added, suggesting that in the absence of additional exogenous carbon sources *C. ljungdahlii* could successfully use the H_2 and CO_2 produced by *P. thermoglucosidasius* as building blocks for acetate via the W-L pathway.

4.4 DISCUSSION

Microbial conversion of syngas into value-added chemicals may provide a sustainable and cost-effective alternative to current industrial strategies. However, most known syngas fermenters are strict anaerobes, which impacts the use of syngas sources which contain even low concentrations of O_2. Besides, very few acetogens have been shown to tolerate only trace amounts of O_2 (Karnholz *et al*., 2002; Takors *et al*., 2018). As such, expensive and often environmentally unfriendly O_2 removal steps are necessary to facilitate effective syngas bioconversion (Heijstra *et al*., 2017). Here we have demonstrated that the facultative anaerobe *P. thermoglucosidasius* provides a biological means for the removal of toxic concentrations of O_2, which allowed for the subsequent growth of the strict anaerobe *C. ljungdahlii*. Moreover, the production of H_2 and CO_2 by *P. thermoglucosidasius* via the WGS reaction provides the building blocks for the synthesis of acetate by *C. ljungdahlii* via the W-L pathway.

The utilization of a thermophile in the first phase of this process presents some additional advantages in that hot flue gases resulting from industrial processes will not need to be cooled down to such a great extent. Most pertinently, the consumption of CO enables a near stoichiometric conversion of CO to H_2 and CO_2, without CO being lost in biomass formation (Mohr *et al*., 2018a). Among other aerobic CO-oxidizing organism, where CO is also used for biomass formation (O_2 + 2.19 CO → 1.83 CO_2 +0.36 cell carbon) (Ragsdale, 2004), *P. thermoglucosidasius* is able to catabolize the entire amount of CO for H_2 and CO_2 production. Hence, more substrate for the acetogenesis is available. The overall yield of the established sequential culture is thus higher than by using other CO metabolizing organisms (King and Weber, 2007).

4.5 CONCLUSIONS

The sequential fermentation system presented here may thus serve as a cost-effective and environmentally friendly methodology for the production of value-added chemicals where it circumvents some of the pitfalls of working with strict anaerobic syngas fermenters while simultaneously linking the fermentative pathways of different taxa for the production of value-added chemicals by a second organism (Takors *et al.,* 2018). Future research will evaluate the application of this sequential fermentation with *P. thermoglucosidasius* and other mesophilic and thermophilic bacteria for the production of a wide variety of bulk chemicals.

REFERENCES FOR CHAPTER 4

Groher A, Weuster-Botz D (2016) Comparative reaction engineering analysis of different acetogenic bacteria for gas fermentation. *Journal of Biotechnology*. **228:** 82–94. DOI:10.1016/j.jbiotec.2016.04.032.

Hatti-Kaul R, Törnvall U, Gustafsson L, Börjesson P (2007) Industrial biotechnology for the production of bio-based chemicals - a cradle-to-grave perspective. *Trends in Biotechnology*. **25(3):** 119-124. DOI:10.1016/j.tibtech.2007.01.001.

Heijstra BD, Leang C, Juminaga A (2017) Gas fermentation: cellular engineering possibilities and scale up. *Microbial Cell Factories*. **16**:60. DOI:10.1186/s12934-017-0676-y.

Hussein AH, Lisowska BK, Leak DJ (2015) The Genus *Geobacillus* and their biotechnological potential. *Advances in Applied Microbiology*. **92**:1-48. DOI:10.1016/bs.aambs.2015.03.001.

Karnholz A, Küsel K, Gößner A, Schramm A, Drake HL (2002) Tolerance and metabolic response of acetogenic bacteria toward oxygen. *Applied and Environmental Microbiology*. **68**:1005–1009. DOI:10.1128/AEM.68.2.1005-1009.2002.

King GM, Weber CF (2007) Distribution, diversity and ecology of aerobic CO-oxidizing bacteria. *Nature Reviews Microbiology*. **5**:107–118. DOI:1 0.1038/nrmicro1595.

Mohr T, Aliyu H, Küchlin R, Polliack S, Zwick M, Neumann A, Cowan D, de Maayer P (2018a) CO-dependent hydrogen production by the facultative anaerobe *Parageobacillus thermoglucosidasius*. *Microbial Cell Factories*. **17**:108. DOI:10.1186/s12934-018-0954-3.

Mohr T, Aliyu H, Küchlin R, Zwick M, Neumann A, Cowan D, de Maayer P (2018b) Comparative genomic analysis of *Parageobacillus thermoglucosidasius* strains

with distinct hydrogenogenic capacities. *BMC Genomics*. **19**:880. DOI:10.1186/s12864-018-5302-9.

Ragsdale SW (2004) Life with carbon monoxide. *Critical Reviews in Biochemistry and Molecular Biology*. **39**:165–195. DOI:10.1080/10409230490496577.

Ragsdale S W (2008) Enzymology of the Wood-Ljungdahl pathway of acetogenesis. *Annals of the New York Academy of Sciences*. **1125**:129–136. DOI:10.1196/annals.1419.015.

Takors R, Kopf M, Mampel J, Bluemke W, Blombach B, Eikmanns B, Bengelsdorf FR, Weuster-Botz D, Dürre P (2018) Using gas mixtures of CO, CO_2 and H_2 as microbial substrates: the do's and don'ts of successful technology transfer from laboratory to production scale. *Microbial Biotechnology*. **11**:606–625. DOI:10.1111/1751-7915.13270.

Teixeira LV, Moutinho LF, Romão-Dumaresq AS (2018) Gas fermentation of C1 feedstocks: commercialization status and future prospects. *Biofuels, Bioproducts and Biorefining* **12:**1103–1117. DOI:10.1002/bbb.1912.

Tirado-Acevedo O, Cotter JL, Chinn MS, Grunden AM (2011) Influence of Carbon Source Pre-Adaptation on *Clostridium ljungdahlii* Growth and Product Formation. *Journal of Bioprocessing & Biotechniques*. **01**:1–5. DOI:10.4172/2155-9821.s2-001.

Zeigler DR (2001) The Genus *Geobacillus*. Introduction and Strain Catalog. *Bacillus Genetic Stock Center. Catalog of Strains*. **7(3)**.

Zhang Y, Liu D, Chen Z (2017) Production of C2-C4 diols from renewable bioresources: New metabolic pathways and metabolic engineering strategies. *Biotechnology of Biofuels*. **10**:1–20. DOI:10.1186/s13068-017-0992-9.

5 INVESTIGATION OF THE EFFECTS OF DIFFERENT OPERATING PARAMETERS ON H_2 PRODUCTION

This chapter is partially based on the submitted manuscript

INVESTIGATION OF THE EFFECTS OF DIFFERENT OPERATING PARAMETERS ON H_2 PRODUCTION BY *PARAGEOBACILLUS THERMOGLUCOSIDASIUS* DSM 6285.

Teresa Mohr, Habibu Aliyu, Lars Biebinger, Roman Gödert, Alex Hornberger, Don Cowan, Pieter de Maayer, Anke Neumann

The findings of this chapter are submitted for publication.

Authors' contribution to this publication

Teresa Mohr designed all experiments and analysed the data, performed the cultivation with Lars Biebinger, Roman Gödert und Alexander Hornberger the experiments and drafted the manuscript.

Habibu Aliyu contributed to the experimental design and drafted the manuscript.

Lars Biebinger, **Roman Gödert** und **Alexander Hornberger** performed the experiments with Teresa Mohr.

Don Cowan edited the manuscript.

Pieter de Maayer conceived the experiments and drafted the manuscript.

Anke Neumann contributed to the experimental design and reviewed the manuscript.

5.1 INTRODUCTION AND ABSTRACT

Comparative analysis revealed different hydrogenogenic capacities of different *P. thermoglucosidasius* strains. As highlighted in Chapter 2, all the hydrogenogenic strains showed the same pattern of growth and H_2 production, subdivided in three phases: (1) rapid aerobic growth (2) a lag phase and (3) a H_2 production phase. In contrast to all hydrogenogenic strains, the strain DSM 6285 commenced H_2 production earlier than the other hydrogenogenic strains. This strain was selected for further investigations. To incorporate this particular strain in industrial H_2 production approaches, further experiments have to be undertaken to optimize the process, more precisely to decrease the lag phase (phase 2) and increase the H_2 production rate in phase 3.

In this chapter, the effects of different operational parameters on H_2 production were investigated. These included different growth temperatures, pre-culture ages and inoculum sizes, as well as different pHs and concentrations of nickel and iron in the medium.

All of the tested parameters were observed to have a substantive effect on both H_2 yield and (specific) production rates. Parameters such as temperature enhanced the optimum growth conditions of *P. thermoglucosidasius*, while others (age of pre-culture and inoculum size) indicated that the H_2 production is linked to the physiological state of the organism rather than to the amount of biomass. A combination of optima for each of these parameters can be used to improve H_2 production with a view of commercialization of this process.

5.2 MATERIALS AND METHODS

5.2.1 Microorganism and medium

P. thermoglucosidasius DSM 6285 was obtained from the Deutsche Sammlung von Mikroorganismen und Zellkulturen (DSMZ, Braunschweig, Germany) and stored at -80°C in glycerol (80%) stocks. The cultivation of *P. thermoglucosidasius* DSM 6285 was performed in 50 mLB (modified Luria-Bertani) medium (Zeigler, 2001). This medium contains tryptone (1% w/v), yeast extract (0.5% w/v), NaCl (0.5% w/v), 1.25 ml/L NaOH (10% w/v) and 1 ml/L of each of the filter-sterilized stock solutions 1.05 M nitrilotriacetic acid, 0.59 M $MgSO_4.7H_2O$, 0.91 M $CaCl_2.2H_2O$ and 0.04 M $FeSO_4.7H_2O$.

5.2.2 Inoculum preparation

A two-step pre-culture approach was adopted for this study. In the first pre-culture, 20 ml mLB medium were inoculated with 20 µl of glycerol stock and cultivated for 24 h. The 2nd pre-culture was inoculated from the first to an initial absorbance (OD_{600}) of 0.1. All pre-cultures were cultivated aerobically in 100 ml shake flasks containing 20 ml mLB medium at 60 °C and 120 rpm (Infors Thermotron, Infors AG, Bottmingen, Switzerland). After 12 hours, an appropriate amount of the 2nd pre-culture was added to 250 ml stoppered serum bottles (containing 50 ml mLB medium total) in an initial gas atmosphere ratio of air and CO at 1 bar atmospheric pressure (at 25 °C). Air was required during all set-ups to ensure biomass production prior to the anaerobic H_2 production. The cultivations were performed in triplicate for a duration of 82 h.

5.2.3 Experimental set up

The effects of different operational parameters on *P. thermoglucosidasius* H_2 production were investigated as per Table 2. To examine the effects of temperature and pH on growth and H_2 production, the cultures were maintained at 50 °C, 55 °C and 60 °C. The pH was adjusted to 5.5, 7.0 and 8.5 using either NaOH (1 M) or HCl

(1 M). Both the CODH and group 4a hydrogenase in *P. thermoglucosidasius* are comprised of a Ni-Fe metallocenter (Mohr *et al.*, 2018a). To determine the effects of higher iron (Fe^{2+}) concentrations on hydrogenogenesis, double the amount of $FeSO_4.7H_2O$ (0.08 mM) normally included in mLB medium (0.04 mM; Mohr *et al.*, 2018a) was added in one experimental set-up. As the mLB medium does not include the addition of nickel (Ni^{2+}), one set-up was prepared containing 0.3 mM $NiSO_4.6H_2O$. The results were compared to those obtained by growing *P. thermoglucosidasius* DSM 6285 in mLB containing only 0.04 mM $FeSO_4.7H_2O$ and no exogenous nickel. The effects of different initial gas compositions on H_2 production were also evaluated using 36:64, 50:50 and 75:25 CO:air ratios. The influence of incubation time and volume of the inoculum were studied by varying the incubation times of the 2nd pre-culture from 4 h, 12 h to 24 h and by using inoculum volumes of the 2nd pre-culture of 2%, 10% and 20% of the final volume.

To investigate the combination of the parameters which resulted in a superior H_2 production, a further experiment was conducted. Here, one condition for each parameter was chosen based on the maximum production rate and highest obtained yield: 55 °C, pH 7.0 (initial), addition of $FeSO_4.7H_2O$ (0.08 mM), 75:25 CO:air ratios (initial gas atmosphere), 4 h incubation time of the 2nd pre-culture, 10% inoculum size. To validate whether the tested parameters have a positive effect on the H_2 production, the experimental set up as in Mohr *et al.* (2018b) was used as a control (60 °C, pH 7.0, addition of 0.04 mM $FeSO_4.7H_2O$, 50:50 CO:air ratios (initial gas atmosphere), 12 h incubation time of the 2nd pre-culture, 2% inoculum size).

Table 2: Overview of the evaluated processing parameters. Different operational parameters were investigated for optimizing hydrogen production: cultivation temperature, initial pH, addition of 0.3 mM $NiSO_4.6H_2O$ + 0.04 mM $FeSO_4.7H_2O$ or 0.08 mM $FeSO_4.7H_2O$, initial gas composition (CO:air ratio), incubation time of 2nd pre-culture and inoculum size.

	Temp.	pH	+$NiSO_4.6H_2O$/ $FeSO_4.7H_2O$	Initial gas composition (CO:air)	Incubation time of 2nd pre-culture	Inoculum size
Temp.	50 °C	7.0	0.0 mM +0.04 mM	50:50	12 h	2%
	55 °C	7.0	0.0 mM +0.04 mM	50:50	12 h	2%
	60 °C	7.0	0.0 mM +0.04 mM	50:50	12 h	2%
pH	60 °C	5.5	0.0 mM +0.04 mM	50:50	12 h	2%
	60 °C	7.0	0.0 mM +0.04 mM	50:50	12 h	2%
	60 °C	8.5	0.0 mM +0.04 mM	50:50	12 h	2%
+$NiSO_4.6H_2O$/ $FeSO_4.7H_2O$	60 °C	7.0	0.0 mM +0.04 mM	50:50	12 h	2%
	60 °C	7.0	0.3 mM +0.04 mM	50:50	12 h	2%
	60 °C	7.0	0.0 mM +0.08 mM	50:50	12 h	2%
Initial gas composition (CO:air)	60 °C	7.0	0.0 mM +0.04 mM	75:25	12 h	2%
	60 °C	7.0	0.0 mM +0.04 mM	50:50	12 h	2%
	60 °C	7.0	0.0 mM +0.04 mM	36:64	12 h	2%
Incubation time of 2nd pre-culture	60 °C	7.0	0.0 mM +0.04 mM	50:50	4 h	2%
	60 °C	7.0	0.0 mM +0.04 mM	50:50	12 h	2%
	60 °C	7.0	0.0 mM +0.04 mM	50:50	24 h	2%
Inoculum size	60 °C	7.0	0.0 mM +0.04 mM	50:50	12 h	2%
	60 °C	7.0	0.0 mM +0.04 mM	50:50	12 h	10%
	60 °C	7.0	0.0 mM +0.04 mM	50:50	12 h	20%

5.2.4 Analytical methods

To determine growth, 1 ml of culture was removed from the bottles through the stoppers using a sterile needle and syringe and absorbance (OD600) was measured using an Ultrospec 1100 pro spectrophotometer (Amersham Biosciences, USA). The medium pH was determined from the same sample using a Profilab pH 597 pH meter (Xylem Analytics Germany Sales GmbH & Co. KG, WTW, Germany). To measure the gas compositions at each time point, a 3 ml gas sample was taken from the head-space of the bottle and injected to a 300 Micro GC gas analyzer (Inficon, Bad Ragaz, Switzerland), fitted with the columns Molsieve and PLOT Q. The column temperature was maintained at 80 °C for a duration of 180 s. Pressure was measured using a manometer (GDH 14 AN, Greisinger electronic, Regenstauf, Germany) prior to and after each sample was extracted from the bottles.

5.2.5 Data analysis

Gas compositions were calculated on the basis of the ideal gas law as previously described (Chapter 2.2.3). In order to compare the results of the different processing parameters, H_2 production rates and the specific production rate between different sampling time points were calculated as per following equation.

$$\text{Production rate} = \frac{\Delta\, m_{\text{hydrogen}}[mmol]}{\Delta\, time\ [h]}$$

$$\text{Specific production rate} = \frac{\Delta\, m_{\text{hydrogen}}[mmol]}{\Delta\, time\ [h] * OD_{600}}$$

The overall H_2 yield for each of the experiments was calculated as a function of CO consumption. This was done for the hydrogenogenic phase from the first time point where H_2 was detected (24 h post-inoculation) until the CO was consumed in most experimental set-ups (72 h post-inoculation):

$$\text{Yield} = \frac{\Delta\, \mathrm{H_2}[mmol]}{\Delta\, \mathrm{CO}\ [mmol]}$$

5.3 RESULTS

5.3.1 Effect of initial gas composition on H_2 production

To evaluate the effect of the initial gas composition, H_2 production with three distinct CO:air ratios (36:64, 50:50 and 75:25) was determined. Spectrophotometeric analysis of the biomass showed that, while *P. thermoglucosidasius* DSM 6285 grown in the 36:64 and 50:50 CO:air gas ratios grew to a maximum absorbance of 0.744 ± 0.103 (after 24 h) and 0.620 ± 0.137 (after 24 h), respectively, it grew substantially less and at a slower rate with a 75:25 CO:air ratio, with a maximum absorbance of 0.476 ± 0.028 after 72 h (Figure 20, Figure 22).

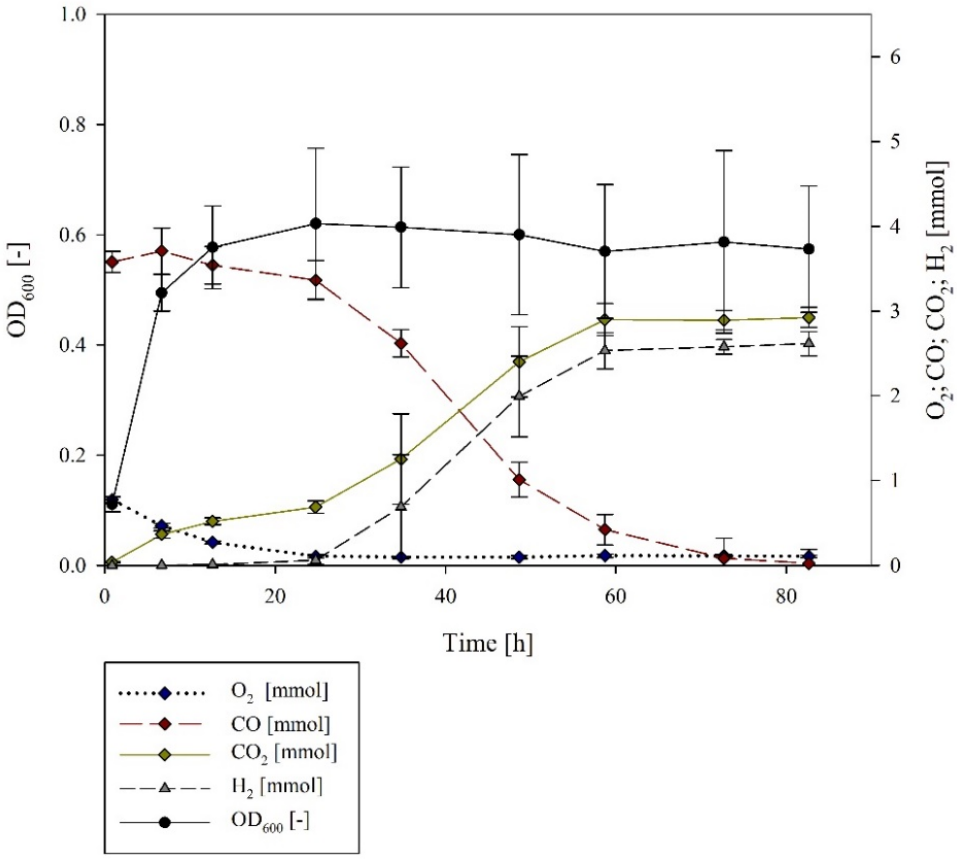

Figure 20: Growth curve and gas composition during the cultivation of *P. thermoglucosidasius* DSM 6285 in the control set up (60 °C, pH 7.0, addition of 0.04 mM FeSO4.7H2O, 50:50 initial gas atmosphere CO:air ratios, 12 h incubation time of the 2nd pre-culture, 2% inoculum size).

This suggests that the lower O_2 concentration affected effective biomass formation in the initial aerobic phase. O_2 reached its minimum for all tested gas compositions after ~24 h, while H_2 was initially detected at approximately the same time. CO was completely consumed at the end of the cultivations in all instances (Figure 21A). Maximum H_2 production rates were observed between the 34 h and 48 h sample points in all cases. The highest values were observed for *P. thermoglucosidasius* exposed to the 75:25% atmosphere, with 0.138 ± 0.009 mmol/h H_2 produced in this time frame. By contrast, substantially lower maximum production rates were observed with 36% and 50% CO in the initial gas atmosphere (0.073 ± 0.006 mmol/h and 0.094 ± 0.016 mmol/h, respectively) (Table 3). With an increasing initial CO concentration, the specific production rate increases from 0.104 ± 0.016 (36% CO), 0.163 ± 0.054 (50% CO) to 0.351 ± 0.038 (75% CO). The overall H_2 yield during the hydrogenogenic phase was also higher with the 75% CO concentration (0.807 ± 0.022 mmol H_2/mmol CO) than when 50% and 36% CO were present in the bottles (5.45 and 7.31% higher, respectively) (Table 3).

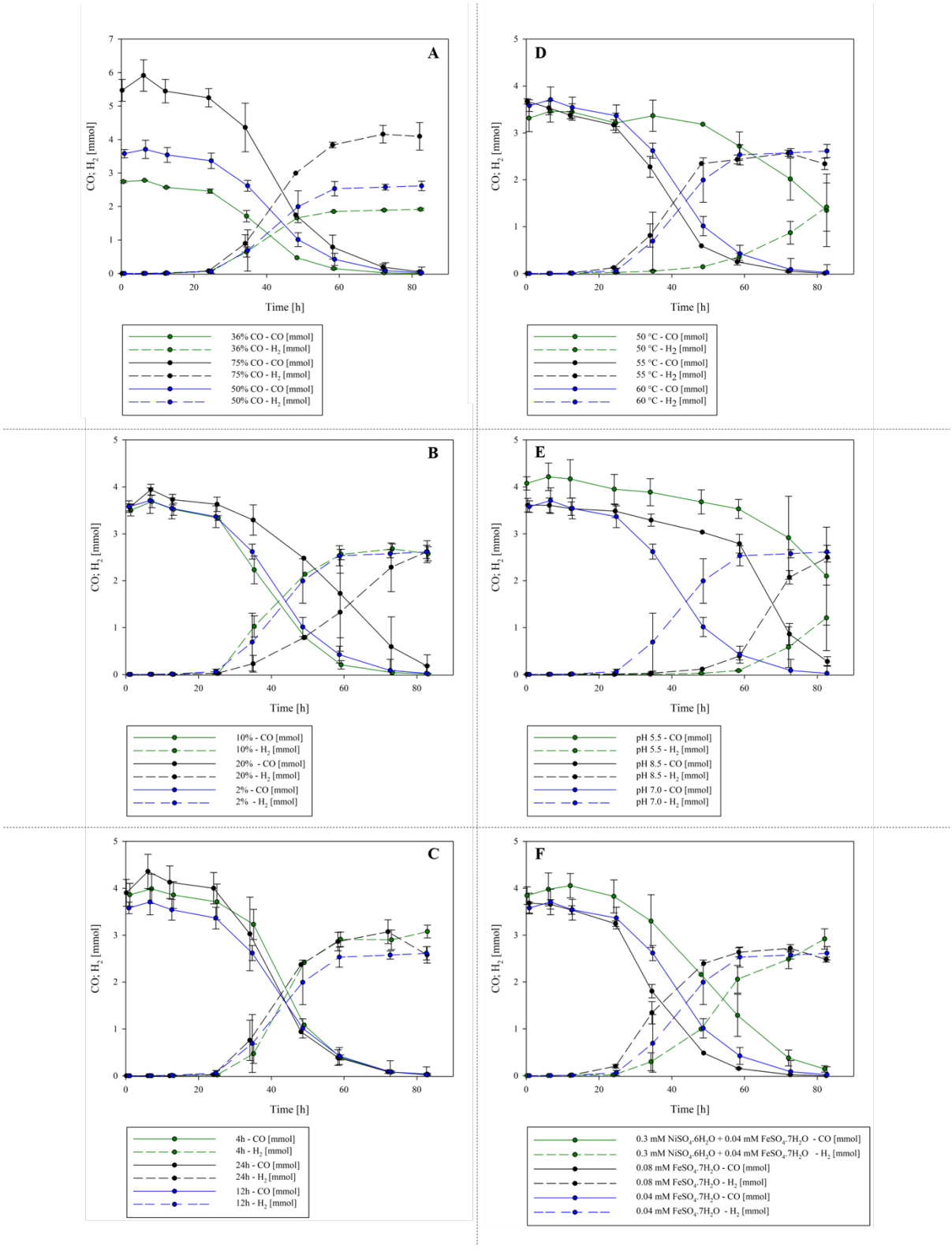

Figure 21: Effects of several operating parameters on CO consumption and H_2 production during the cultivation of *P. thermoglucosidasius*. (A) initial gas composition, (B) inoculum size, (C) age of 2nd pre-culture, (D) temperature, (E) initial pH and (F) addition of $FeSO_4.7H_2O$ and $NiSO_4.6H_2O$.

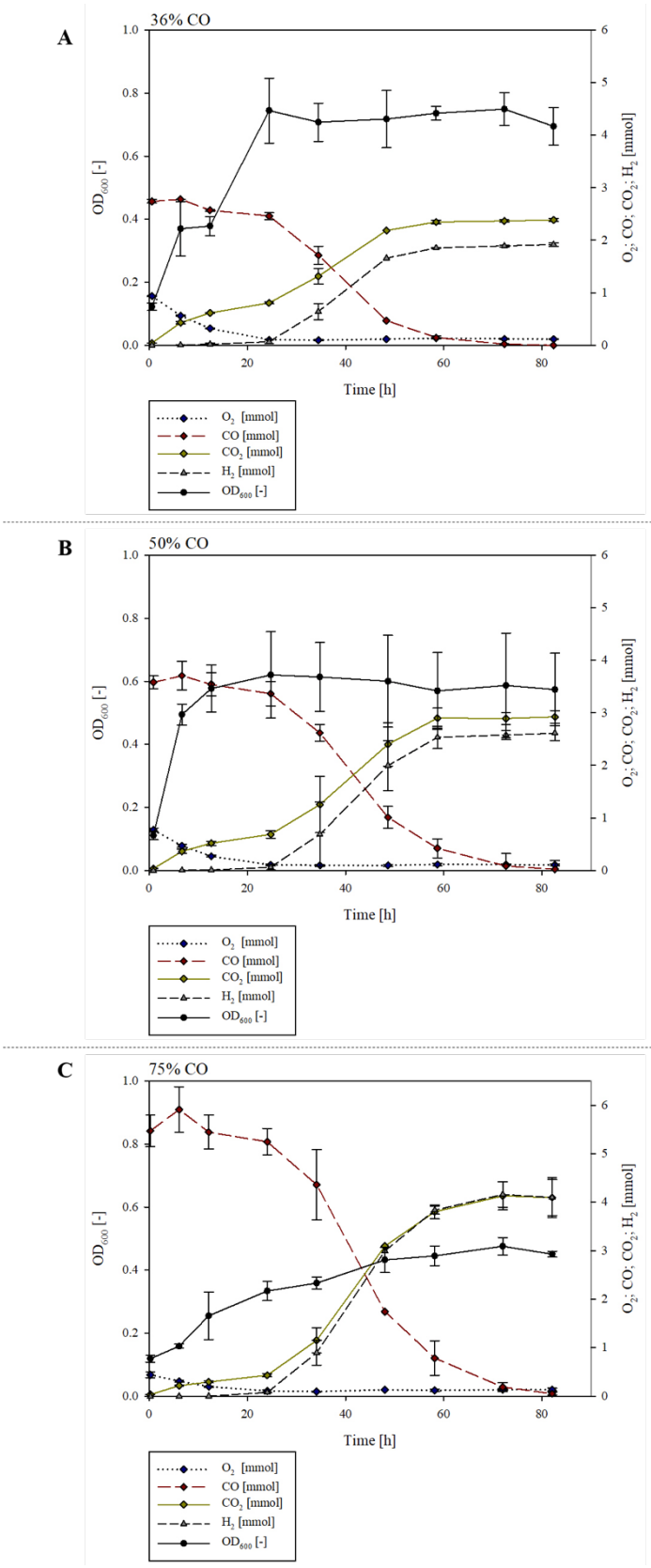

Figure 22: Effect of initial gas composition on H_2 production. Growth curve and gas composition during the cultivation of *P. thermoglucosidasius* DSM 6285 with an initial gas atmosphere of (A) 36% CO + 64% air (B) 50% CO + 50% air (C) 75% CO + 25% air.

5.3.2 Effect of inoculum preparation on H_2 production

The effect of different inoculum preparations on H_2 production by *P. thermoglucosidasius* DSM 6285 was determined using different inoculum sizes (2%, 10%, 20%) and incubation times of the 2nd pre-cultures (4 h, 12 h, 24 h). Maximum OD_{600} was observed after ~72 and 24 hours when inocula (incubated for 12 h) of 2% (OD_{600} = 0.620 ± 0.137) and 10% (OD_{600} = 0.923 ± 0.054) were added, respectively (Figure 20, Figure 23). The highest OD_{600} was observed when the highest cell concentration (20%) was added, with a maximum absorbance of 1.057 ± 0.063 ~ 7 h post-inoculation (Figure 23). However, during the aerobic growth phase the highest growth rate was observed for the 2% inoculum (0.14 1/h) (Table 3). O_2 reached its minimal plateau ~24 hours post-inoculation for all three inoculum sizes, and H_2 was first detected at this time when a 10% inoculum (0.021 ± 0.010 mmol) and 20% inoculum (0.024 ± 0.015 mmol) was used (Figure 21B). By contrast, with the 2% inoculum, 0.009 ± 0.003 mmol of H_2 could already be detected ~12 h after inoculation and 0.103 ± 0.027 mmol was detected after 24 h. CO was mostly depleted after ~83 hours (10% inoculum, 2% inoculum), while 0.179 ± 0.239 mmol CO was still present at this time point with the 20% inoculum (Figure 21B). When considering H_2 production rate, the highest production rate was observed with the 10% inoculum (0.101 ± 0.022 mmol/h), and occurred between 25-35 h post-inoculation (Table 3). A slightly lower maximum production rate (0.094 ± 0.016 mmol/h) was seen with the 2% inoculum and occurred later (between 35-48 h post-inoculation) than with the 10% inoculum. Maximum production rate for the highest inoculum size (20%) was achieved only between the 59-73 h time intervals and was 48.52% and 38.24% less than was observed with the 10% and 2% inocula, respectively (Table 3). Though the specific production rate was the highest for the 2% inocula (0.14 mmol/h/OD_{600}), the overall H_2 yield is highest for the 10% inoculum (Table 3), and this inoculum size was thus selected as the optimal parameter for further experiments.

Substantial differences in the growth, maximum production rates and H_2 yields could also be observed when distinct pre-culture inocula ages were evaluated. For the 4 h pre-culture, it took ~12 h to reach its maximum absorbance (OD_{600} = 0.50 ± 0.01), while it took ~24 h for the 12 h (0.620 ± 0.137) and 24 h inocula (0.56 ± 0.124) to reach their maximum absorbances (Figure 20, Figure 24). Growth rates during the aerobic phase also differed. Cultures inoculated with a 2nd pre-culture cultivated for 4 h, showed the highest growth rate (0.327 1/h) (Table 3). While in all cases maximum production rate occurred between the same time points, 36-48 h post-inoculation, the maximal production rate and H_2 yield were highest with the 4 h pre-inoculum (0.129 ± 0.018 mmol/h between 35-49 h; 0.796 ± 0.029 mmol H_2/mmol CO). The same pattern was observed for the specific production rate (Figure 21C, Table 3).

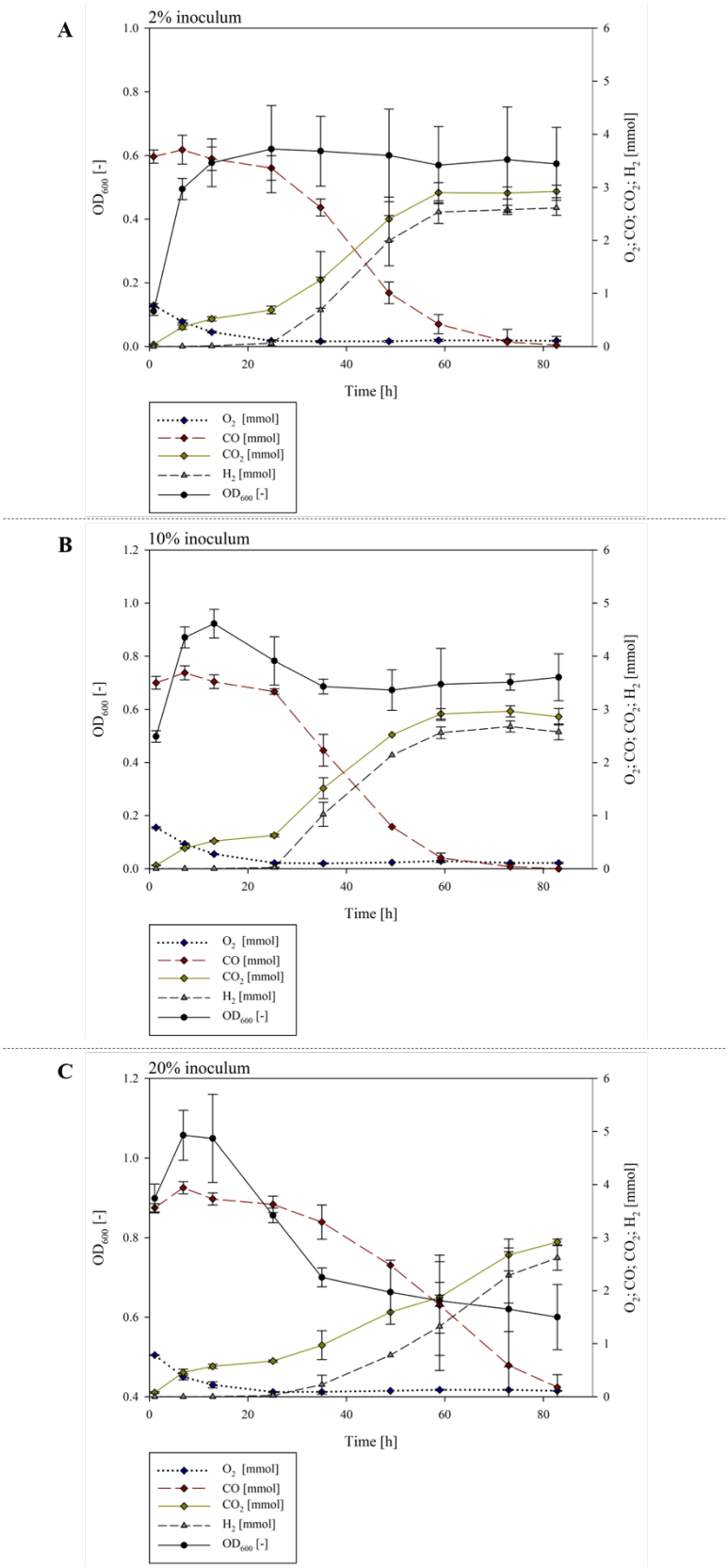

Figure 23: Effect of inoculum preparation on H_2 production – inoculum size. Growth curve and gas composition during the cultivation of *P. thermoglucosidasius* DSM 6285 with different inoculum sizes of (A) 2% (B) 10% and (C) 20%.

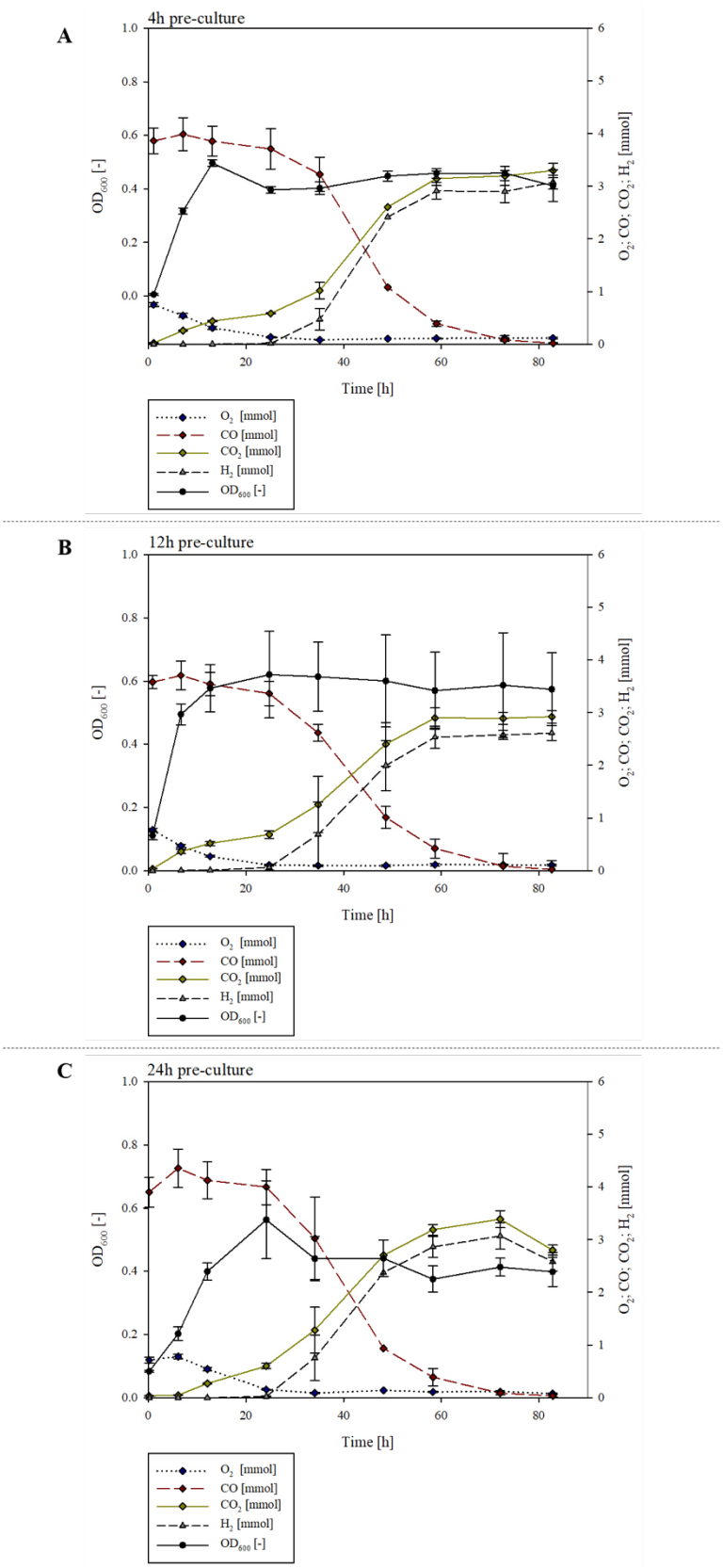

Figure 24: Effect of inoculum preparation on H_2 production - incubation time of the 2nd pre-culture. Growth curve and gas composition during the cultivation of *P. thermoglucosidasius* DSM 6285 with variations in the incubation time of the 2nd pre-culture: (A) 4 h (B) 12 h (C) 24 h.

5.3.3 Effect of temperature and initial pH on H_2 production

Different medium pHs (5.5, 7.0, 8.5) and cultivation temperatures (50 °C, 55 °C, 60 °C) were evaluated for their effects on H_2 production. The maximum OD_{600} was observed in cultures maintained at 55 °C (maximum OD_{600} = 0.854 ± 0.141 after 48 h; OD_{600} = 0.846 ± 0.118 after 24 h), followed by growth at 50 °C (maximum OD_{600} = 0.787 ± 0.039 after 24 h) and 60 °C (maximum OD_{600} = 0.620 ± 0.137 after 24 h) (Figure 20, Figure 25). During aerobic growth, the growth rate during the cultivation at 55 °C was highest (0.172 1/h), followed by 50 °C (0.163 1/h) and 60 °C (0.140 1/h) (Table 3). Depletion of O_2 (~24 hours) and CO (after ~72 h) occurred earlier at 55 °C and 60 °C than at 50 °C (O_2 depletion after ~36 h; 1.346 ± 0.772 mmol CO after 72 h) (Figure 21D, Figure 25). This correlated with both the higher maximum H_2 production rates and yields observed at the higher temperatures. Highest production rates at these temperatures occurred between 34-48 h post-inoculation, while at 50 °C this was only achieved in the last part (73-82 h) of the experiment (Figure 21D). Only marginal differences in both maximum production rates and yield were observed with the other experimental temperatures, with both factors being slightly higher (0.004 mmol/h more H_2 produced between 34-48 h; yield: 0.085 mmol more H_2 per mmol CO) at 55 °C than at 60 °C (Table 3). Given these marginal differences and the superior growth rate at 55 °C, this temperature was selected as the optimal condition for further experimentation although the specific production rate was the lowest during the cultivation at 55 °C.

More substantial differences could be observed for *P. thermoglucosidasius* grown in media which were adjusted prior inoculation to pH 5.5, 7.0 and 8.5. The highest OD_{600} was observed for the pH 7.0 cultures (maximum absorbance of 0.620 ± 0.137 after ~24 h), while *P. thermoglucosidasius* grew least well at pH 8.5 (maximum absorbance of 0.463 ± 0.018 after 6 hours) (Figure 26). The growth rate (aerobic phase) during the cultivation with a pH of 7.0 was also higher than with the other two medium pHs. Differences in O_2 consumption were also observed. Whereas O_2

reached its minimal plateau after ~24 h for the cultivations with medium pH 7.0 and 8.5, it only reached its minimum after 48 h at pH 5.5 (Figure 20, Figure 26). The highest maximal H_2 production rate (0.122 ± 0.005 mmol/h) and yield (0.786 ± 0.018 mmol H_2/mmol CO) were observed at pH 8.5. However, maximum production rate occurred substantially later (59-72 h post-inoculation) when a medium pH of 7.0 was used (35-48 h post-inoculation) (Figure 21E, Figure 26). By contrast, the specific production rate was higher at pH 5.5 and pH 8.5 than at pH 7.0, but occurred 12-24 h later. As the concept of parametric optimization should not be considered solely on the basis of yield, but also the time-efficiency of the process, the pH of 7.0 was selected as the optimum condition for H_2 production.

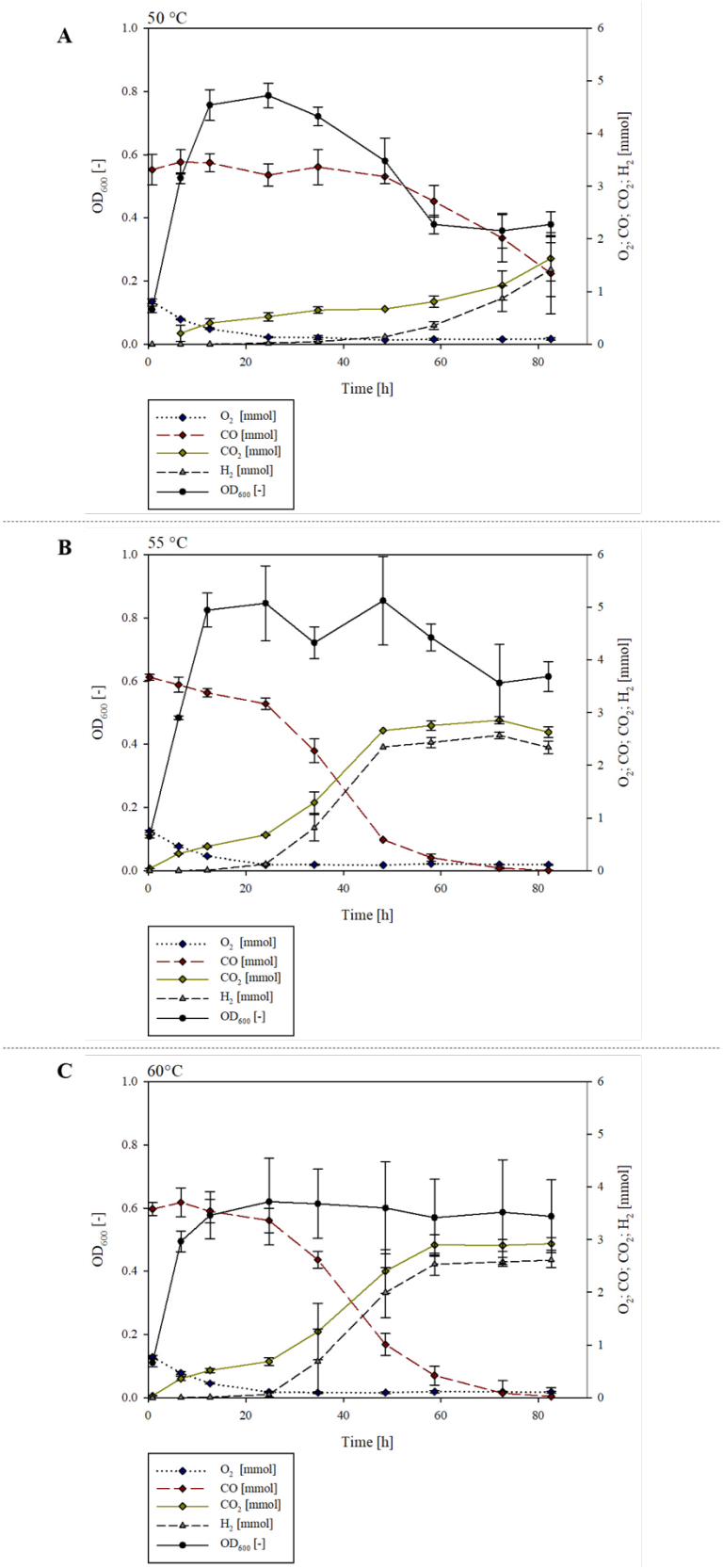

Figure 25: Effect of cultivation temperature on H_2 production. Growth curve and gas composition during the cultivation of *P. thermoglucosidasius* DSM 6285 with different cultivation temperatures: (A) 50 °C (B) 55 °C (C) 60 °C.

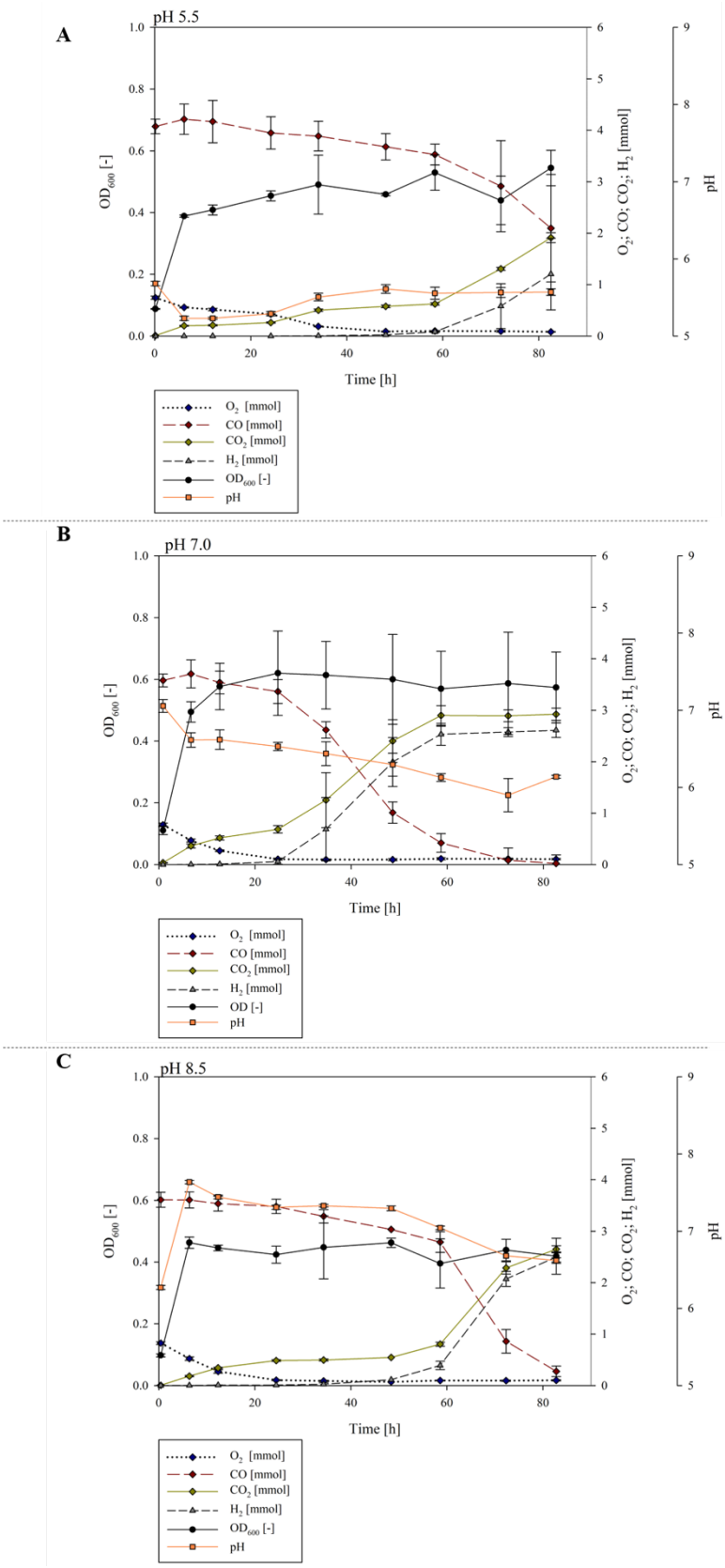

Figure 26: Effect of initial pH on H_2 production. Growth curve and gas composition during the cultivation of *P. thermoglucosidasius* DSM 6285 with different initial pHs: (A) pH 5.5 (B) pH 7.0 (C) pH 8.5.

5.3.4 Effect of nickel and iron concentration on H_2 production

Both the carbon monoxide dehydrogenase (CODH) and the hydrogenase that catalyses the WGS contain nickel (Ni^{2+}) and iron (Fe^{2+}) as co-factors (Can *et al.*; 2014; Peters *et al.*, 2015; Mohr *et al.*, 2018a). Exogenous nickel and iron were added to the medium in order to evaluate their effect on hydrogenogenesis. The addition of nickel resulted in a maximal absorbance (OD_{600}) of 0.486 ± 0.022 after 24 h. When more iron was added, the OD_{600} rose to a maximum of 0.572 ± 0.066 after 12 h (Figure 27). By contrast, the control fermentation (no additional nickel or iron) showed a higher maximum absorbance of 0.620 ± 0.137 after 24 h (Figure 27). However, the aerobic growth rate was less if no extra nickel or more iron was added. In all set-ups O_2 attained its minimum after ~24 h. H_2 was detected for the first time after ~12 h without added iron (0.009 ± 0.003 mmol) and after 24 h with additional iron (0.199 ± 0.038 mmol), while when nickel was added H_2 production only commenced after 24 h (0.017 ± 0.012 mmol). CO was completely consumed after 82 h when iron was added and in the control samples, whereas 0.144 ± 0.069 mmol was still available when nickel was added (Figure 21F). The addition of nickel also resulted in a substantially lower maximal production rate (0.078 mmol/h between 48-60 h post-inoculation), which was 17.02% less than was achieved without addition of nickel and iron, 36-48 h post-inoculation. By contrast, addition of iron resulted in a higher maximum production rate (0.115 mmol/h), which occurred twelve hours earlier than the without the addition of iron. Furthermore, the overall yield was ~2% and 8% higher with the addition of iron than when nickel was added or when no nickel or added iron were included (Table 3). Therefore, the addition of 0.08 mM $FeSO_4.7H_2O$ was selected for subsequent experiments.

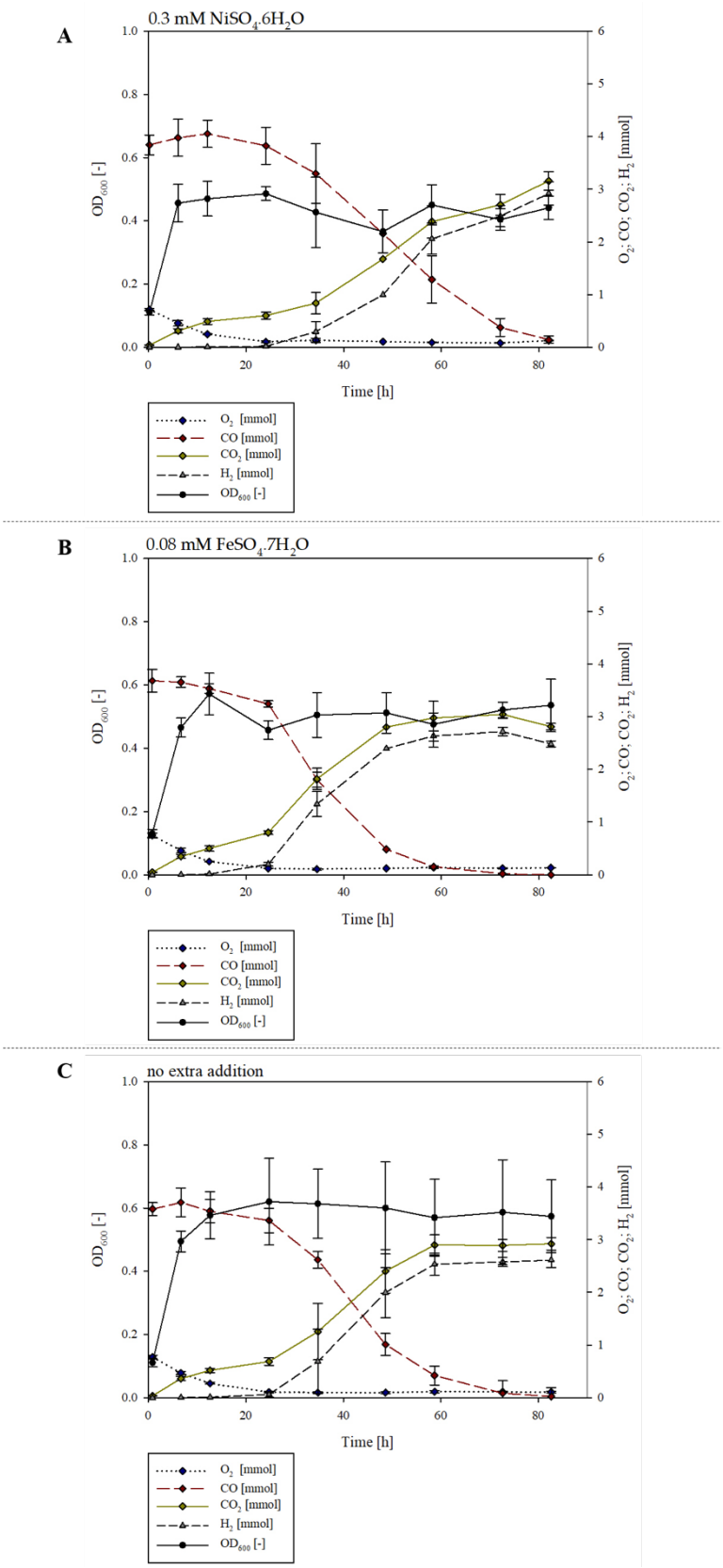

Figure 27: Effect of Nickel and Iron concentration on H_2 production. Growth curve and gas composition during the cultivation of *P. thermoglucosidasius* DSM 6285 with addition of trace elements:(A) 0.3 mM $NiSO_4.6H_2O$ + 0.04 mM $FeSO_4.7H_2O$ and (B) 0.08 mM FeSO4.7H2O (C) 0.04 mM $FeSO_4.7H_2O$.

Table 3: Summary of the differential calculated values for hydrogen production rate (mmol/h), yield (H_2 mmol/CO mmol) and growth for the tested parameters.

	H_2 production rate		H_2 specific production rate		H_2 yield *	aerobic growth phase	
parameter	**maximum [mmol/h]**	**time [h]**	**maximum [mmol/h*OD_{600}]**	**time [h]**	**[H_2 mmol/CO mmol]**	**ΔOD_{600} (t12-t0)**	**μ [1/h]**
control: 60°C; pH 7; 0.04 mM Fe^{2+}; no Ni^{2+}; 50% CO; 12 h pre-culture; 2% inoculum	0.094 ± 0.016	35-48	0.163 ± 0.054	35-48	0.763 ± 0.026	0.467 ± 0.073	0.14
50°C	0.055 ± 0.027	73-82	0.144 ± 0.06	73-82	0.698 ± 0.068	0.647 ± 0.044	0.163
55°C	0.098 ± 0.006	34-48	0.124 ± 0.001	34-48	0.783 ± 0.014	0.716 ± 0.059	0.172
pH 5.5	0.06 ± 0.025	72-82	0.358 ± 0.103	72-82	0.606 ± 0.168	0.127 ± 0.035	0.128
pH 8.5	0.122 ± 0.005	59-72	0.294 ± 0.028	59-72	0.786 ± 0.018	0.348 ± 0.006	0.127
0.3 mM $NiSO_4.6H_2O$ + 0.04 mM FeSO4.7H2O	0.078 ± 0.015	48-58	0.192 ± 0.035	48-58	0.716 ± 0.032	0.36 ± 0.056	0.122
0.08 mM $FeSO_4.7H_2O$	0.115 ± 0.020	25-35	0.24 ± 0.052	25-35	0.782 ± 0.012	0.442 ± 0.052	0.127
36:64 CO:air	0.073 ± 0.006	34-48	0.104 ± 0.016	34-48	0.748 ± 0.006	0.256 ± 0.042	0.095
75:25 CO:air	0.138 ± 0.009	34-48	0.351 ± 0.038	34-48	0.807 ± 0.022	0.136 ± 0.083	0.064
4 h pre-culture	0.129 ± 0.018	35-49	0.303 ± 0.046	35-49	0.796 ± 0.029	0.491 ± 0.015	0.372
24 h pre-culture	0.115 ± 0.025	34-48	0.27 ± 0.098	34-48	0.779 ± 0.013	0.316 ± 0.027	0.132
10% inoculum	0.101 ± 0.022	25-35	0.137 ± 0.025	25-35	0.806 ± 0.025	0.425 ± 0.063	0.052
20% inoculum	0.068 ± 0.023	59-73	0.108 ± 0.029	59-73	0.741 ± 0.028	0.151 ± 0.131	0.013
combined: 55°C, pH 7.0, 0.8mM Fe2+, no Ni2+, 75% CO; 4 h pre-culture; 10% inoculum	0.182 ± 0.009	34-58	0.566 ± 0.024	34-58	0.808 ± 0.01	0.323 ± 0.02	0.32

***calculated between 24 h and 72 h cultivation time**

5.3.5 Optimized H_2 production

From the experiments evaluating the individual parameters, all tested parameters were observed to have substantial effects on both H_2 yield and maximum production rates. In a further experiment, the effects of a combination of the optimum parameters (55 °C, pH 7.0, addition of $FeSO_4.7H_2O$ (0.08 mM), 75:25 CO:air ratios (initial gas atmosphere), 4 h incubation time of the 2nd pre-culture, 10% inoculum size) on hydrogenogenesis was established. In this experiment, *P. thermoglucosidasius* growth to a maximum absorbance was observed after ~48 h (OD_{600}= 0.388 ± 0.018), while O_2 was depleted earlier (after ~24 h). At this time, H_2 was detected for the first time (0.071 ± 0.02 mmol) (Figure 28).

Comparison to the previously evaluated control set-up (60 °C, pH 7.0, 0.04 mM $FeSO_4.7H_2O$, 50:50 CO:air ratio, 12 h incubation time of the 2nd pre-culture, 2% inoculum size; Mohr *et al.* 2018b) showed a modest increase in H_2 yield (2% higher) when the optimized conditions were used (Table 3). However, marked increases in both the maximum (1.94x higher) and specific H_2 production rate (3.47x higher) could be observed with the optimized parameters, occurring ~35-48 h post-inoculation in both cases. These factors were also substantially higher than each of the single tested parameters, with a 1.61x and 5.44x fold increase in specific H_2 production rate for the best (75:25 CO:air ratio) and worst (36:64 CO:air ratio) performing individual parameter, respectively (Table 3).

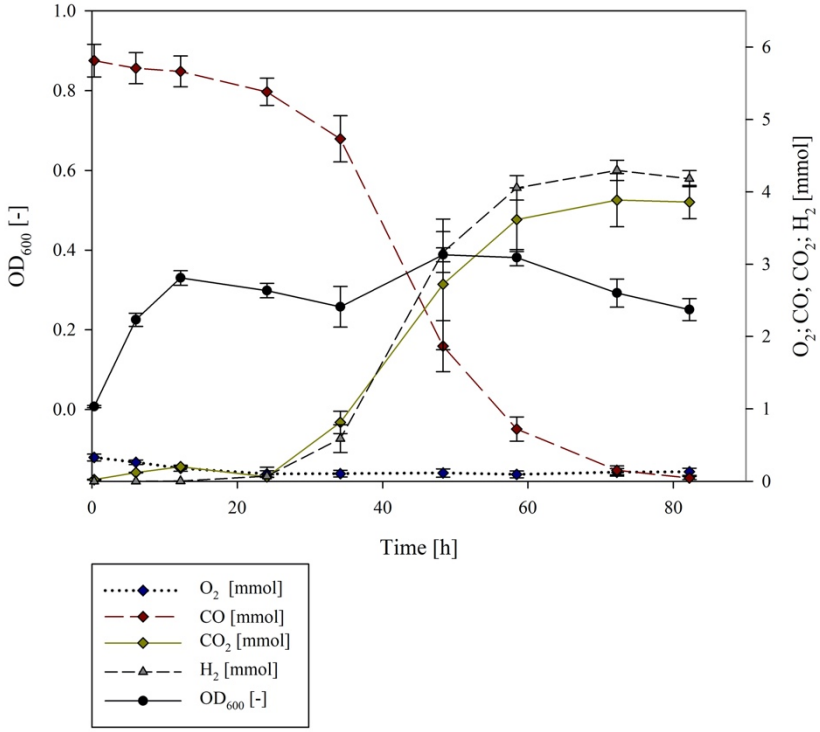

Figure 28: Growth curve and gas composition during the cultivation of *P. thermoglucosidasius* DSM 6285 with the combined superior parameters (55 °C, pH 7.0, addition of 0.08 mM $FeSO_4.7H_2O$, 75:25 initial gas atmosphere CO:air ratios, 4 h incubation time of the 2nd pre-culture, 10% inoculum size).

5.4 DISCUSSION

A critical aspect of microbial fermentations that involve gas as the main substrate or e^- acceptor is the solubility of the gas and the threshold concentration that does not inhibit the metabolism of the microorganisms (Bertsch & Müller, 2015). In general, high gas concentrations can have an inhibitory effect while low gas concentrations can result in a low volumetric mass transfer coefficient resulting in limited substrate availability (Daniell *et al*., 2012; Mohammadi *et al*., 2014). This was evident in the fermentations with *P. thermoglucosidasius* DSM 6285 as less growth (biomass) was observed with increasing CO concentrations and concomitantly lower concentration of O_2 as terminal electron acceptor during the aerobic growth phase. However, poorer growth at higher CO concentrations did not have a negative effect on the hydrogenogenic capacity of *P. thermoglucosidasius* DSM 6285, with the highest H_2 production rate observed with the 75:25 CO:air mixture. The higher production rate with 75% CO, which grew to the lowest optical density, suggests that H_2 production is a function of the availability of CO, rather than being dependent on the amount of biomass. To investigate the influence of the amount of biomass prior the H_2 production phase, cultivations in bottles were undertaken using different inoculum sizes.

The size and age of inocula can have substantial effects on H_2 fermentations, as has been observed in the fermentative thermophile *Thermoanaerobacterium thermosaccharolyticum* and the photosynthetic purple non-sulphur bacterium *Rhodobacter sphaeroides* (Japaar *et al*., 2011; Seengenyoung *et al*., 2011). The highest production rate was detected with the 10% inoculum size, while the lowest production rate was achieved with the highest inoculum size (20%). Similar results were obtained with the fermentative H_2-producer *Bacillus coagulans* IIT-BT S1, where higher H_2 production rates were observed with a 10% inoculum volume, but decreased with larger (15% and 20%) inoculum sizes (Kotay and Das, 2007). As such, H_2 production appears not to be directly linked to the amount of biomass but may rather be a function

of the physiological state of *P. thermoglucosidasius*. To confirm this hypothesis, different cultivation times (4 h, 12 h, 24 h) of the 2nd pre-culture were tested. Although the maximum production rate was detected at the same time points, H_2 production with the shortest incubation time of the 2nd pre-culture (4 h) showed the highest production rate. The 4 h pre-cultures may be in the lag growth phase preceding exponential growth (12-24 h), the preparative phase where bacteria adapt optimally to new environments (i.e., the exposure of *P. thermoglucosidasius* to CO) (Bertrand, 2019). This pre-adaptive physiological state may explain the highest production rate observed with the 4h pre-culture. Similarly, the lower H_2 production rates with the 20% inoculum size may be due to the cells reaching the post-lag exponential phase more rapidly than the optimal 10% inoculum size.

P. thermoglucosidasius strains grow optimally at temperatures of 61-63 °C and an initial medium pH of 6.5-8.5 (Suzuki *et al.*, 1984). The strain utilized in this study, DSM 6285, is reported to grow optimally at 55 °C, with some growth at 75 °C (Gurujeyalakshmi & Oriel, 1989). In the current study, a growth temperature of 55 °C and a medium pH of 7.0 resulted in optimal H_2 production. Although the highest H_2 production rate was obtained with the pH=8.5 set up, the lag phase between O_2 consumption and the commencement of H_2 production was substantially longer (24 h later than at pH 7.0).

Nickel (Ni^{2+}) and iron (Fe^{2+}) are both essential co-factors in the catalytic sites of a broad range of enzymes (Waldron & Robinson, 2009), and both the Ni-Fe CODH and Ni-Fe group 4a hydrogenase that catalyse the WGS are reported to contain both of these co-factors (Mohr *et al.*, 2018a). Thus, the addition of both of these elements to the *P. thermoglucosidasius* growth medium might be expected to have a positive effect on hydrogenogenesis. When doubling the amount of Fe^{2+} (0.08 mM $FeSO_4.7H_2O$) normally added to mLB medium, there was an evident decrease in the lag phase between O_2 consumption and H_2 production and the maximum H_2 production rate was 8% higher than at lower concentrations. However, the addition of $NiSO_4.6H_2O$ had a negative impact on both the growth of *P. thermoglucosidasius* DSM 6285, the

length of the pre-hydrogenogenic lag phase, H_2 yield and maximum H_2 production rate. A study of the effects of nickel on H_2 production by anaerobic sludge bacteria showed that increasing the nickel concentration from 0.0 mM up to 0.01 mM led to an increase of H_2 production, while higher nickel concentration had a negative effect on H_2 production. Furthermore, the lag phase of H_2 production could be decreased to 6 h by using 0.01 mM nickel (Wang *et al*., 2008). As such, further fine-tuning of the amount of nickel added may be necessary for improved *P. thermoglucosidasius* hydrogenogenesis.

The current study highlights that WGS catalyzed hydrogenogenesis in *P. thermoglucosidasius* is a finely balanced process with variations in all the tested operational parameters having either a positive or negative impact on H_2 yield, maximal (specific) production rates, as well as the time frame of the lag phase preceding hydrogenogensis and the growth. The optima for each parameter combined in a further experiment resulted in the highest production rate compared to the single tested conditions. This study can serve as a basis for up-scale fermentations. However, the effects of additional parameters such as the stirrer rate and flow rate of the feed gas inherent to up-scale fermentations will also need to be evaluated.

5.5 CONCLUSIONS

Hydrogenogenesis via the WGS in *P. thermoglucosidasius* is a finely balanced process, which is influenced by key operational parameters. While some parameters such as temperature and initial medium pH reflect the optimum growth conditions for *P. thermoglucosidasius* others such as the age of the pre-culture and inoculum volume are more complex and may rather indicate the importance of the physiological state of *P. thermoglucosidasius* on its hydrogenogenic capacity. Further investigations, including gene expression analysis and metabolic profiling may shed light on additional factors influencing H_2 production which, together with additional fine-tuning of operational parameters, can be used to develop up-scale fermentations with a continuous CO feed for commercial H_2 production using the facultatively anaerobic thermophilic carboxydotroph *P. thermoglucosidasius*.

REFERENCES FOR CHAPTER 5

Bertrand RL (2019) Lag phase is a dynamic, organized, adaptive, and evolvable period that prepares bacteria for cell division. *Journal of Bacteriology*. **201(7)**: e00697-18. DOI:10.1128/JB.00697-18.

Bertsch J, Müller V (2015) CO Metabolism in the Acetogen *Acetobacterium woodii*. *Applied Environmental Microbiology*. **81(17)**:5949-5956. DOI:10.1128/AEM.01772-15.

Can M, Armstrong FA, Ragsdale SW (2014) Structure, Function, and Mechanism of the Nickel Metalloenzymes, CO Dehydrogenase, and Acetyl-CoA Synthase. *Chemical Reviews*. **114(8)**:4147-4174. DOI:10.1021/cr400461p.

Daniell J, Kopke M, Simpson SD (2012) Commercial biomass syngas fermentation. *Energies*. **5(12)**:5372–417. DOI:10.3390/en5125372.

Gurujeyalakshmi G, Oriel P (1989) Isolation of phenol-degrading *Bacillus stearothermophilusand* partial characterization of the phenol hydroxylase. *Applied Environmental Microbiology*. **55**: 500-502.

Japaar SZ, Kalil MS, Ali E, Anuar N (2011) Effects of age of inoculum, size of inoculum and headspace on hydrogen production using *Rhodobacter sphaeroides*. *Journal of Bacteriology*. **1**:16-23. DOI:10.3923/bj.2011.16.23.

Kotay SM, Das D (2007) Microbial hydrogen production with *Bacillus coagulans* IIT-BT S1n isolated from anaerobic sewage sludge. *Bioresource Technology*. **98**:1183-1190. DOI:10.1016/j.biortech.2006.05.009.

Mohammadi M, Mohamed AR, Najafpour GD, Younesi H, Uzir MH (2014) Kinetic studies on fermentative production of biofuel from synthesis gas using *Clostridium ljungdahlii*. *Scientific World Journal*.910590. DOI:10.1155/2014/910590.

Mohr T, Aliyu H, Küchlin R, Polliack S, Zwick M, Neumann A, Cowan D, de Maayer P (2018a) CO-dependent hydrogen production by the facultative anaerobe

Parageobacillus thermoglucosidasius. *Microbial Cell Factories*. **17**:108. DOI:10.1186/s12934-018-0954-3.

Mohr T, Aliyu H, Küchlin R, Zwick M, Neumann A, Cowan D, de Maayer P (2018b) Comparative genomic analysis of *Parageobacillus thermoglucosidasius* strains with distinct hydrogenogenic capacities. *BMC Genomics*. **19**:880. DOI:10.1186/s12864-018-5302-9.

Peters JW, Shut GJ, Boyd ES, Mulder DW, Shepard EM, Broderick JB, King PW, Adams MWW (2015) [FeFe]- and [NiFe]-hydrogenase diversity, mechanism, and maturation. **1853(6)**:1350-1369. DOI:10.1016/j.bbamcr.2014.11.021.

Seengenyoung J, O-Thong S, Imai T, Prasetsan P (2011) Effect of inoculum size for biohydrogen production from palm oil mill effluent. TIChE International Conference, 2011.

Suzuki Y, Kishigami T, Inoue K, Mizoguchi Y, Eto N, Takagi M, Abe S (1984) *Bacillus thermoglucosidasius* sp. Nov., a New Species of Obligately Thermophilic Bacilli. *Systematic and Applied Microbiology*. **4(4)**:487-495. DOI:10.1016/S0723-2020(83)80006-X.

Waldron KJ, Robinson NJ (2009) How do bacterial cells ensure that metalloproteins get the correct metal? *Nature Reviews Microbiology*. **6:**25-35. DOI:10.1038/nrmicro2057.

Wang J, Wan W (2008) Influence of Ni2+ concentration on biohydrogen production. *Bioresource Technology*. **99**:8864-8868. DOI:10.1016/j.biortech.2008.04.052.

Zeigler DR (2001) The Genus *Geobacillus*. Introduction and Strain Catalog. *Bacillus Genetic Stock Center. Catalog of Strains*. **7(3)**.

6 CONCLUSIONS

Sustainable H_2 production is regarded as an attractive alternative to fossil-dependent fuels because it carries the highest energy content and its combustion only produces heat and water ($2\ H_2 + O_2 \rightarrow 2\ H_2O$). Besides the need to develop processes to produce clean energy, it is crucial to reduce toxic emissions to the Earth's atmosphere and to move towards a modern, sustainable society. One such process, which can contribute towards clean energy by producing H_2 and reducing CO at the same time, is presented in this thesis. The thesis highlights the potential of a thermophilic facultative anaerobic organism *Parageobacillus thermoglucosidasius*.

Genomic analysis of different *Parageobacillus* and *Geobacillus* strains revealed the presence of genes encoding for a carbon monoxide dehydrogenase (CODH) and a group 4a hydrogenase in *P. thermoglucosidasius*. These enzymes are involved in the water-gas shift (WGS) reaction, whereby the oxidation of CO is coupled with the splitting of a water molecule yielding in CO_2 and H_2 ($CO + H_2O \rightleftharpoons CO_2 + H_2$). Cultivation of *P. thermoglucosidasius* DSM 2542^T at an initial gas atmosphere of 50% CO and 50% air showed a near-equimolar conversion from CO to H_2. The production of H_2 is divided into three different phases: aerobic growth (1), lag phase (2) and H_2 production (3), where O_2 is removed prior H_2 production. By undertaking this

reaction, *P. thermoglucosidasius* was able to gain energy for growth from the WGS reaction. Furthermore, it shows the ability to tolerate high concentrations of CO. These properties are unique features of *P. thermoglucosidasius*, which in contrast to other hydrogenogenic carboxydotrophic bacteria that use the WGS pathway, is a facultative anaerobe.

In a follow up study, the ability of different *P. thermoglucosidasius* strains to produce H_2 was investigated. Three of the four strains were hydrogenogenic, while one did not produce any H_2. Additionally, one hydrogenogenic strain stands out because of its superior H_2 production and by its shorter lag phase (phase 2). To investigate the differences in H_2 production, comparative genomics were undertaken. Comparative genomic analysis revealed extensive differences in the proteins encoded on the genomes of the tested strains. Moreover, SNPs (Single Nucleotide Polymorphisms) in the CODH-NiFe hydrogenase loci were identified in the non hydrogenogenic strain that could impact H_2 production. The superior strain DSM 6285 was selected for further experiments due to its higher production rate and the shorter lag phase.

Also the microbial conversion of syngas or industrial waste gas to value-added chemicals has gained great interest. However, one issue with using industrial waste gases as a substrate, is the presence of O_2 as most known syngas bioconverting organisms are strict anaerobes. Residual O_2 in the waste gas has to be removed first which is expensive and often environmentally unfriendly. In Chapter 4 a sequential cultivation was undertaken whereat a gas mixture containing O_2 was anaerobised biologically to make it accessible for anaerobic bacteria. Via a two-phase system, O_2 was removed by *P. thermoglucosidasius*, which allowed a subsequent culturing of *Clostridium ljungdhalii*, a strict anaerobe. Additionally, *P. thermoglucosidasius* produced H_2 and CO_2, which provided the building blocks for the acetogenesis of *C. ljungdhalii* via the Wood Ljungdahl pathway. This sequential cultivation may serve as an environmentally friendly methodology wherein *P. thermoglucosidasius* represents a

biological cleaning tool for removing O_2 to make industrial waste gases accessible to strict anaerobes.

One crucial step for a commercial H_2 production is the investigation of different operational parameters on H_2 production. Therefore, several parameters were evaluated for their potential an enhancement of hydrogenogenesis. Some parameters (temperature, initial pH) had a direct influence on the growth conditions, while others (the age of the pre-culture and inoculum volume) revealed a more complex impact on H_2 production. The production of H_2 depends rather on the physiological state of the microorganism than of the available amount of biomass. However, this study indicates that *P. thermoglucosidasius* is able to produce H_2 under several conditions. It also shows that the WGS reaction is a finely balanced process which indicates a more complex integration in the organism's metabolism.

In this thesis the hydrogenogenesis of *P. thermoglucosidasius* was investigated on genome level, strain selection, process optimization and as well as possible alternative to remove O_2 sustainable from waste gas. It was shown that *P. thermoglucosidasius* is characterized by its ability to produce H_2 in a broad range of conditions, tolerating high concentrations CO by concomitantly tolerating O_2 and the ability to grow via the produced energy of the WGS reaction. The combination of these features makes *P. thermoglucosidasius* an attractive candidate for a commercial biohydrogen production.

LIST OF ALL REFERENCES

Albright L, Crynes B, Corcoran W, Pyrolysis: Theorie and Industrial Practice (Eds.: Albright L, Crynes B, Corcoran W) Academic Press, New York 1983.

Alfano A, Cavazza C (2018) The biologically mediated water-gas shift reaction: structure, function and biosynthesis of monofunctional [NiFe]- carbon monoxide dehydrogenase. *Sustainable Energy & Fuels*. **2**:1653-1670. DOI:10.1039/C8SE00085A.

Aliyu H, Lebre P, Blom J, Cowan D, De Maayer P (2016) Phylogenomic re-assessment of the thermophilic genus *Geobacillus*. *Systematic and Applied Microbiology*. **39(8):**527-533. DOI:10.1016/j.syapm.2016.09.004.

Andrews S, Mattatall NR, Arnold D, Hill BC (2005) Expression, purification, and characterization of the Cu_A–cytochrome c domain from subunit II of the *Bacillus subtilis* cytochrome caa_3 complex in *Escherichia coli. Protein Expression and Purification*. **2**:227-235. DOI:10.1016/j.pep.2004.11.009.

Andrews SC, Berks BC, McClay J, Ambler A, Quail MA, Golby P, et al. (1997) A 12-cistron *Escherichia coli* operon (*hyf*) Encoding a putative proton-translocating formate hydrogenlyase system. *Microbiology*. **143**:3633–47. DOI:10.1099/00221287-143-11-3633.

Bankevich A, Nurk S, Antipov D, Gurevich AA, Dvorkin M, Kulikov AS, Lesin VM, Nikolenko SI, Pham S, Prjibelski AD, Pyshkin AV, Sirotkin AV, Vyahhi N, Tesler G, Alekseyev MA, Pevzner PA (2012) SPAdes: a new genome assembly algorithm and its

applications to single-cell sequencing. *Journal of Computational Biology*. **5**: 455-477. DOI:10.1089/cmb.2012.0021.

Bengtsson J, Tjalsma H, Rivolta C, Hederstedt L (1999) Subunit II of *Bacillus subtilis* cytochrome *c* oxidase is a lipoprotein. *Journal of Bacteriology*. **181**: 685-688.

Bertrand RL (2019) Lag phase is a dynamic, organized, adaptive, and evolvable period that prepares bacteria for cell division. *Journal of Bacteriology*. **201(7)**: e00697-18. DOI:10.1128/JB.00697-18.

Bertsch J, Müller V (2015) CO Metabolism in the Acetogen *Acetobacterium woodii*. *Applied Environmental Microbiology*. **81(17)**:5949-5956. DOI:10.1128/AEM.01772-15.

Besemer J, Lomsadze A, Borodovsky M (2001) GeneMarkS: a self-training method for prediction of gene starts in microbial genomes. Implications for finding sequence motifs in regulatory regions. *Nucleic Acids Research*. **29**:2607–18. DOI:10.1093/nar/29.12.2607.

Blumenthal I (2001) Carbon monoxide poisoning. *Journal of the Royal Society of Medicine*. **94(6)**:270-272.

Bosi E, Donati B, Galardini M, Brunetti S, Sagot MF, Lió P, Crescenzi P, Fani R, Fondi M (2015) MeDuSa: a multi-draft based scaffolder. *Bioinformatics*. **31**: 2443–2451. DOI:10.1093/bioinformatics/btv171.

BP (2016). Statistical Review of World Energy 2016. 68th edition.

Brumm PJ, Land ML, Mead DA (2015) Complete genome sequence of *Geobacillus thermoglucosidasius* C56-YS93, a novel biomass degrader isolated from obsidian hot spring in Yellowstone National Park. *Standards in Genomic Science*. **10(73)**:73. DOI:10.1186/s40793-015-0031-z.

Can M, Armstrong FA, Ragsdale SW (2014) Structure, Function, and Mechanism of the Nickel Metalloenzymes, CO Dehydrogenase, and Acetyl-CoA Synthase. *Chemical Reviews*. **114(8)**:4147-4174. DOI:10.1021/cr400461p.

Chan KH, Lee KM, Wong KB (2012) Interaction between hydrogenase maturation factors HypA and HypB is required for [NiFe]-hydrogenase maturation. PLoS One. 7:e.32592. DOI:10.1371/journal.pone.0032592.

Chen K, Lio C, Huang S, Shen H, Shieh Y, Chiu H, Lu C (2017): CSAR: a contig scaffolding tool using algebraic rearrangements. *Bioinformatics*. **34**: 109-111. DOI:10.1093/bioinformatics/btx543.

Chen SD, Lee KS, Lo YC, Chen WM, Wu JF, Lin CY, Chang JS (2008) Batch and continuous bio-hydrogen production from starch hydrolysate by *Clostridium* species. *International Journal of Hydrogen Energy*. **33**:3289-3294. DOI:10.1016/j.ijhydene.2008.01.028.

Conrad R, Seiler W (1980) Role of microorganism in the consumption and production of atmospheric carbon monoxide by soil. *Applied Environmental Microbiology*. **40**:437-445.

Cripps RE, Eley K, Leak DJ, Taylor M, Todd M, Boakes S, Martin S, Atkinson T (2009) Metabolic engineering of *Geobacillus thermoglucosidasius* for high yield ethanol production. *Metabolic Engineering*, **11**: 398-408. DOI:10.1016/j.ymben.2009.08.005.

Daas MJA, van de Weijer AHP, de Vos WM, van der Oost J, van Kranenburg R (2016) Isolation of a genetically accessible thermophilic xylan degrading bacterium from compost. *Biotechnology for Biofuels*. **9**:210. DOI:10.1186/s13068-016-0618-7.

Daniell J, Kopke M, Simpson SD (2012) Commercial biomass syngas fermentation. *Energies*. **5(12)**:5372–417. DOI:10.3390/en5125372.

Daniels L, Fuchs G, Thauer RK, Zeikus JG (1977) Carbon monoxide oxidation by methanogenic bacteria. *Journal of Bacteriology*. **132**:118–126.

Darling AE, Mau B, Perna, NT. (2010) progressiveMauve: multiple genome alignment with gene gain, loss and rearrangement. *PLoS One 5*. e11147. DOI:10.1371/journal.pone.0011147.

Das D, Veziroğlu TN (2001) Hydrogen production by biological processes: a survey of literature. *International Journal of Hydrogen Energy*. **26**:13-28. DOI:10.1016/S0360-3199(00)00058-6.

De Maayer P, Brumm PJ, Mead DA, Cowan DA (2014) Comparative analysis of the *Geobacillus* hemicellulose utilization locus reveals a highly variable target for improved hemicellulolysis. *BMC Genomics*. **15**: 836. DOI:10.1186/1471-2164-15-836.

De Maayer P, Brumm PJ, Mead DA, Cowan DA (2014) Comparative analysis of the *Geobacillus* hemicellulose utilization locus reveals a highly variable target for improved hemicellulolysis. *BMC Genomics*. **15**:836. DOI:10.1186/1471-2164-15-836.

DeWeerd KA, Mandelco L, Tanner RS, Woese CR, Suflita JM (1990) *Desulfomonile tiedjei* gen. nov. and sp. nov., a novel anaerobic, dehalogenating, sulfate-reducing bacterium". *Archives of Microbiology*. **154(1)**:22-30. DOI:10.1007/BF00249173.

Diekert G (1990) CO_2 reduction to acetate in anaerobic bacteria. *FEMS Microbiology Review*. **87**:391-396. DOI:10.1016/0378-1097(90)90484-8.

Diender M, Stams AJM, Sousa DZ (2015) Pathways and Bioenergetics of Anaerobic Carbon Monoxide Fermentation. *Frontiers in Microbiology*. **6**:1275. DOI:10.3389/fmicb.2015.01275.

Dobbek H, Svetlitchnyi V Gremer L, Huber R, Meyer O (2001) Crystal structure of a carbon monoxide dehydrogenase reveals a [Ni-4Fe-5S] cluster. *Science*. **293**:1281–1285. DOI:10.1126/science.1061500.

Dutta D, De D, Chaudhuri S, Bhattacharya SK (2005) Hydrogen production by Cyanobacteria. *Microbial Cell Factories*. **4**:36–46. DOI:10.1186/1475-2859-4-36.

Ebbesen SD, Mogensen M (2009) Electrlysis of carbon dioxid in Solid Oxide Electrolysis cells. *Journal of Power Sources*. **193(1)**:349-358. DOI:10.1016/j.jpowsour.2009.02.093.

Eitinger T, Mandrand-Berthelot MA (2000) Nickel transport systems in microorganisms. *Archives of Microbiology*. **173**: 1-9.

Ellabban O, Abu-Rub H, Blaabjerg F (2014) Renewable energy resources: Current status, future prospects and their enabling technology. *Renewable and Sustainable Energy*, **39**:748-764. DOI:10.1016/j.rser.2014.07.113.

Emms DM, Kelly S (2015) OrthoFinder: solving fundamental biases in whole genome comparisons dramatically improves orthogroup inference accuracy. *Genome Biology*. **16**:157. DOI:10.1186/s13059-015-0721-2.

Engel RR, Matsen JM, Chapman SS, Schwartz S (1972) Carbon monoxide production from heme compounds by bacteria. *American Society for Microbiology*. **112(3)**: 1310-1315.

Esteves-Ferreira AA, Cavalcanti JHF, Vaz MGMV, Alvarenga LV, Nunes-Nesi A, Araújo WL (2017) Cyanobacterial nitrogenases: Phylogenetic diversity, regulation and functional predictions. *Genetics and Molecular Biology*. **40**:261–75. DOI:10.1590/1678-4685-GMB-2016-0050.

Fabiano B, Perego P (2002) Thermodynamic study and optimization of hydrogen production by *Enterobacter aerogenes*. *International Journal of hydrogen Energy*. **27**:149-156. DOI:10.1016/S0360-3199(01)00102-1.

Ferry JG (1995) CO dehydrogenase. *The Annual Review of Microbiology*. **49**:305–333. DOI:10.1146/annurev.mi.49.100195.001513.

Fischer F, Zillig W, Stetter KO, Schreiber G (1983) Chemolithoautotrophic metabolism of anaerobic extremly thermophilic archaebacteria. *Nature*. **301**:511–513. DOI:10.1371/journal.pone.0024222.

Flachsbart PG (1999) Human exposure to carbon monoxide from mobile sources. *Chemosphere – Global Change Science*. **1**: 301-329). DOI:10.1016/S1465-9972(99)00030-6.

Fox JD, Kerby RL, Roberts GP, Ludden PW (1996) Characterization of the CO-induced, CO-tolerant hydrogenase from *Rhodospirillum rubrum* and the gene encoding the large subunit of the enzyme. *Journal of Bacteriology*. **178**:1515–1524. DOI:10.1128/jb.178.6.1515-1524.

Garcia JL, Patel BK, Ollivier B (2000) Taxonomic, phylogenetic, and ecological diversity of methanogenic Archaea. *Anaerobe*. **6**:205–226. DOI:10.1006/anae.2000.0345.

Ghimire A, Frunzo L, Pirozzi F, Trably E, Escudie R, Lens PNL, Esposito G (2015) A review on darf fermentative biohydrogen production from organic biomass: Process parameters and use of by-products. *Applied Energy*. **144**:73-95. DOI:10.1016/j.apenergy.2015.01.045.

Grant JR, Stothard P (2008) The CGView Server: a comparative genomics tool for circular genomes. *Nucleic Acids Research*. **36**:181–4. DOI:10.1093/nar/gkn179.

Greening C, Biswas A, Carere CR, Jackson CJ, Taylor MC, Stott MB, Cook GM, Morales SE (2016) Genomic and metagenomic surveys of hydrogenase distribution indicate H_2 is a widely utilised energy source for microbial growth and survival. *ISME Journal*. **10(3)**:761-77. DOI:10.1038/ismej.2015.153.

Greening C, Biswas A, Carere CR, Jackson CJ, Taylor MC, Stott MB, Cook GM, Morales SE (2016) Genomic and metagenomic surveys of hydrogenase distribution indicate H_2 is a widely utilised energy source for microbial growth and survival. *ISME Journal*. **10**:761–77. DOI:10.1038/ismej.2015.153.

Groher A, Weuster-Botz D (2016) Comparative reaction engineering analysis of different acetogenic bacteria for gas fermentation. *Journal of Biotechnology*. **228:** 82–94. DOI:10.1016/j.jbiotec.2016.04.032.

Guindon S, Gascuel O (2003) A simple, fast, and accurate algorithm to estimate large phylogenies by maximum likelihood. *Systematic Biology*. **52**:696–704. DOI:10.1080/10635150390235520.

Gurujeyalakshmi G, Oriel P (1989) Isolation of phenol-degrading *Bacillus stearothermophilusand* partial characterization of the phenol hydroxylase. *Applied Environmental Microbiology*. **55**: 500-502.

Hall TA (1999) Bioedit: a user-friendly biological sequence alignment editor and analysis program for Windows 95/98/NT. *Nucleic Acids Symposiums Series*. **41**:95–8.

Hallenbeck PC, Benemann JR (2002) Biological hydrogen production; fundamental and limiting processes. *International Journal of Hydrogen Energy*. **27**:1185-1193. DOI:10.1016/S0360-3199(02)00131-3.

Hatti-Kaul R, Törnvall U, Gustafsson L, Börjesson P (2007) Industrial biotechnology for the production of bio-based chemicals - a cradle-to-grave perspective. *Trends in Biotechnology*. **25(3):** 119-124. DOI:10.1016/j.tibtech.2007.01.001.

Heijstra BD, Leang C, Juminaga A (2017) Gas fermentation: cellular engineering possibilities and scale up. *Microbial Cell Factories*. **16**:60. DOI:10.1186/s12934-017-0676-y.

Hino S, Tauchi H (1987) Production of carbon monoxide from aromatic amino acid by *Morganella morganii*. *Archieves of Microbiology*. **148(3)**:167-171. DOI:10.1007/BF00414807.

Holmqvist M, Lindberg P, Agervald Å, Stensjö K, Lindblad P (2011) Transcript analysis of the extended *hyp*-operon in the cyanobacteria *Nostoc* sp. strain PCC 7120 and *Nostoc punctiforme* ATCC 29133. *BMC Research Notes*. **4**:186. DOI:10.1186/1756-0500-4-186.

Huerta-Cepas J, Szklarczyk D, Forslund K, Cook H, Heller D, Walter MC, Rattei T, Mende DR, Sunagawa S, Kuhn M, Jensen LJ, von Mering C, Bork P (2016) eggNOG 4.5: a hierarchical orthology framework with improved functional annotations for eukaryotic, prokaryotic and viral sequences. *Nucleic Acids Research*. **44 D1**: D286-D293. DOI:0.1093/nar/gkv1248.

Hussein AH, Lisowska BK, Leak DJ (2015) The Genus *Geobacillus* and their biotechnological potential. *Advances in Applied Microbiology*. **92**:1-48. DOI:10.1016/bs.aambs.2015.03.001.

Hussein AH, Lisowska BK, Leak DJ (2015) The Genus *Geobacillus* and their biotechnological potential. *Advances in Applied Microbiology*. **92**:1-48. DOI:10.1016/bs.aambs.2015.03.001.

Inaoka T, Wang G, Ochi K (2009) ScoC regulates bacilysin production at the transcription level in *Bacillus subtilis*. *Journal of Bacteriology*. **191**: 7367-7371. DOI:10.1128/JB.01081-09.

Japaar SZ, Kalil MS, Ali E, Anuar N (2011) Effects of age of inoculum, size of inoculum and headspace on hydrogen production using *Rhodobacter sphaeroides*. *Journal of Bacteriology*. **1**:16-23. DOI:10.3923/bj.2011.16.23.

Jeoung JH, Fesseler J, Goetzl S, Dobbek H (2014) Carbon Monoxide. Toxic Gas and Fuel for Anaerobes and Aerobes: Carbon Monoxide Dehydrogenase. *Metal ions in life science.* **14**:37-69. DOI:10.1007/978-94-017-9269-1_3.

Jones WJ, Leigh JA, Mayer F, Woese CR, Wolfe RS (1983) *Methanococcus jannaschii* sp. nov., an extremely thermophilic methanogen from a submarine hydrothermal vent. *Archives Microbiology*. **136**:254–261. DOI:10.1007/BF00425213.

Kallio PT, Fagelson JE, Hoch JA, Strauch MA (1991) The transition state regulator Hpr of *Bacillus subtilis* is a DNA-binding protein. *Journal of Biological Chemistry*. **266**: 13411-13417.

Kanai T, Imanaka H, Nakajima A, Uwamori K, Omori Y, Fukui T, Atomi H, Imanaka T (2005) Continuous hydrogen production by the hyperthermophilic archaeon, *Thermococcus kodakaraensis* KOD1. *Journal of Biotechnology*. **116(3)**:271-282. DOI:10.1016/j.jbiotec.2004.11.002.

Kapdan IK, Kargi F (2006) Bio-hydrogen production from waste materials. *Enzyme and Microbial Technology*. **38**:569–82. DOI:10.1016/j.enzmictec.2005.09.015.

Karnholz A, Küsel K, Gößner A, Schramm A, Drake HL (2002) Tolerance and metabolic response of acetogenic bacteria toward oxygen. *Applied and Environmental Microbiology*. **68**:1005–1009. DOI:10.1128/AEM.68.2.1005-1009.2002.

Kerby R, Ludden P, Roberts G (1995) Carbon monoxide-dependent growth of *Rhodospirillum rubrum*. *Journal of Bacteriology*. **177**:2241-2244. DOI:10.1128/jb.177.8.2241-2244.1995.

Kerby R, Ludden P, Roberts G (1997) In vivo nickel insertion into the carbon monoxide dehydrogenase of *Rhodospirillum rubrum*: molecular and physiological characterization of cooCTJ. *Journal of Bacteriology*. **179**:2259-2266. DOI:10.1128/jb.179.7.2259-2266.1997.

King GM (1999) Characteristics and significance of atmospheric carbon monoxide consumption by soils. *Chemosphere*. **1**:53–63. DOI:10.1016/S1465-9972(99)00021-5.

King GM, Weber CF (2007) Distribution, diversity and ecology of aerobic CO-oxidizing bacteria. *Nature Reviews Microbiology*. **5**:107–118. DOI:1 0.1038/nrmicro1595.

Kodgire P, Rao KK (2009) *hag* expression in *Bacillus subtilis* is both negatively and positively regulated by ScoC. *Microbiology*. **155**: 142-149. DOI:10.1099/mic.0.021899-0.

Köpke M, Mihalcea C, Liew F, Tizard JH, Ali MS, Conolly JJ, Al- Sinawi B, Simpson SD (2011) 2,3-Butanediol production by acetogenic bacteria, an alternative route to chemical synthesis using industrial waste gas. *Applied Environmental Microbiology*. **77**:5467-5475. DOI:10.1128/AEM.00355-11.

Kotay SM, Das D (2007) Microbial hydrogen production with *Bacillus coagulans* IIT-BT S1n isolated from anaerobic sewage sludge. *Bioresource Technology*. **98**:1183-1190. DOI:10.1016/j.biortech.2006.05.009.

Kotay SM, Das D (2008) Biohydrogen as renewable energy resource – Prospects and potentials. *International Journal of Hydrogen Energy*. **33(1)**:258-263. DOI: 10.1016/j.ijhydene.2007.07.031.

Krueger NJ, von Schaewen A (2003) The oxidative pentose phosphate pathway: structure and organization. *Current Opinion in Plant Biology*. **6(3)**:236-246. DOI:10.1016/S1369-5266(03)00039-6.

Lee I, Ouk Kim Y, Park SC, Chun J (2016) OrthoANI: An improved algorithm and software for calculating average nucleotide identity. *International Journal of Systematic and Evolutionary Microbiology*. **66**: 1100-1103. DOI:10.1099/ijsem.0.000760.

Lefort V, Longueville J, Gascuel O (2017) SMS: Smart Model Selection in PhyML. *Molecular Biology and Evolution*. **34**:2422–4. DOI:10.1093/molbev/msx149.

Lelieveld J, Dentener FJ, Peters W, Krol MC (2004) On the role of hydroxyl radicals in the self-cleansing capacity of the troposphere. *Atmospheric Chemistry and Physics*. **4**:2337-2344. DOI:10.5194/acp-4-2337-2004.

Lenz O, Friedrich B (1998) A novel multicomponent regulatory system mediates H_2 sensing in *Alcaligenes eutrophus*. *Proceedings of the National Academy of Sciences of the United States of America*. **95**:12474–9. DOI:10.1073/pnas.95.21.12474.

Levin DB, Pitt L, Love M (2004) Biohydrogen production: prospects and limitations to practical application. *International Journal of Hydrogen Energy*, **29**:173–85. DOI:10.1016/S0360-3199(03)00094-6.

Li C, Fang HHP (2007a) Fermentative hydrogen production from wastewater and solid wastes by mixed cultures. *Critical Reviews in Environmental Science and Technology*. **37(1)**:1-39. DOI:10.1080/10643380600729071.

Lin PP, Rabe KS, Takasumi JL, Kadisch M, Arnold FH, Liao JC (2014) Isobutanol production at elevated temperatures in thermophilic *Geobacillus thermoglucosidasius*. *Metabolic Engineering*. **24**:1-8. DOI:10.1016/j.ymben.2014.03.006.

Lindahl PA (2002) The Ni-containing carbon monoxide dehydroge- nase family: light at the end of the tunnel? *Biochemistry*. **41**:2097–2105. DOI:10.1021/bi015932+.

Liou JS, Balkwill DL, Drake GR, Tanner RS (2005) *Clostridium carboxidivorans* sp. nov., a solvent-producing clostridium iso- lated from an agricultural settling lagoon, and reclassification of the acetogen *Clostridium scatologenes* strain SL1 as *Clostridium drakei* sp. nov. *International Journal of Systematic and Evolutionary Microbiology*. 55:2085–2091. DOI:10.1099/ijs.0.63482-0.

Lu Y, Khalil MAK (1993). Methane and carbon monoxide in OH chemistry: the effects of feedbacks and reservoirs generated by the reactive products. *Chemosphere*. **26**:641–655. DOI:10.1016/0045-6535(93)90450-J.

Maier T, Binder U, Böck A (1996) Analysis of the hydA locus of *Escherichia coli*: two genes (hydN and hypF) involved in formate and hydrogen metabolism. *Archives of Microbiology*. **165**:333–41. DOI:10.1007/s002030050335.

Marbán G, Valdés-Solís T (2007) Towards the hydrogen economy? *Science Direct*. **32**:1625-1637. DOI:10.1016/j.ijhydene.2006.12.017.

Marchler-Bauer A, Bryant SH (2004) CD-Search: protein domain annotations on the fly. *Nucleic Acids Research*. **32**(W): 327-331. DOI:10.1093/nar/gkh454.

Meier-Kolthoff JP, Auch AF, Klenk HP, Göker M (2013) Genome sequence-based species delimitation with confidence intervals and improved distance functions. *BMC Bioinformatics*. **14:** 1–14. DOI:10.1186/1471-2105-14-60.

Meyer O, Schlegel HG (1978) Reisolation of the carbon monoxide utilizing hydrogen bacterium *Pseudomonas carboxydovorans* (Kistner) comb. nov. *Archieves of Microbiology*. **118**:35–43.

Mohammadi M, Mohamed AR, Najafpour GD, Younesi H, Uzir MH (2014) Kinetic studies on fermentative production of biofuel from synthesis gas using *Clostridium ljungdahlii*. *Scientific World Journal*.910590. DOI:10.1155/2014/910590.

Mohr T, Aliyu H, Küchlin R, Polliack S, Zwick M, Neumann A, Cowan D, de Maayer P (2018a) CO-dependent hydrogen production by the facultative anaerobe *Parageobacillus thermoglucosidasius*. *Microbial Cell Factories*. **17**:108. DOI:10.1186/s12934-018-0954-3.

Mohr T, Aliyu H, Küchlin R, Zwick M, Neumann A, Cowan D, de Maayer P (2018b) Comparative genomic analysis of *Parageobacillus thermoglucosidasius* strains with distinct hydrogenogenic capacities. *BMC Genomics*. **19**:880. DOI:10.1186/s12864-018-5302-9.

Mörsdorf G, Frunzke K, Gadkari D, Meyer O (1992) Microbial growth on carbon monoxide. *Biodegradation* **3**:61–82.

Mukherjee M, Vajpai M, Sankararamakrishnan R (2017) Anion-selective Formate/ nitrite transporters: taxonomic distribution, phylogenetic analysis and subfamily-specific conservation pattern in prokaryotes. *BMC Genomics*. **18**:1–19. DOI:10.1186/s12864-017-3947-4.

Nagarajan D, Lee DJ, Kondo A, Chang JS (2016) Recent insights into biohydrogen production by microalgae – From biophotolysis to dark fermentation. *Bioresource Technology*. **227**:373-387. DOI:10.1016/j.biortech.2016.12.104.

Nath K, Das D (2004) Biohydrogen production as a potential energy resource- Present state-of-art. *Journal of Scientific & Industrial Research*. **63**:729-738.

Nazina TN, Tourova TP, Poltaraus AB, Novikova EV, Grigoryan AA, Ivanova AE, Lysenko AM, Petrunyaka VV, Osipov GA, Belyaev SS, Ivanov MV (2001) Taxonomic study of aerobic thermophilic bacilli: descriptions of *Geobacillus subterraneus* gen. nov., sp. nov. and *Geobacillus uzenensis* sp. nov. from petroleum reservoirs and transfer of *Bacillus stearothermophilus, Bacillus thermocatenulatus, Bacillus thermoleovorans, Bacillus kaustophilus, Bacillus thermoglucosidasius* and *Bacillus thermodenitrificans* to *Geobacillus* as the new combinations *G. stearothermophilus, G. thermocatenulatus,*

G. thermoleovorans, G. kaustophilus, G. thermoglucosidasius and *G. thermodenitrificans*. *International Journal of Systematic and Evolutionary Microbiology*. **51**:433-446.

Ni M, Leung DYC, Leung MKH, Sumathy K (2006) An overview of hydrogen production from biomass. *Fuel Processing Technology*. **87**:461-472. DOI:10.1016/j.fuproc.2005.11.003.

Nikolaidis P, Poullikkas A (2017) A comparative overview of hydrogen production processes. *Renewable & Sustainable Energy Reviews*. **67**:597–611. DOI:10.1016/j.abb.2004.08.032.

Odgen JM (1999) Prospects for Building A Hydrogen Energy Infrastructure. *Annual Review of Energy and The Environment*. **24**:227-279. DOI:10.1146/annurev.energy.24.1.227.

Oelgeschläger, E, Rother, M (2008) Carbon monoxide-dependent energy metabolism in anaerobic bacteria and archaea. *Archives of Microbiology*. **190**:257–269. DOI:0.1007/s00203-008-0382-6.

Overbeek R, Olson R, Pusch GD, Olsen GJ, Davis JJ, Disz T. Edwards RA, Gerdes S, Parrello B, Shukla M, Vonsetin V, Wattam AR, Xia F, Stevens R (2014) The SEED and the Rapid Annotation of microbial genomes using Subsystems Technology (RAST). *Nucleic Acids Research*. **42**(Database issue): D206-214. DOI:10.1093/nar/gkt1226.

Parshina SN, Sipma J, Nakashimada Y, Henstra AM, Smidt H, Lysenko AM, Lens PN, Lettinga G, Stams AJ (2005) *Desulfotomaculum carboxydivorans* sp. nov., a novel sulfate-reducing bacterium capable of growth at 100% CO. *International Journal of Systematic and Evolutionary Microbiology*. **55**:2159-2165. DOI:10.1099/ijs.0.63780-0.

Peng C, Huang D, Shi Y, Zhang B, Sun L, Li M, Deng X, Wang W (2019) Comparative transcriptomic analysis revealed the key pathways responsible for organic sulfur removal by thermophilic bacterium *Geobacillus thermoglucosidasius* W-2. *Science of the total Environment*. **676**:639-650. DOI:10.1016/j.scitotenv.2019.04.328.

Peters JW, Shut GJ, Boyd ES, Mulder DW, Shepard EM, Broderick JB, King PW, Adams MWW (2015) [FeFe]- and [NiFe]-hydrogenase diversity, mechanism, and maturation. **1853(6)**:1350-1369. DOI:10.1016/j.bbamcr.2014.11.021.

Philip EA, Clark OG, Londry K, Yu Steven, Leonard J (2013) *Compost science & utilization*. **19(3)**:170-177. DOI:10.1080/1065657X.2011.10736996.

Preuster P, Alekseev A, Wasserscheid P (2017) Hydrogen Storage Technologies for Future Energy Systems. *Annual Review of Chemical and Biomolecular Engineering*. **8**:445-471. DOI:10.1146/annurev-chembioeng-060816-101334.

Ragsdale S W (2008) Enzymology of the Wood-Ljungdahl pathway of acetogenesis. *Annals of the New York Academy of Sciences*. **1125**:129–136. DOI:10.1196/annals.1419.015.

Ragsdale SW (2004) Life with Carbon Monoxide. *Critical Reviews in Biochemistry and Molecular Biology*. **39**:165–95. DOI:10.1080/10409230490496577.

Rahman SNA, Msdar MS, Rosli MI, Majlan EH, Husaini T, Kamarudin SK, Daud WRW (2016) Overview of biohydrogen technologies and application in fuel cell technology. *Renewable & Sustainable Energy Reviews*. **66**:137-162. DOI:10.1016/j.rser.2016.07.047.

Ramachandran R, Menon RK (1998) An overview of industrial uses of hydrogen. *International Journal of Hydrogen Energy*. **23(7)**:593-598. DOI:10.1016/S0360-3199(97)00112-2.

Reed CJ, Lewis H, Trejo E, Winston V, Evilia C (2013) Protein adaption in archeael extremophiles. *Archaea*. 373275. DOI:10.1155/2013/373275.

Reimert R, Marschner F, Renner HJ, Boll W, Supp E, Brejc M, Liebner W, Schaub G (2011) Gas production, 2. Processes. *Ullmann's Encyclopedia of Industrial Chemistry*, Wiley-VCH, Weinheim. DOI:10.1002/14356007.o12_o01.

Sargent F, Bogsch EG, Stanley NR, Wexler M, Robinson C, Berks BC, Palmer T (1998) Overlapping functions of components of a bacterial Sec-independent protein export pathway. *EMBO Journal*. **17**:3640–50. DOI:10.1093/emboj/17.13.3640.

Schmidt U, Conrad R, (1993) Hydrogen, carbon monoxide, and methane dynamics in Lake Constance. *Limnology and Oceanography*, **38**:1214–1226. DOI:10.4319/lo.1993.38.6.1214.

Schneider SH (1989) The Greenhouse Effect: Science and Policy. *Science*. **243(4892)**:771-781. DOI:10.1126/science.243.4892.771.

Schwartz E, Fritsch J, Friedrich B (2013) H_2-Metabolizing Prokaryotes. In: The Prokaryotes: Prokaryotic Physiology and Biochemistry, Rosenberg E, DeLong EF, Lory S, Stackebrandt E, Thomson F, editors. Berlin: Springer. Berlin. pp 119–199.

Seengenyoung J, O-Thong S, Imai T, Prasetsan P (2011) Effect of inoculum size for biohydrogen production from palm oil mill effluent. TIChE International Conference, 2011.

Shahinyan G, Margaryan A, Panosyan H, Trchounian A (2017) Identification and sequence analyses of novel lipase encoding novel thermophillic bacilli isolated from Armenian geothermal springs. *BMC Microbiology*. **17**:1-11. DOI:10.1186/s12866-017-1016-4.

Sharma S, Ghoshal SK (2014) Hydrogen the future transportation fuel: From production to applications. *Renewable and Sustainable Energy Review*. **43**:1151-1158. DOI:10.1016/j.rser.2014.11.093.

Sipma J, Henstra AM, Parshina SM, Lens PN, Lettinga G, Stams AJ (2006) Microbial CO conversions with applications in synthesis gas purification and bio-desulfurization. *Critical Reviews in Biotechnology*. **26**:41–65. DOI:10.1080/07388550500513974.

Soboh B, Linder D, Hedderich R (2002) Purification and catalytic properties of a CO-oxidizing: H_2-evolving enzyme complex from *Carboxydothermus hydrogenoformans*. *European Journal of Biochemisty*. **269**:5712–21. DOI:10.1046/j.1432-1033.2002.03282.x.

Solovyev V, Salamov A (2011) Automatic annotation of microbial genomes and metagenomic sequences. In: Metagenomics and its applications in agriculture, biomedicine and environmental studies. *Ed. Robert W, Nova Science Publishers*. New York, USA p. 61-78.

Søndergaard D, Pedersen CNS, Greening C (2016) HydDB: A web tool for hydrogenase classification and analysis. *Scientific Report*. **6**:1–8. DOI:10.1038/srep34212.

Sørensen B, Spazzafumo G (2011) Hydrogen and Fuel Cells. *Emerging Technologies and Application*. DOI:10.1016/C2009-0-63881-2.

Srirangan K, Akawi L, Moo-Young M, Chou CP (2012) Towards sustainable production of clean energy carriers from biomass resources. *Applied Energy*, **100**:172-186. DOI:10.1016/j.apenergy.2012.05.012.

Stettner AI, Segrè D (2013) The cost of efficiency in energy metabolism. *PNAS*. **110(24)**:9629-9630. DOI:10.1073/pnas.1307485110.

Suzuki Y, Kishigami T, Inoue K, Mizoguchi Y, Eto N, Takagi M, Abe S (1983) *Bacillus thermoglucosidasius* sp. Nov. a new species of obligately thermophilic bacilli. I*nternational Journal of Systematic and Evolutionary Microbiology.* **4**: 487-495

Svetlichny V, Sokolova T, Gerhardt M, Ringpfeil M, Kostrikina N (1991) *Carboxydothermus hydrogenoformans* gen. nov., sp. nov., a CO-utilizing thermophilic anaerobic bacterium from hydrothermal environments of Kunashir Island. *Systematic and Applied Microbiology*. **14**:254-260. DOI:10.1016/S0723-2020(11)80377-2.

Takors R, Kopf M, Mampel J, Bluemke W, Blombach B, Eikmanns B, Bengelsdorf FR, Weuster-Botz D, Dürre P (2018) Using gas mixtures of CO, CO_2 and H_2 as microbial

substrates: the do's and don'ts of successful technology transfer from laboratory to production scale. *Microbial Biotechnology*. **11**:606–625. DOI:10.1111/1751-7915.13270.

Talavera G, Castresana J (2007) Improvement of phylogenies after removing divergent and ambiguously aligned blocks from protein sequence alignments. *Systematic Biology*. **56**:564–77. DOI:10.1080/10635150701472164.

Tang YJ, Sapra R, Joyner D, Hazen TC, Myers S, Reichmuth D, Blanch H, Keasling JD (2008) Analysis of metabolic pathways and fluxes in a newly discovered thermophilic and ethanol-tolerant *Geobacillus* strain. *Biotechnology and Bioengineering*. **102(5)**:1283-1525. DOI:10.1002/bit.22181.

Taylor, JA, Zimmerman, PR, Erickson III, DJ (1996) A 3-D modeling study of the sources and sinks of atmospheric carbon monoxide. *Ecological Modelling*, **88**:53–71. DOI:10.1016/0304-3800(95)00069-0.

Techtmann SM, Colman AS, Robb FT (2009) 'That which does not kill us only makes us stronger': the role of carbon monoxide in thermophilic microbial consortia. *Environmental Microbiology*. **11**:1027–1037. DOI:10.1111/j.1462-2920.2009.01865.

Techtmann SM, Lebedinski AV, Colman AS, Sokolova TG, Woyke T, Goodwin L, Robb FT (2012) Evidence for horizontal gene transfer of anaerobic carbon monoxide dehydrogenases. *Frontiers in Microbiology*. **3**:1–16. DOI:10.3389/fmicb.2012.00132.

Teixeira LV, Moutinho LF, Romão-Dumaresq AS (2018) Gas fermentation of C1 feedstocks: commercialization status and future prospects. *Biofuels, Bioproducts and Biorefining* **12:**1103–1117. DOI:10.1002/bbb.1912.

Tfsitescan: http://www.ifti.org/Tfsitescan. Accessed 20 April 2018.

Thebti W, Riahi Y, Belhadj O (2016) Purification and Characterization of a New Thermostable, Haloalkaline, Solvent Stable, and Detergent Compatible Serine Protease from *Geobacillus toebii* Strain LBT 77. *BioMed Research International.* DOI:10.1155/2016/9178962.

Thomé R, Gust A, Toci R, Mendel R, Bittner F, Magalon A, Walburger A (2012) A sulfurtransferase is essential for activity of formate dehydrogenases in *Escherichia coli*. *Journal of Biological Chemistry*. **287**:4671–8. DOI:10.1074/jbc.M111.327122.

Thompson JD, Higgins DG, Gibson TJ (1994) Clustal W: improving the sensitivity of progressive multiple sequence alignment through sequence weighting, position-specific gap penalties and weight matrix choice. *Nucleic Acids Research*. **22**: 4673-4680.

Timm B (1963) 50 Jahre Ammoniak-Synthese. *Chemie Ingenieur Technik*. **35**(12):817-823. DOI:10.1002/cite.330351202.

Tirado-Acevedo O, Chinn MS, Grunden AM (2010) Production of biofuels from synthesis gas using microbial catalysts. *Advances in Applied Microbiology*. **70**:57–92.

Tirado-Acevedo O, Cotter JL, Chinn MS, Grunden AM (2011) Influence of Carbon Source Pre-Adaptation on *Clostridium ljungdahlii* Growth and Product Formation. *Journal of Bioprocessing & Biotechniques*. **01**:1–5. DOI:10.4172/2155-9821.s2-001.

Valladares Juárez AG, Dreyer J, Göpel PK, Kosche N, Frank D, Märkl H, Müller R (2009) Characterisation of a new hermoalkaliphilic bacterium for the production of high-quality hemp fibres, *Geobacillus thermoglucosidasius* strain PB94A. *Applied Microbiology and Biotechnology*. **83(3)**:521-527.

van der Oost J, von Wachenfeldt C, Hederstedt L, Saraste M (1991) *Bacillus subtilis* cytochrome oxidase mutants: biochemical analysis and genetic evidence for two aa_3-type oxidases. *Molecular Microbiology*. **5**: 2063-2072.

Vignais PM, Billoud B (2007) Occurrence, classification, and biological function of hydrogenases: an overview. *Chemical Reviews*. **107**:4206–72. DOI:10.1038/ismej.2015.153.

Vignais PM, Billoud B, Meyer J (2001) Classification and phylogeny of hydrogenases. *FEMS Microbiology Reviews*. **25**:455–501. DOI:10.1111/j.1574-6976.2001.tb00587.x

Vignais PM, Elsen S, Colbeau A (2005) Transcriptional regulation of the uptake [NiFe] hydrogenase genes in *Rhodobacter capsulatus*. *Biochemical Society Transactions*. **33**:28–32. DOI:10.1042/BST0330028.

Waldron KJ, Robinson NJ (2009) How do bacterial cells ensure that metalloproteins get the correct metal? *Nature Reviews Microbiology*. **6:**25-35. DOI:10.1038/nrmicro2057.

Wallace IM, Sullivan OO, Higgins DG, Notredame C (2006) M-Coffee: combining multiple sequence alignment methods with T-Coffee. *Nucleic Acids Research*. **34**:1692–9. DOI:10.1093/nar/gkl091.

Wang J, Wan W (2008) Influence of Ni2+ concentration on biohydrogen production. *Bioresource Technology*. **99**:8864-8868. DOI:10.1016/j.biortech.2008.04.052.

World Energy Outlook 2018 (www.iae.org) accessed on 04/04/2018.

Wu M, Ren Q, Durkin AS, Daugherty SC, Brinkac LM, Dodson RJ, Madupu R, Sullivan SA, Kolonay JF, Haft DH, Nelson WC, Tallon LJ, Jones KM, Ulrich LE, Gonzales JM, Zhulin IB, Robb FT, Eisen JA (2005) Life in hot carbon monoxide: the complete genome sequence of *Carboxydothermus hydrogenoformans* Z-2901. *PloS Genetics*. e60.

Yu J, Takahashi P (2007) Biophotolysis-based hydrogen production by cyanobacteria and green microalgae. *Communicating Current Research and Educational Topics and Trends in Applied Microbiology*. **1**:79–89.

Zafiriou OC, Andrews SS, Wang W (2003) Concordant estimates of oceanic carbon monoxide source and sink processes in the Pacific yield a balanced global 'blue- water' CO budget. *Global Biogeochemical Cycles*. **17**:1–13. DOI:10.1029/2001GB001638.

Zavarazin GA, Nozhevnikova AN (1977) Aerobic carboxydobacteria. *Microbial Ecology*. **3**:305-326. DOI:10.1007/BF02010738.

Zeigler DR (2001) The Genus *Geobacillus*.Introduction and Strain Catalog. *Bacillus Genetic Stock Center. Catalog of Strains*. **7(3)**.

Zeigler DR (2014) The Geobacillus paradox: why is a thermophilic bacterial genus so prevalent on a mesophilic planet? *Microbiology*. **160**:1–11. DOI:10.1099/mic.0.071696-0.

Zeng K, Zhang D (2010) Recent progress in alkaline water electrolysis for hydrogen production and application. *Progress in Energy and Combustion Science*. **36**:307-326. DOI:10.1016/j.pecs.2009.11.002.

Zhang T, Liu H, Fang HHP (2003) Biohydrogen production from starch in wastewater under thermophilic conditions. *Journal of Environmental Management*. **69(2)**:149-156. DOI:10.1016/S0301-4797(03)00141-5.

Zhang Y, Liu D, Chen Z (2017) Production of C2-C4 diols from renewable bioresources: New metabolic pathways and metabolic engineering strategies. *Biotechnology of Biofuels*. **10**:1–20. DOI:10.1186/s13068-017-0992-9.

Zhou Y, Liang Y, Lynch KH, Dennis JJ, Wishart DS (2011) PHAST: a fast phage search tool. *Nucleic Acids Research* **39**(Web Server issue):W347-52. DOI:10.1093/nar/gkr485.

LIST OF FIGURES

LIST OF TABLES

APPENDIX

Appendix 1

Annotations of the CODH and [Ni-Fe] hydrogenase loci of *P. thermoglucosidasius* DSM 2542^T. The locus tags, sizes, protein names as well as the functions of the proteins in the three [Ni-Fe] hydrogenase loci and the anaerobic CODH locus of *P. thermoglucosidasius* DSM 2542^T. BlastP data (locus tag, average amino acid identity, bitscore and e-value) for the closest non-*Parageobacillus* orthologue and the top conserved domain for each *P. thermoglucosidasius* DSM 2542^T protein are shown.

Available: https://static-content.springer.com/esm/art%3A10.1186%2Fs12934-018-0954-3/MediaObjects/12934_2018_954_MOESM2_ESM.xlsx in Mohr T, Aliyu H, Küchlin R, Polliack S, Zwick M, Neumann A, Cowan D, de Maayer P (2018a) CO-dependent hydrogen production by the facultative anaerobe *Parageobacillus thermoglucosidasius*. *Microbial Cell Factories*. 17:108. DOI:10.1186/s12934-018-0954-3.

Appendix 2

Orthologous [Ni-Fe] hydrogenase and anaerobic CODH loci in *Parageobacillus* and other taxa. The locus size, G+C content, G+C deviation of the orthologous [Ni-Fe] hydrogenase and anaerobic CODH loci of other *P. thermoglucosidasius* strains and distinct taxa. The number of protein orthologous and average amino acid identity of these proteins to those encoded on the *P. thermoglucosidasius* DSM 2542^{T} loci are indicated.

Available: https://static-content.springer.com/esm/art%3A10.1186%2Fs12934-018-0954-3/MediaObjects/12934_2018_954_MOESM2_ESM.xlsx in Mohr T, Aliyu H, Küchlin R, Polliack S, Zwick M, Neumann A, Cowan D, de Maayer P (2018a) CO-dependent hydrogen production by the facultative anaerobe *Parageobacillus thermoglucosidasius*. *Microbial Cell Factories*. **17**:108. DOI:10.1186/s12934-018-0954-3.

Appendix 3

Annotations of the protein families shared and unique among the compared *P. thermoglucosidasius* strains. The protein family datasets which are shared between different combinations of the four compared strains or unique to a particular strain were functionally annotated by RAST, comparison against the Conserved Domain Database and classification according to their COG function using EggNOG mapper (Overbeek *et al*., 2014; Zhou *et al*., 2011). The proportions (%) of proteins (unique to strains or shared among different combinations of strains) belonging to each COG are graphically presented.

Available: https://static-content.springer.com/esm/art%3A10.1186%2Fs12864-018-5302-9/MediaObjects/12864_2018_5302_MOESM3_ESM.xlsx in Mohr T, Aliyu H, Küchlin R, Zwick M, Neumann A, Cowan D, de Maayer P (2018b) Comparative genomic analysis of Parageobacillus thermoglucosidasius strains with distinct hydrogenogenic capacities. BMC Genomics. 19:880. DOI:10.1186/s12864-018-5302-9.

Appendix 4

SNPs occurring in the CODH-NiFe group 4a locus genes of the compared *P. thermoglucosidasius* strains. The number of SNPs occurring in the individual CODH-NiFe group 4a genes of particular strains are indicated. The number in brackets indicates the number of non-synonymous amino acid substitutions observed in the amino acid sequence alignments for each individual gene.

Gene	Protein product	Gene size (nt)	SNPs (non-synonymous amino acid substitutions)			Total SNPs
			DSM 6285	DSM 21625	DSM 21625 + DSM 6285	
cooC	Carbon monoxide dehydrogenase maturation factor	765	-	10 (6)	-	10 (6)
cooS	Carbon monoxide dehydrogenase catalytic subunit	1926	2 (1)	9 (0)	-	11 (1)
cooF	Carbon monoxide dehydrogenase iron-sulfur protein	489	-	-	-	-
phcA	[Ni-Fe]-hydrogenase 4 component B	2010	1 (0)	1 (1)	6 (1)	8 (2)
phcB	Hydrogenase 3 membrane subunit	942	5 (0)	2 (1)	6 (3)	13 (4)
phcC	[Ni-Fe]-hydrogenase 4 component E	648	-	1 (1)	-	1 (1)
phcD	[Ni-Fe]-hydrogenase 4 component F	1479	-	4 (2)	-	4 (2)
phcE	[Ni-Fe]-hydrogenase 4 component D	1439	-	4 (2)	-	4 (2)
phcF	[Ni-Fe]-hydrogenase large subunit	1725	1 (1)	8 (4)	-	9 (5)
phcG	[Ni-Fe]-hydrogenase 4 component H (4Fe-4S ferredoxin)	519	-	2 (0)	-	2 (0)
phcH	[Ni-Fe]-hydrogenase small subunit	744	-	2 (1)	-	2 (1)
phcI	Formate hydrogenlyase maturation protein	432	-	1 (0)	-	1 (0
phcJ	Hydrogenase maturation protease	423	2 (0)	-	-	2 (0)
phcK	Hydrogenase maturation nickel metallochaperone	471	2 (2)	-	-	2 (2)
phcL	Hydrogenase accessory protein	696	-	1 (1)	2 (2)	3 (3)
		TOTAL	13 (4)	45 (19)	14 (6)	72 (29)